DYNAMIC SIMULATION AND COMPUTER CONTROL OF A PILOT SCALE FLUIDIZED BED REACTOR

by

© RANDALL CHARLES McFARLANE

A thesis submitted to the Department of Chemical Engineering in conformity with the requirements for the degree of Master of Engineering

McMaster University
Hamilton, Ontario, Canada

November, 1980

MASTER OF ENGINEERING — McMASTER UNIVERSITY

(Chemical Engineering) — Hamilton, Ontario

TITLE: Dynamic Simulation and Computer Control of a Pilot Scale Fluidized Bed Reactor

AUTHOR: Randall Charles McFarlane, B.A.Sc. (University of Waterloo)

SUPERVISORS: Professors J.F. MacGregor and T.W. Hoffman

NUMBER OF PAGES: xii, 176

ABSTRACT

A dynamic simulation of the pilot scale fluidized bed reactor in the Department of Chemical Engineering is developed based on mass/energy balance equations of the process. The unknown parameters in the model equations are estimated using dynamic data from the reactor. A preliminary control strategy for the reactor system is tested by simulation, and the results are used to aid in the implementation of the control system to the reactor. The control strategy is a cascade control system in which the inner loop regulates reaction temperature by proportional-integral control, using the ratio of hydrogen to n-butane feedrates as manipulated variable. The outer loop is a Dahlin's algorithm controller, which maintains the selectivity of propane at a specified setpoint by manipulating the reaction temperature setpoint to the inner loop.

The control system performed less favourably on the real system than it did on the simulation model. This result is attributed primarily to the inability of fixed-parameter controllers to deal with highly non-linear and time varying processes. Alternate control methods are suggested which are designed to deal with these problems.

ACKNOWLEDGEMENTS

I wish to express my sincere appreciation to Dr. J.F. MacGregor and Dr. T.W. Hoffman, for their guidance and supervision throughout this project. I am also particularly grateful to Dr. P.A. Taylor for his very helpful input into the project.

Financial support from the Ontario Government and McMaster University is gratefully acknowledged.

I would also like to thank the following individuals:

- Miss Sau Man Yang, for her assistance in preparing the sofware and reactor for the final control runs.
- Mrs. Amy Stott, for the careful typing of the manuscript

Acknowledgement is made to the Donors of The Petroleum Research Fund, administered by the American Chemical Society, for support of this research.

TABLE OF CONTENTS

INDEX OF FIGURES

INDEX OF TABLES

NOMENCLATURE

KINETIC EXPRESSIONS, SECTION 3.2.1

ΔE	activation energy, kcal/g-mole
F'	= .9, fraction of n-butane that reacts to form propane
k/k_o	catalyst activity, dimensionless
K_{B1}, K_{P1}, K_{E2}	frequency factors, gmoles/sec-cm^3-atm^{m-n}
K_{P2}, K_{E1}	rates of frequency factors, dimensionless
m, m', m''	exponents on n-butane, propane and ethane partial pressures, respectively, dimensionless
n, n', n''	exponents on hydrogen partial pressures in rate expressions for n-butane, propane and ethane respectively, dimensionless
P	partial pressure, atm
r_i	rate of reaction of component i, gmoles/sec-g catalyst
T	reaction temperature, ^oK

MASS/ENERGY BALANCES SECTION 3.2

a	pellet area per weight of catalyst, cm^2/g-catalyst
A_c	area for heat transfer between oil in heating/cooling coil and wall, cm^2
A_w	area for heat transfer between catalyst bed and wall, cm^2
C	concentration, gmoles/cm^3
C_{pB}	heat capacity of catalyst particles, cal/g-^oC
$\bar{C}_{pg}$	average molal heat capacity of gas, cal/gmole-^oC
C_{poil}	heat capacity of oil, cal/g-^oC
C_{pw}	effective heat capacity of wall, cal/g-^oC
D_b	bubble diameter, cm

d_p	average particle diameter, cm
g	acceleration due to gravity, cm/sec^2
h	heat transfer coefficient between solid catalyst and gas phase, $cal/sec\text{-}cm^2\text{-}^oC$
H	height of bed at fluidization conditions, cm
ΔH_j	heat of reaction of the jth reaction, cal/gmole
h_c	effective heat transfer coeeficient between oil and wall, $cal/sec\text{-}cm^2\text{-}^oC$
k_G	mass transfer coefficient for diffusion, cm/sec
m_w	mass of reactor wall, g
N	number of bubbles per unit volume of bed, cm^{-3}
P	partial presure, atm
q	net volumetric inflow and outflow in the bubble phase, cm^3/sec
Q	transfer rate, $cm^3/sec\text{-bubble}$
Q_e	heat input to heating tank from immersion heaters, cal/sec
R	gas law constant, $atm\text{-}cm^3/mole\text{-}^oK$
r_v	rate of reaction of a component, $gmoles/sec\text{-}cm^3$
R_j	rate of reaction of the jth reaction, gmoles/sec-g catalyst
S	cross sectional area of bed, cm^2
S	surface area of bubble, cm^2
T	temperature, ^oC

subscripts for T:

air,in	air entering air cooler
air,out	air exiting air cooler
oil,in	oil entering heating/cooling coil

$T_{oil,out}$	oil exiting heating/cooling coil
T_R	reactor catalyst bed
T_{TANK}	circulating oil heating tank
T_{OIL}	average bulk temperature of oil in heating/cooling coil, ^{o}C
U	overall heat transferr coefficient between air and oil in air air cooler, $cal/sec\text{-}cm^2\text{-}^{o}C$
u_b	bubble rise velocity, cm/sec
u_{mf}	superficial velocity at minimum fluidization, cm/sec
V	= SH, bed volume under fluidizing conditions, cm^3
V_b	average bubble volume, cm^3
V_e	volume of emulsion phase, cm^3
v_o	total volumetric flowrate of inlet gas, cm^3/sec
V_{TANK}	volume of oil in heating tank, cm^3
W	weight of catalyst, g
W_{OIL}	mass flowrate of oil in heating/cooling circulating system, g/sec
y	distance from distributor plate, cm
GREEK LETTERS	
ϵ	bed void fraction, dimensionless
$\bar{\rho}_g$	average molal density of gas, $gmoles/cm^3$
ρ_{OIL}	density of oil, g/cm^3
ρ_P	average particle density, g/cm^3
Subscripts	
b	bubble phase
e	emulsion phase
o	feed

CHAPTER 1

INTRODUCTION

With the advent of inexpensive and reliable minicomputer systems has come a dramatic increase in the number of installations of these systems in the chemical process and related industries. It is now common practice that new plants include the minicomputer system and related interface hardware at the design stage. However, there exists a reluctance in industry to fully utilize these systems in a control sense. Cost/benefit considerations make it difficult to justify the expense (in human and capital resources) required to develop a control strategy for a particular plant. The cost is easily evaluated but the projected benefits are not; often it is difficult to state with reasonable certainty that the contemplated control strategy will in fact be successful in meeting the stated control objectives. The impetus for this study is the need to demonstrate the applicability of control methods to chemical processes of industrial interest.

This project is the first in what is anticipated to be a series of control studies on the pilot scale fluidized bed reactor in the Department of Chemical Engineering. The objectives of this study are stated as follows. The dynamic behaviour of the reactor system will be studied to develop a base of knowledge for the design of control strategies. This will be accomplished by developing a dynamic simulation, based on a mechanistic description of the system. A

preliminary control strategy will be developed, the performance of which will be tested by simulation and by application to the real system. It is hoped that this study will provide a sound basis for the continuation of control studies on this reactor system.

The outlines of the chapters of this thesis are given below.

2. This chapter provides a description of the fluidized bed pilot plant and the interface system which was installed for the purpose of on-line control implementation.

3. The development of the dynamic model of the fluidized bed system is presented. The previous work of Shaw (11,12), Orlickas (9,10) and coworkers on this particular system, has been used extensively in this development, and a summary of their work is given. A modular dynamic simulation is developed using the DYNSYS simulation executive.

4. The unknown parameters in the model equations are estimated using dynamic data from the fluidized bed reactor.

5. The control problem is discussed, and a preliminary solution in the form of a cascade control system is presented. The control system is tuned and tested by simulation.

6. The control system designed and tested in Chapter 5, was implemented on the real system, and the results are described in this chapter.

7. This chapter presents the major conclusions of the study. The control problems in this system are summarized and suggestions are made for alternate control methods to deal with these problems.

CHAPTER 2

FLUIDIZED BED PILOT PLANT

2.1 INTRODUCTION

The fluidized bed pilot plant in the Department of Chemical Engineering was designed by Shaw(1) and coworkers. The reactor diameter, 8", is large for a research reactor of this type, and was chosen so as to avoid slugging in the catalyst bed and to minimize wall effects. Because of the physical size of the reactor, and the complexity of its support systems, many of the operating characteristics of this pilot plant resemble those of industrial scale plants. Control studies on this pilot plant can be considered to be especially relevant to the advancement of the application of control theory to complex chemical engineering systems.

Since any control theory to be applied to this system must be implemented using a minicomputer, a process interface has been intalled between the pilot plant and the department's minicomputer system. A description of the minicomputer facilities is given in Section 2.3 and details of the interface are given in Section 2.4. In Section 2.2, a general description of the fluidized bed reactor pilot plant is provided. The reader is referred to Shaw (1) for a more detailed description.

2.2 DESCRIPTION OF THE FLUIDIZED BED PILOT PLANT

A flow diagram of the pilot plant is shown in Figure 2.1. The locations of interface instrumentation, to be described in Section 2.4, are also shown in this diagram.

The fluidized bed reactor consists of three sections: bottom cone, reactor barrel and disengaging section. Feed gas enters the bottom of the reactor and passes through the bottom cone which is packed with 3/4" stainless steel rings to disperse the flow over the cross section of the reactor barrel. The feed gas then flows into the reactor barrel, which holds the catalyst bed, through a distributor plate drilled with 230, .055 in. holes. The reactor barrel is constructed of 16 gauge stainless steel and is 7.986 in. I.D. and 6 ft. high. Catalyst is held in place with a sheet of 200 mesh stainless steel screening, bolted in place immediately below the distributor plate. Above the reactor barrel is a disengaging section 2 ft. high by 18 in. in diameter. Gas exiting the reactor passes through a cyclone which returns entrained catalyst particles to the catalyst bed. A pressure release valve on the exit line is set to 5 p.s.i.g.

Cooling of the reactor is accomplished with a circulating oil system from which heat is removed in an air cooled heat exchanger (single pass, stainless steel, 1.2 ft^2). Stainless steel (Type 316) 1/2 in. tubing is spiralled at 2 in. centers around the reactor barrel and approximately 1/2 of the disengaging section, providing heat transfer

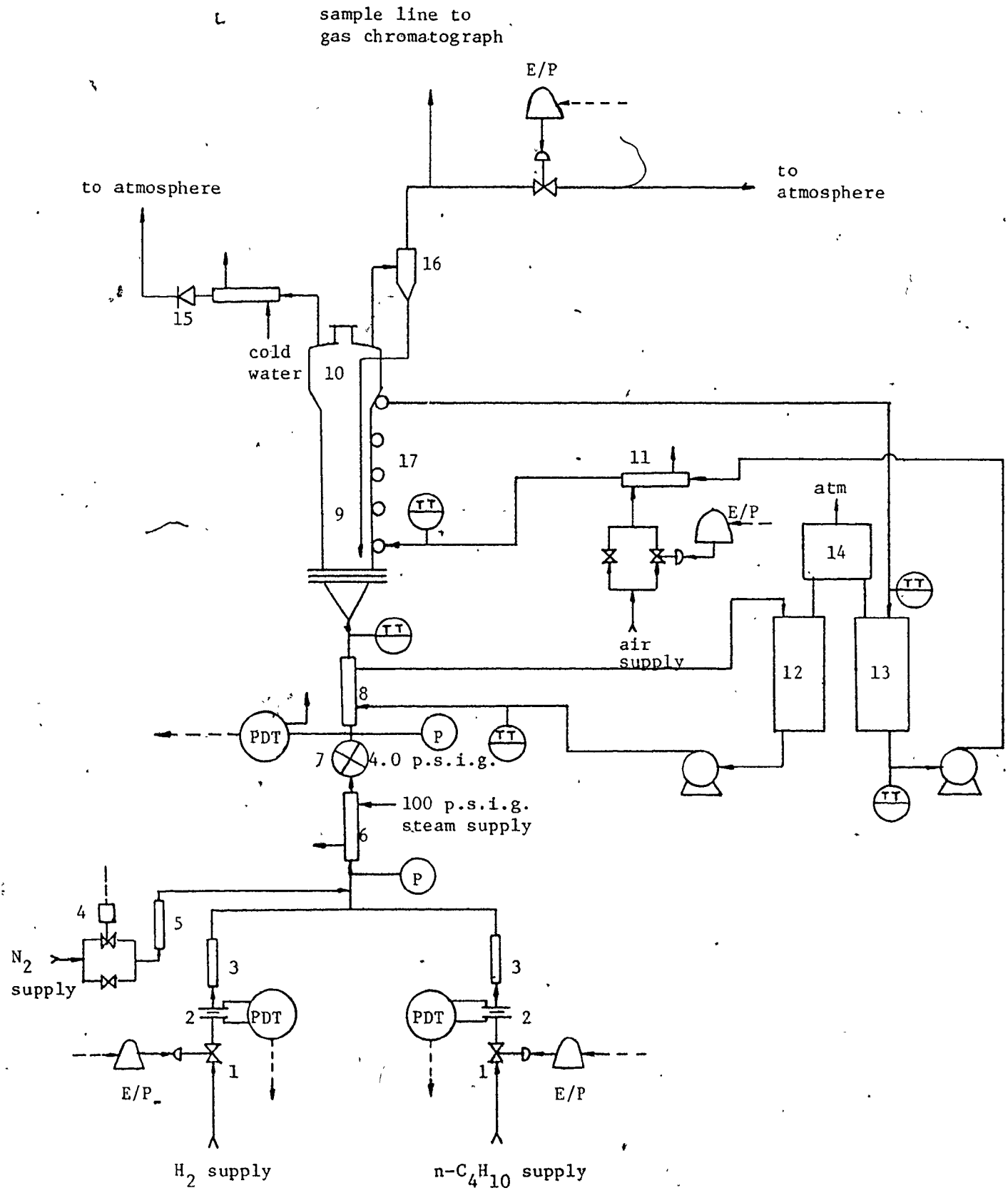

FIGURE 2.1 Flow diagram of Fludized Bed Pilot Plant.

Legend for FIGURE 2.1


control valve


pressure relief valve


on-off solenoid valve

multiplexed thermocouple

differential pressure transmitter

pressure gauge


back pressure regulator

electro-pneumatic transducer

1. H_2 and n-butane control valves
2. H_2 and n-butane orifice plates
3. H_2 and n-butane rotameters
4. N_2 solenoid valve
5. N_2 flow indicator
6. feed preheater (steam)
7. backpressure regulator for feed system
8. feed preheater (circulating oil)
9. fluidized bed reactor, reaction chamber
10. fludized bed reactor, disengaging section
11. air cooler (circulating oil system for heating/cooling coil)
12. heating tank, feed preheat circulating oil system
13. heating tank, heating/cooling coil circulating oil system
14. expansion chamber
15. reactor pressure relief valve
16. exit gas cyclone
17. heating/cooling coil

between the reactor wall and the circulating heat transfer oil. Heat transfer compound is caulked between the coils and the reactor wall to improve the heat transfer characteristics of this arrangement. During reactor start up the circulating oil system is used to heat the reactor wall to increase the temperature of the catalyst bed to reaction conditions. Heat is added to the oil by electrical immersion heaters installed in the circulating oil tank.

Feed gas is heated to approximately reaction temperature by flowing it through two pre-heaters. The first is a brass shell and tube heat exchanger (single pass, 1.2 ft^2) which is supplied with 100 p.s.i.g steam. The second consists of 2 heat exchangers in series (each single pass, 2 ft^2) supplied with hot oil in a circulating system similar to the reactor heating/cooling circulating oil system. Measurement and manipulation of feed flows is described in Section 2.4.2.

A nitrogen purge system, which can be operated manually or from the minicomputer, provides for emergency cooling of the catalyst bed.

Exit gas composition is measured with an on-line process gas chromatograph (Beckman Model 6700) with an analysis time of 360 seconds. The operation of the gas chromatograph is described in Section 2.3.

The catalyst is 10% nickel on silica gel. The silica gel is Davidson grade 81 with a reported size range of 70 to 297 microns. The bed depth employed for these studies is 47.6 cm.

2.3 MINICOMPUTER SYSTEM

The real-time computer facilities in the Department of Chemical

Engineering are centered around two Data General NOVA 1200 16 bit minicomputers (A and B). These minicomputers share a fixed head 0.5 Mbyte disc and are capable of direct communication via an inter-processor bus (IPB).

The peripheral devices on Minicomputer A include a high speed line printer, a teletype, a paper tape punch and a paper tape reader. Minicomputer B is interfaced to a video console and keyboard, and two 5 Mbyte discs, one of which is removable. Each minicomputer has access to 16 analog to digital (A/D) input channels which are multiplexed to a 10-bit analog to digital converter, 6 10-bit digital to analog converters, 16 relays and 16 contact sense inputs. In addition, Minicomputer B is able to transfer data directly to the University's main Control Data Corporation CDC CYBER computer. The system configuration is shown in Figure 2.2.

All user software for this study was written in a real-time extension of Data General Corporation Fortran IV. The computer facility and user software is supported by Data General's Real-Time Disc Operating System (RDOS).

2.4 DETAILS OF PROCESS INTERFACE

This section describes the process equipment and interfacing installed on the fluidized bed pilot plant for the purpose of datalogging and control implementation.

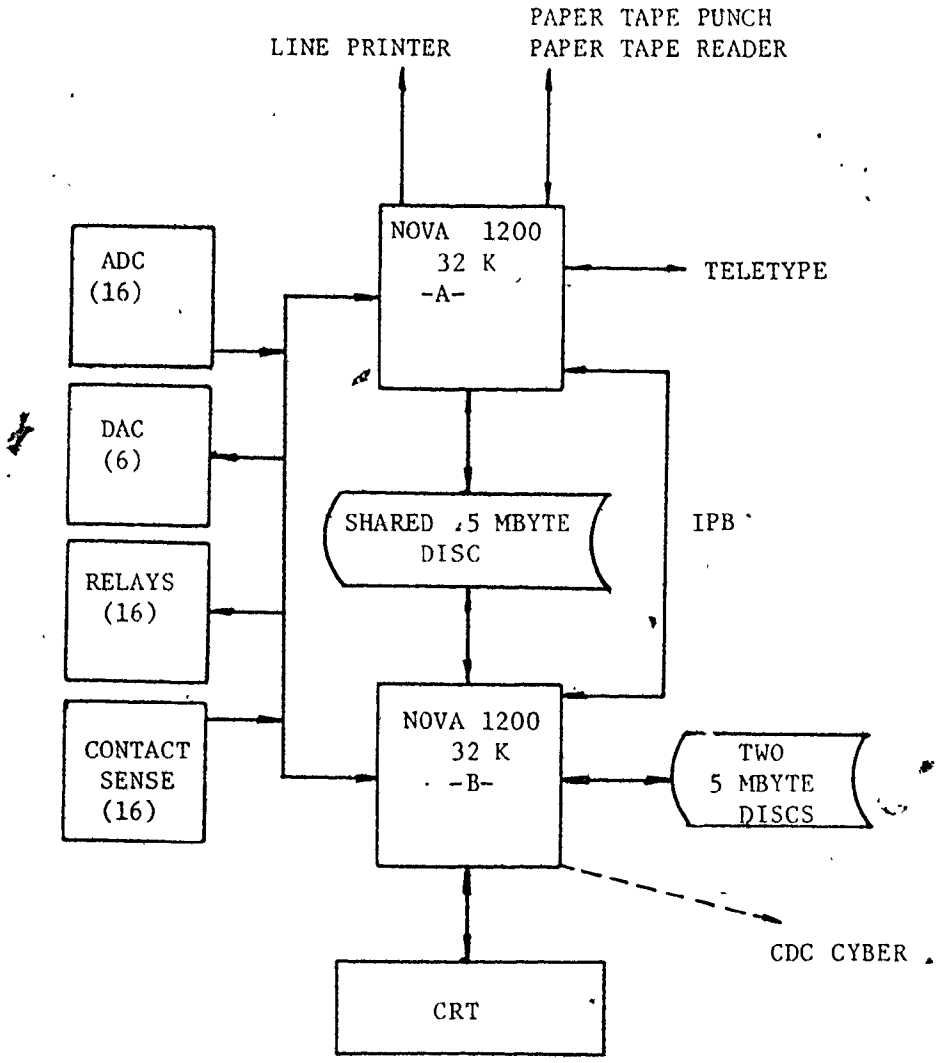

FIGURE 2.2 Configuration of Minicomputer Facility

2.4.1 Temperature measurement

A multiplexing system reduces up to 16 thermocouple signals to 2, which require amplification and transmission to A/D input channels. A block diagram of the multiplexing system is shown in Figure 2.3. The relay box contains 8, 4-pole single throw sealed reed relays. The relays are consecutively closed with voltages applied from the multiplexer. Two thermocouples are sampled when a relay is closed. The multiplexer is advanced (causing the next relay to close) by opening and closing DGDAC relay N.C. (normally closed) contacts which are connected to the multiplexer input. Input and output connections for the relay box and multiplexer are given in Appendix A2.1.

Thermocouple locations in the pilot plant flow network are shown in Figure 2.1. Thermocouple locations in the reaction chamber and at the reactor wall are given in Appendix A2.2. All thermocouples are chromel-alumel (k-type).

2.4.2 Flow Measurement and Manipulation

The primary manipulated variables for this system are the feed flowrates of n-butane and hydrogen. Rotameters provide visual indication of these flowrates at the reactor. A backpressure regulator (Fisher, Type 38L 2-7 p.s.i.g.) installed downstream of the rotameters is adjusted to 4 p.s.i.g., and maintains a constant pressure on the rotameters for calibration purposes. Orifice plates (n-butane: diam = 2.50 mm, hydrogen: diam = 2.00 mm) and pressure differential (ΔP) transmitters (Rosemount Alphaline, model C1151DPE22MBCE, 4-20 ma output)

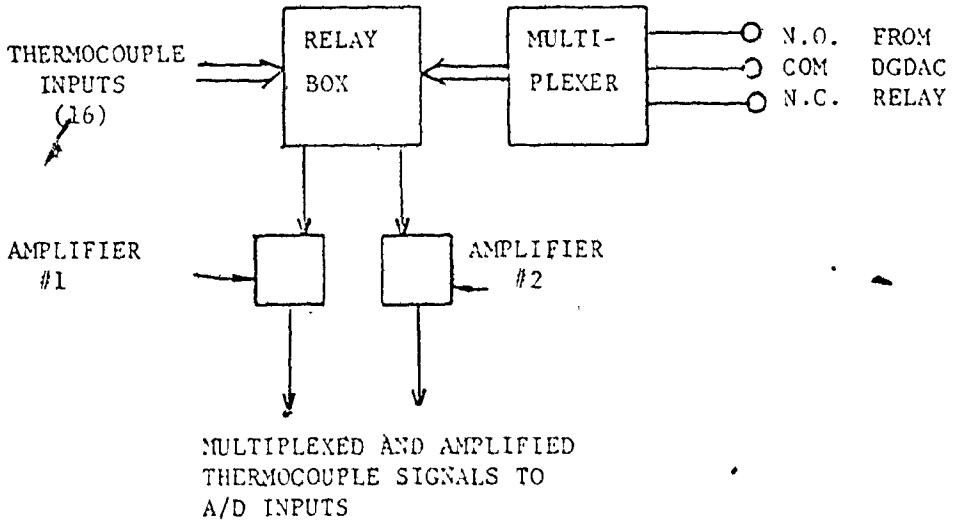

FIGURE 2.3 Block Diagram of Thermocouple Multiplexing System

are installed upstream of each rotameter and provide for computer datalogging of feed flowrates. Dropping resistors across the outputs of the ΔP transmitters produce a voltage signal for transmission to the A/D inputs. A schematic of this section of the interface is given in Appendix A2.3. Calibration procedures are described in Appendix A2.8.

Hydrogen and n-butane feedrates are manipulated with pneumatically actuated control values (Badger Meter Inc. Research valves, air to open, type TY7SS, n-butane: trim H, hydrogen: trim C). Electro-pneumatic E/P converters (Fisher Controls Co., Type 546) linearly convert control voltages to pneumatic signals which actuate the control valves. These particular E/P converters require a current

input signal in the range 2-50 ma (corresponding to a 3 - 15 p.s.i.g. pneumatic output signal to the control valve), whereas the control signal for this installation is a voltage in the range 1-9V. Therefore, voltage to current converters are required between the voltage control source and these two particular transducers. A schematic for these devices is on file with the department's electronic technician.

Two additional pneumatically actuated control valves are installed in the system. A control valve on the reactor exit line is adjusted to maintain positive pressure on the reactor to provide a sufficient driving force for chromatograph sample flow. A constant pressure in the sample line is also required for the chromatograph since its calibration is pressure dependent. Originally, reactor pressure was to be measured (a ΔP transmitter, Foxboro d/p cell, 613 DM, is in place but has not been used to date) and controlled in a feedback loop with this valve. It is recommended that this system be replaced with a backpressure regulator set at the desired reactor pressure (approximately 1-2 p.s.i.g.).

Cooling air flowrate to the heating/cooling oil heat exchanger (referred to hereafter as the air cooler) is manipulated with a pneumatically actuated control valve (Badger Meter Inc, Type TY7SS, trim G). This valve is undersized however, and does not allow sufficient air flowrate to effect the desired magnitude of changes to the circulating oil temperature. A manual bypass value across the control valve has been used to date to effect changes to the cooling rate. A larger control valve, and possibly a larger heat exchanger is required. The

E/P converters driving the exit line control valve and the air control valve have standard input 1-9V (Fisher Control Co., Type 546, 1-9V input).

A 'MANUAL/COMPUTER' switch at the bench adjacent to the reactor is used to select the source of voltage for manipulation of control valve positions. In the 'MANUAL' position, the voltage sources are 4 variable voltage supplies located at the reactor bench. When the output voltage is 1 volt, a control valve is fully closed and at 9 volts it is fully open (for air to open valves). As suggested earlier, the exit line control valve should be replaced with a backpressure regulator. This would leave the voltage source free for another use, or as backup. In the 'MANUAL' mode, manipulation of valve stem positions is possible only from the variable voltage supplies at the reactor. Reactor start-up (as described by Shaw(1)) and manual control of the reactor is convenient in this mode. In the 'COMPUTER' mode, the voltage sources are from the computer via the D/A converter output channels. The voltages to be transmitted to the E/P converters are set within the user software (in terms of computer units, 0-4095 computer units corresponds to 0-10V at the D/A output).

A contact sense function has been included in the switch to alert the computer when a change in operating mode has been made. Datalogging functions are not affected by switching the mode of operation, unless specifically programmed by the user. For instance a faster sampling rate might be required upon switching from 'MANUAL' mode, where datalogging only was occuring, to 'COMPUTER' mode, where a control loop

might be activated. To effect the change in sampling rate automatically, the user software would be required to process the contact sense signal and adjust the appropriate parameters as required.

A schematic of the interface circuitry associated with control valve manipulation is given in Appendix A2.4.

2.4.3 Description of Gas Chromatograph System

On-line measurement of exit gas composition is accomplished using a Beckman Model 6700 Gas Chromatograph. This chromatograph was previously in service on the packed bed pilot plant, in which the reaction system occurring is also the hydrogenolysis of n-butane. The chromatograph therefore, can be used with the fluidized bed reactor without major modification. However, some small modifications in hardware and operating procedure were found necessary, and these are described in this section. Component calibration is different for the two pilot plant systems, because different ranges of component compositions are expected due to the different operating conditions of the reactors. Also, the calibration procedure as described by Tremblay (2) has been simplified. To facilitate movement of the chromatograph analyzer between pilot plants, some changes have been made to the sampling network. A modification to the digital timer control circuitry in the programmer has been made to simplify user software - programmer communication. A startup procedure for on-line operation of the chromatograph is given in this section.

Finally, the adjustment procedure for the analyzer and programmer electronics has been compiled from several sources, and included in Appendix A2.9. Comments and modifications to procedure and operating conditions are included. Calibration procedure is described in this appendix.

Summarizing, this section includes descriptions of

1. modification to digital timer circuitry
2. the sampling network
3. chromatograph start-up procedure, which includes a reference to Appendix A2.9 for chromatograph adjustment and calibration procedures.

1 MODIFICATION TO DIGITAL TIMER BOARD

Previous workers on the packed bed system have used the chromatograph on-line by operating the programmer in the 'CONTINUOUS CYCLE' mode. In this mode a new cycle is begun immediately after the previous one is completed. The programmer generates interupts to alert the computer of events in the analysis cycle. At the end of an analysis cycle an interupt is generated which signals the user software to read the A/D inputs. Data handling in this manner is inconvenient since chromatograph data become available at random and unknown times. This problem has been eliminated by installing a switch in the digital timer circuitry to allow external cycle initiation control. This 'AUXILIARY MODE' switch is mounted on the right hand side of the programmer main frame. With the switch in the 'COMPUTER' position a single cylce is

initiated from the user software by opening a DGDAC relay-out normally closed contact. This signal is required from the user software every time a new cycle is to be initiated. In the 'MANUAL' position, cycle control is achieved at the programmer in the usual way. Since the analysis time is fixed (360 seconds), chromatograph data become available at regular and known intervals. Control intervals and timing within the user software can be adjusted to accommodate the chromatograph analysis time. A schematic of this modification is shown in Figure 2.4. The procedure for switching from 'MANUAL' to 'COMPUTER' operation is described in 3 steps:

1. Place the front panel 'MODE' switch to 'RESET', the 'TIMER' switch to 'OFF' and the 'SINGLE-CONTINUOUS' switch on the DIGITAL TIMER BOARD to 'SINGLE'.

2. Place the 'AUXILIARY MODE' switch to 'COMPUTER', the 'MODE' switch to 'RUN' and the 'TIMER' switch to 'ON'. (If the timer begins counting at this point indicating the start of an analysis cycle, then an open circuit exists somewhere between channel 14007 relay contacts at the DGDAC and the programmer. Check that G.C. Cable #1 is properly connected at the programmer and at the DGDAC, and that the relay channel 14007 normally closed contacts are in fact closed).

3. A single cycle is initiated within the user software by momentarily changing the status of relay output 14007. The normally closed contacts must be left open for at least 1000 ms for the programmer to recognize the change.

To switch back to cycle control from the programmer, place the 'AUXILIARY MODE' switch back to the 'MANUAL' position.

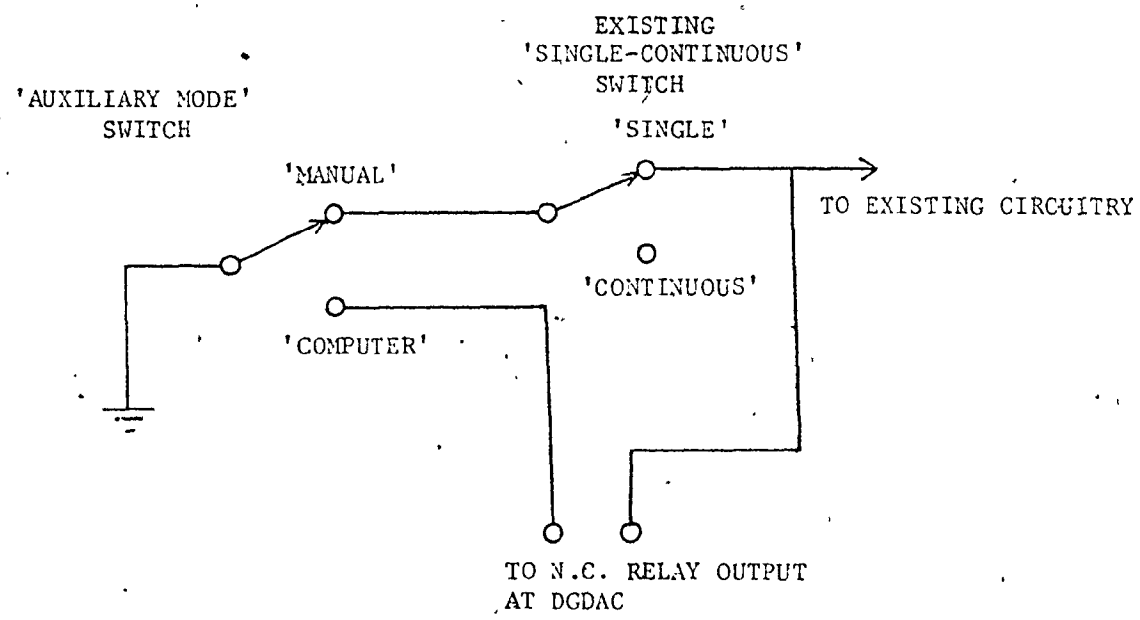

FIGURE 2.4 Schematic of Modification to Programmer (Digital Timer Board #632196)

2. SAMPLING NETWORK

A few changes were made to the chromatograph sampling network to facilitate movement of the analyzer between the fluidized bed and packed bed pilot plants. The flow controller and indicator are now mounted on the analyzer frame so that sample flowrate can be adjusted when the sample is taken from either reactor or from the calibration bomb. A flow diagram of the new arrangement is shown in Figure 2.5. To calibrate the chromatograph, it can be placed in either position I (packed bed) or II (fluidized bed). Solenoid valve A is activated and either valve B or C is opened, depending on the position of the analyzer, to allow the calibration mixture to flow to the analyzer. To sample product gas from either reactor, the analyzer is placed at the desired position and valves B and C are set to allow sample to flow to the analyzer.

3. CHROMATOGRAPH START-UP

The start-up sequence to prepare the gas chromatograph for on-line operation is as follows:

1. Place the analyzer at the desired pilot plant and connect the sample inlet line to the analyzer as shown in Figure 2.5.

2. Verify the operation and calibration of the chromatograph according to the procedure in Appendix A2.9.

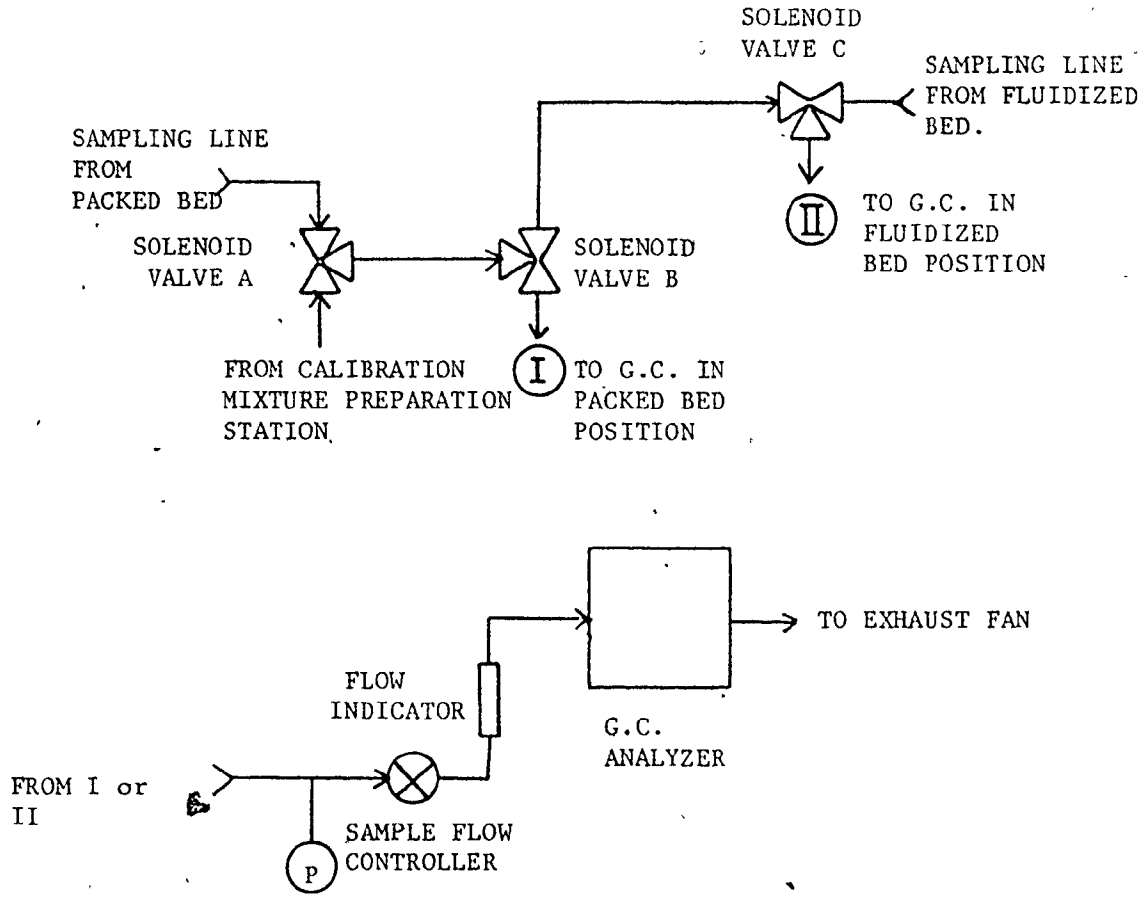

FIGURE 2.5 Flow Diagram of Chromatograph Sampling Network

3. If step 2 is satisfactory, switch valve C (for fluidized bed) or valve B (for packed bed) to allow sample mixture to flow from the reactor to the analyzer. The programmer should be in the 'COMPUTER' mode from Step 2, since verification of calibration must be performed in this mode. With the reactor at operating conditions ensure that a backpressure is placed on the reactor equal to the sample pressure used for calibration (≈ 1 p.s.i.g.) and that sample flow is adjusted to 1 cc/sec (as measured with the bubble meter) using the sample flow controller shown in Figure 2.5.

4. A single analysis cycle is initiated from user software as described above. After 360 seconds the A/D inputs for the four components are read and mole fractions calculated using the calibration equations.

CHAPTER 3

DEVELOPMENT OF THE DYNAMIC SIMULATION MODEL

3.1 INTRODUCTION

In developing a model for a system it is imperative to keep in mind what the end use of the model will be. A model which will be used primarily for process design and scale-up purposes will have greater demands put on it and will require a more sophisticated level of modelling than a model which is intended to simulate the performance of an existing system. In this latter case, the designer has more freedom in choosing the complexity of the model and the degree of empiricism used in it, since its adequacy can be checked by comparison of its predictions with plant data. When a model is to be used as an integral part of a control strategy, a question arises concerning the relationship between level of complexity of the model and quality of control attained. Many workers have pointed to the lack of adequate process models as one impediment to successful application of modern control theory(for example, Foss (3), Weekman and Lee (4)). It is generally recognized, however, that a high level of model complexity is not always required for control purposes. A model which is able to predict the dominant dynamic effects in the system will often be adequate. The question of what constitutes a major dynamic effect is not easily answered, and Foss (3) suggests that studies aimed at defining in some way the relationship between model complexity and

quality of control are required.

For this study, a dynamic model of an existing fluidized bed pilot plant is required. Initially, the model will be used to study the open loop dynamic behaviour of the reactor, and to simulate some preliminary control schemes. In future studies, it is anticipated that the model will form the basis for a linearized state space model which in combination with a Kalman filter will be used in the design of a multivariable stochastic control scheme for on-line implementation. With this latter use particularly in mind, a dynamic model for the system was developed.

Shaw (1) has evaluated extensively the performance of possible alternate steady-state fluidized bed models using data from this particular reactor. Shaw's experience suggests a suitable steady state model to form the basis for the reactor mass balance for this study. The complexity of the models examined by him varied widely in the description of the fluid mechanical behaviour of the bed. The major differences occur primarily in the descriptions of:

1. the makeup, size and mixing behaviour of the bubble, cloud and wake regions
2. the flow of solids and gas in the emulsion phase
3. the interchange of species between the bubble and emulsion gas

The models studied by Shaw are summarized in Table 3.1

The use of the Kunii and Levenspiel model was not pursued because of prohibitively long computational times. The two models of Orcutt et al are the simplest available because they assume only a

TABLE 3.1 Summary of Steady State Models Studied by Shaw

MODEL	PHASES	UPFLOW PHASE	DENSE PHASE	INTERCHANGE
Orcutt, Davidson Pigford (5)	1 Bubble 2 Emulsion	spherical bubbles, perfectly mixed with no solids, constant size	no solids mixing A) gas flow at u_{mf}, perfectly mixed (ORCMIX) B) gas flow at u_{mf}, plug flow upwards (ORCPLG)	by bubble circulation and diffusion
Partridge and Rowe (6)	1 bubble, cloud 2 Emulsion	Murray bubble model 2 dimensional measurements perfectly mixed bubble and cloud	no solids mixing gas flow at u_{mf}, plug flow upwards	empirical mass transfer coefficient calculated
Kunii and Levenspiel (7)	1 Bubble 2 Cloud, wake 3 Emulsion	Davidson bubble model, constant size with cloud and wake	solids, mixing, gas flow calculated, in plug flow, allows flow reversal	Bubble to cloud as Orcutt model. Cloud to Emulsion with Higbie Penetration model
Kato and Wen (8) KATWEN (0)	1 Bubble Cloud 2 Emulsion	growing spherical bubble and cloud Kobayashi size perfectly mixed cloud and bubble	solids mixing gas mixing in compartments no vertical gas flow	gas interchange per volume of bubble $F_o = 11/D_b$
Kato and Wen modification (Katwen(1))	same as Katwen (0) but assumes a larger cloud volume			
Kato and Wen modification (KWMIX)	no. of phases, upflow phase and interchange the same as KATWEN (0) but emulsion phase assumed to be perfectly mixed.			

bubble (pure gas) and an emulsion phase, without the complications of bubble cloud and bubble wake which contains solid particles. The Orcutt models also assume that the bubbles have a constant average size throughout the bed. Although both of these assumptions do not correspond to reality, the success of these models in predicting the performance of the fluidized bed is surprisingly good. Computationally, the perfectly mixed emulsion model of Orcutt et al is about twenty times faster than the next fastest, because the mathematical formulations involve algebraic rather than differential expressions.

Shaw's experimental program allowed him to discriminate among the possible models proposed. The field of competing models was reduced to ORCMIX, KWMIX, KATWEN (0) and KATWEN (1). The plug flow model of Orcutt et al and the Partridge and Rowe model were not included because of excessive computation times. In the final assessment of the remaining models, discrimination was achieved by calculating posterior probabilities for each model at two bed heights. The effect of uncertainty in the estimated parameters, namely the kinetic parameters, the interchange parameter and the catalyst activity, was eliminated from this discrimination method by integrating out these parameters in the calculation of the posterior probability. At a bed height of 77 cm, KATWEN (0) was found to be vastly superior to all other models considered. At a bed height of 47.6 cm, Shaw found that the KATWEN (0) model indicated the poorest performance, whereas the KWMIX model proved the best. The ORCMIX model, although not as good as KWMIX, was superior to KATWEN (0). Since the relative predictive power of each model

depended on bed height, it may be concluded that none of the models was completely adequate in describing the fluid mechanical behaviour of the fluidized bed reactor. On the other hand, all of the models predicted conversion and selectivity reasonably well over the entire range of the operating variables; certainly the trends and response were correct in all cases. It is important to note that the experimental conditions were such that the responses were about equally sensitive to the fluid mechanical and chemical kinetic aspects of the model. It should be noted also that Shaw estimated separate catalyst activity and interchange parameters from each set of experimental data for each model. Based on these observations it is judged that all of the models above would be adequate for use in control studies, particularly when the estimated parameters appropriate to the model and bed depth are used in it. Keeping in mind that the model selected will eventually be used in state space form, it is desirable to choose a model which can be written in terms of ordinary differential equations. Models which assume a perfectly mixed emulsion phase, when extended to the dynamic case, satisfy this requirement. Because of the computational simplicity of the ORCMIX model, it was chosen to form the basis for the dynamic mass balance equations for the fluidized bed reactor. It has been assumed that the pilot plant reactor will have a bed depth of about 48 cm, where the ORCMIX performance was best. Also, Shaw's parameter estimates obtained for the ORCMIX model at this bed depth should pertain.

The model equations for the entire fludized bed system, including

the reactor, the oil heater and the air cooler are developed in Section 3.2. A description of the kinetic system is given in Section 3.2.1. In Section 3.3, the development of the system equations into a modular simulation using DYNSYS is presented.

3.2 DYNAMIC MODELLING OF THE REACTOR SYSTEM

3.2.1 Kinetic System

The reaction occurring in the fluidized bed reactor is the hydrogenolysis of n-butane on a 10% nickel on silica gel catalyst. This complicated series-parallel reaction is characterized by high heats of reaction and activation energies (ca. 50 kcal/mole-^{o}K). As a result the reaction is extremely temperature sensitive.

A considerable effort has been expended by Orlickas (9,10) and Shaw (1,11) in developing mechanistic rate expressions for this reaction system, and estimating the parameters in these expressions. The result of their work is a reliable mechanistic kinetic model for the system. A summary of the development of this model is given below. Four individual reactions occur, of which three are independent:

$$n - C_4H_{10} + H_2 \xrightarrow{F'} C_3H_8 + CH_4 \qquad 3.1$$

$$n - C_4H_{10} + H_2 \xrightarrow{(1-F')} 2C_2H_6 \qquad 3.2$$

$$C_3H_8 + H_2 \longrightarrow C_2H_6 + CH_4 \qquad 3.3$$

$$C_2H_6 + H_2' \longrightarrow 2CH_4 \qquad 3.4$$

where F' is defined in Figure 3.1

The conversion of n-butane and propane directly to methane is

assumed not to occur because of the low probability of breaking two or three carbon-carbon bonds simultaneously. The hypothesized overall reaction scheme is shown in Figure 3.1. The compounds labelled C_1, C_2, C_3 and C_4 are the hydrocarbon species in the gas phase and C_1^*, C_2^*, C_3^* and C_4^* represent activated hydrocarbon species adsorbed onto the surface of the catalyst.

FIGURE 3.1 Overall Reaction Scheme for Hydrogenolysis of n-butane

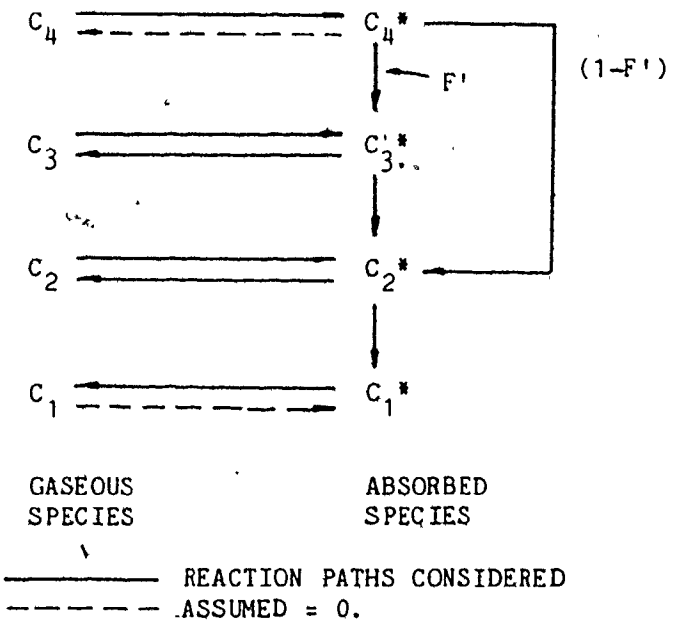

where F' = 0.9, the fraction of C_4^* that reacts to produce C_3^* and C_1^*

Normal butane is adsorbed onto the catalyst surface to form an activated species which can desorb or react to form activated propane and methane, or two activated molecules of ethane. Desorption of C_4^*,

and adsorption of C_1, are considered equal to zero in this scheme since the final rate equations which are developed consider net rates for n-butane and methane. Activated propane may desorb, with possible re-adsorption, or further react to form activated ethane. Ethane may similarly desorb, with possible re-adsorption, or react to form activated methane. The original rate expressions developed by Orlickas considered re-adsorption of ethane to be negligible. After some additional experimentation, however, Shaw found the re-adsorption of ethane to be significant, particularly at high reaction rates. The rate expressions re-derived by Shaw to include re-adsorption of ethane are given by Equations 3.5 to 3.9:

$$r_{C_4} = (\frac{k}{k_o})k_{B1} \cdot \exp(-\Delta E_B/RT)\ P_{C_4}^m\ P_{H_2}^n \qquad 3.5$$

$$r_{C_3} = F'r_{C_4} - (\frac{k}{k_o}) \cdot k_{P1} \cdot \exp(-\Delta E_{P1}/RT)P_{C_3}^{m'}\ P_{H_2}^{n'} \qquad 3.6$$

$$r_{C_2} = \frac{(2-F')r_{C_4} - r_{C_3} - (\frac{k}{k_o})K_{E2} \cdot \exp(-\Delta E_{E2}/RT)P_{C_2}^{m''}\ P_{H_2}^{n'}}{1 + K_{E1} \cdot \exp(-\Delta E_{E1}/RT)} \qquad 3.7$$

$$r_{C_1} = 4r_{C_4} - 3r_{C_3} - 2r_{C_2} \qquad 3.8$$

$$r_{H_2} = 3r_{C_4} - 2r_{C_3} - r_{C_2} \qquad 3.9$$

Literature data for similar reaction systems indicate that reaction rates are essentially first order with respect to hydrocarbon partial pressure. Therefore, the parameters m, m' and m'' are assumed equal to one. The parameters ΔE_{P1} and ΔE_{P2} are highly correlated and

difficult to estimate independently. This is also the case for ΔE_{E1} and ΔE_{E2}. For the purpose of parameter estimation therefore, it was assumed that these parameters differ by a constant amount. Two additional model equations were added into the kinetic model:

$$\Delta E_{P1} = \Delta E_{P2} - 10,000$$

$$\Delta E_{E2} = \Delta E_{E1} - 10,000$$

The remaining parameters to be estimated were

$$K_{B1},\ \Delta E_{B},\ n,\ K_{P1},\ K_{P2},\ n',\ K_{E2},\ K_{E1},\ n''$$

Catalyst activity k/k_o was assigned a value of 1.0. The parameters were estimated from integral data from a lab scale tubular fixed bed reactor, using catalyst from the fluidized bed. The final parameter estimates are reported in Shaw's Ph.D. thesis (1).

3.2.2 Reactor mass/energy balances

The two phase model proposed by Orcutt et al, in which the emulsion phase is perfectly mixed, is based on the following assumptions:

1. Gas flows up the reactor in separate bubble and emulsion phases. The bubble cloud and emulsion phase are at the same concentration.

2. All gas in excess of that required for minimum fluidization flows as bubbles
3. There is no catalyst in the bubble phase, i.e., reaction occurs only in the emulsion phase. Spherical bubbles of uniform average size move upward at bubble rise velocity, u_b.
4. Radial concentration is uniform in the bubble phase.
5. The system is completely isothermal
6. The bubbles do not break up or coalesce as they move up the bed
7. Interchange of gas between the bubble and emulsion phase occurs at a uniform rate over the bed height
8. The emulsion phase is perfectly mixed with partial pressure of any component, Pe, $Pe \neq f(\text{height})$
9. The bubble phase is perfectly mixed at any height with partial pressure of any component, Pb, $Pb = f(\text{height})$

This two phase representation is shown in Figure 3.2.

MASS BALANCE

For any component in the entire emulsion phase, taken across the entire bed

Rate of accumulation	=	Mass transfer to emulsion phase from feed by bulk flow	+	mass transfer from bubbles by diffusion and circulating flow
	-	mass transfer to bubbles by diffusion and circulating flow	-	rate of disappearance by reaction

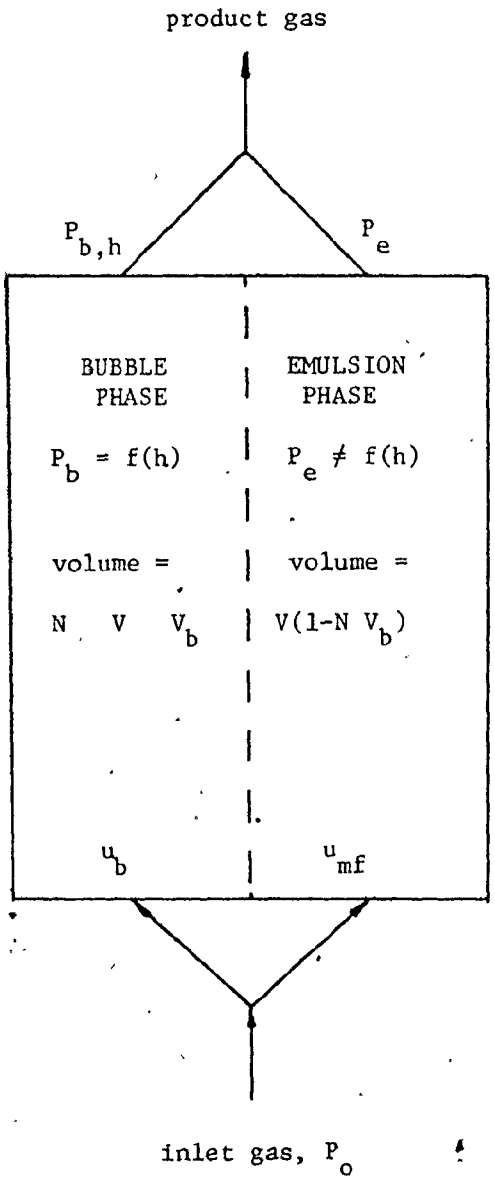

FIGURE 3.2 Two-phase representation of fluidized bed reactor.

$$V_e \frac{dC_e}{dt} = u_{mf} S(C_o - C_e) + NQ \int_0^H C_b S \, dy$$

$$- NQSH\, Ce - r_v V_e \qquad 3.10$$

An expression for C_b as a function of height is found by solving the material balance on the bubble phase. Consider a simple bubble rising up through the bed:

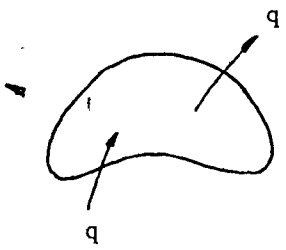

where q represents the volumetric inflow and outflow of gas to and from the bubble (cm^3/sec).

A material balance on the bubble is written as

$$V_b \frac{dC_b}{dt} = (q + k_G S)(C_e - C_b)$$

$$\text{B.C.: } C_b = C_o \text{ at } t = 0 \qquad 3.11$$

The term $k_G S(C_e - C_b)$ represents the rate of mass transfer between the bubble and emulsion phases by molecular diffusion. Define a new quantity, Q, the transfer rate from a bubble:

$$Q \equiv q + k_G S$$

Also since $u_b = \frac{y}{t}$,

$$dt = \frac{dy}{u_b} \qquad 3.13$$

Substituting Equations 3.12 and 3.13 into 3.11 yields

$$V_b\, u_b \frac{dC_b}{dy} = Q(C_e - C_b)$$

$$\text{B.C.:}\quad C_b = C_o \text{ at } y = 0 \qquad 3.14$$

Equation 3.14 is separable since V_b, u_b, C_e, q, K_G and S are assumed to be independent of height. Integration of Equation 3.14 from y = o to y = y gives the desired expression for C_b as a function of height:

$$C_b = C_e + (C_o - C_e)\exp(-Qy/u_b\, V_b) \qquad 3.15$$

Substituting Equation 3.15 into Equation 3.10 and performing the integration gives the result, after rearrangement:

$$V_e \frac{dC_e}{dt} = S(C_o - C_e)(u_{mf} + Nu_b\, V_b\{1 - \exp[-\frac{QH}{u_b V_b}]\})$$

$$-r_v\, V_e \qquad 3.16$$

Using $V_e = V(1 - N\, V_b)$ and H = V/S, Equation 3.16 becomes

$$H(1 - N\ V_b)\frac{dC_e}{dt} = (C_o - C_e)(u_{mf} + Nu_b\ V_b\ \{1 - \exp[-\frac{QH}{u_b V_b}]\}) - H(1 - N\ V_b)r_v \qquad 3.17$$

Substituting H for y in Equation 3.15, gives an expression for the exit concentration of the bubble phase:

$$C_{b,H} = C_e + (C_o - C_e)\ \exp(-QH/u_b\ V_b) \qquad 3.18$$

Equations 3.17 and 3.18 are solved simultaneously for each component, and knowing the division of flow into each phase, the reactor exit concentration is calculated.

Several empirical correlations are available from the literature (see Shaw et al (12)) for predicting certain physical phenomena in the bed:

1. bubble diameter as a function of height

$$D_b = 0.14\ \rho_p d_p y\ (\frac{u}{u_{mf}}) + [6(\frac{u - u_{mf}}{n_o \pi})]^{0.4}\ g^{-0.2} \qquad 3.19$$

The second term on the right side of Equation 3.19 gives the initial bubble size from a perforated plate with hole concentration n_o cm^{-2}. Observation from the top of the fluidized bed at operating conditions indicated a maximum bubble diameter at the top of the bed of no greater than 10 cm. The Orcutt model makes the simplification that bubble size is constant over the bed height. Bubble diameter as a function of height was calculated using Equation 3.19 until the maximum bubble diameter

was reached. Thereafter the bubble diameter was maintained constant. An integrated average bubble size was then calculated for use with the Orcutt model.

2. Q, interchange rate between bubble and emulsion phase

$$Q = \frac{0.11}{D_b} \cdot V_b \qquad 3.20$$

3. u_b, bubble rise velocity

$$u_b = 0.711 (g D_b)^{1/2} + (u - u_{mf}) \qquad 3.21$$

Enthalpy balances on reactor contents

Enthalpy balances on the gas present in the bed, which includes gas in the bubble and emulsion phases, and the solid catalyst, are written separately.

For the gas,

Accumulation = Net input of enthalpy from inlet flow + input of heat from reactor wall + input of heat from catalyst pellets

$$\varepsilon V \bar{\rho}_g \bar{C}_{pg} \frac{dT_R}{dt} = v_o \bar{C}_{pg} \bar{\rho}_g (T_o - T_R) + h_w A_w (T_w - T_R) + h_a w (T_p - T_R) \qquad 3.22$$

where $v_o \bar{C}_{pg} \bar{\rho}_g = \sum_{\substack{comp \\ i}} F_i C_{pi}$

Under assumption #5 above, the last term in Equation 3.22 disappears.

For the solid catalyst

Accumulation = input of heat from gas + heat generation due to reaction

$$W C_{pB} \frac{dT_p}{dt} = h_a w (T_R - T_p) + \sum_{j=1}^{r} R_j \overline{\Delta H}_j W \qquad 3.23$$

where r = number of reactions where heat is generated

Note that again the first term on the right side of Equation 3.23 disappears ($T_p = T_R$ from assumption #5). Combining Equations 3.22 and 3.23 yields

$$(W C_{pB} + \varepsilon V \bar{\rho}_g \bar{C}_{pg}) \frac{dT_R}{dt} = v_o \bar{C}_{pg} \bar{\rho}_g (T_o - T_R) + h_w A_w (T_w - T_R) + \sum_{j=1}^{r} R_j \overline{\Delta H}_j W \qquad 3.24$$

It is further assumed that the molal average heat capacity and density of the reaction gas mixture and feed are equal.

The second term on the left side of Equation 3.24 is small compared to the first term and can be neglected, leaving

$$W C_{pB} \frac{dT_R}{dt} = v_o \bar{C}_{pg} \bar{\rho}_g (T_o - T_R) + h_w A_w (T_w - T_R) + \sum_{j=1}^{r} R_j \overline{\Delta H}_j W \qquad 3.25$$

Equation 3.25 is the final form of the enthalpy balance on the reactor contents.

Enthalpy balance on wall

The wall, cooling coils and supporting structures in thermal contact with the wall all have significant mass; thus they were judged to affect significantly the dynamic response of the reactor temperature to changes in oil temperature. As a simplification, all of these elements were assumed to be at a uniform temperature over the bed height and are referrred to here as the wall. To describe the thermal dynamics of the wall, the enthalpy balance is written as

$$m_w C_{pw} \frac{dT_w}{dt} = h_w A_w (T_R - T_w) + h_c A_c (T_{oil} - T_w) \qquad 3.26$$

Note that an effective mass and heat capacity of the wall is used. Also, heat loss from the wall is assumed negligible.

Heating/cooling coil enthalpy balance

The mass of oil in the heating/cooling coil is much less than the

mass of the wall. It is assumed therefore that the average oil temperature in the coil is at pseudo-steady state with respect to the wall temperature. That is, at any instant, the oil temperature is determined by the temperature of the wall. If it is assumed that the thermal capacity of the wall is much larger than that of the oil, the instantaneous outlet oil temperature may be calculated from the effectiveness factor of a heat exchanger with constant heat source temperature. The effectiveness factor in this case is defined as

$$\varepsilon = \frac{1 - \exp[-(NTU)(1-R)]}{1 - R \exp[-NTU(1-R)]} \qquad 3.27$$

where,

$$R = \frac{(w\, C_p)_{oil}}{m_w\, C_{pw}} \simeq 0$$

and $$NTU = \frac{h_c A_c}{(wC_p)_{oil}}$$

also, $$\varepsilon = \frac{T_{oil,\,out} - T_{oil,in}}{T_w - T_{oil,in}} \qquad 3.28$$

Knowing T_w and $T_{oil,in}$, Equations 3.27 and 3.28 are combined to eliminate ε and to calculate $T_{oil,out}$. The mean bulk temperature of oil in the heating/cooling coil is taken as the arithmetic average of the oil inlet and outlet temperatures:

$$T_{oil} = T_{oil,in} + \frac{(T_{oil,out} - T_{oil,in})}{2} \qquad 3.29$$

3.2.3 Pseudo steady-state assumption on mass balance

For most solid catalysed gas reactions, the ratio of the concentration wave velocity to the thermal wave velocity is large. A disturbance in reactant concentration produces initially a rapid dynamic response in product concentration. After this initial response is complete, product concentrations begin to drift slowly, following directly the slower thermal dynamics of the solid catalyst. This latter effect is a result of product concentrations being coupled directly to reaction temperature through the temperature dependent terms in the rate expressions. The time constant of the mass balance Equation 3.17 is in the order of magnitude of 10 seconds, while the time constant of the reactor contents enthalpy balance Equation 2.25 is around 500 seconds. Therefore, a pseudo steady-state assumption is made on the concentration dynamic response by equating the left hand side of Equation 3.17 to zero, leaving

$$(C_o - C_e)(u_{mf} + Nu_b V_b \{1 - \exp[\frac{-QH}{u_b V_b}]\}) = H(1 - N V_b)r_v \qquad 3.30$$

Equations 3.30 and 3.18 are solved simultaneously for each component, but now the calculation is strictly algebraic (steady state).

3.2.4 Reaction Rates and Heats of Reaction

The rate expressions, Equations 3.5 to 3.9, provide net rates of reaction of chemical species. The catalyst bed enthalpy balance Equation 3.25 requires rates of reactions expressed in terms of the rate

of the hydrocarbon reacting. The following conversion is required. Equations 3.1 and 3.2 are rewritten respectively, as

$$F' C_4H_{10} + F'H_2 \longrightarrow F'C_3H_8 + F'CH_4 \qquad 3.31$$

$$(1-F')C_4H_{10} + (1-F')H_2 \longrightarrow 2(1-F')C_2H_6 \qquad 3.32$$

These are added to give

$$C_4H_{10} + H_2 \longrightarrow F'C_3H_8 + 2(1-F')C_2H_6 + F'CH_4 \qquad 3.33$$

Equations 3.3, 3.4 and 3.33 are three heat producing reactions for which heats of reaction will be calculated; thus r=3 in Equation 3.25. The rates of reactions of Equations 3.3, 3.4 and 3.33 are found as follows. The net rates of reactions for three independent species, n-butane, propane and ethane are calculated using Equations 3.5, 3.6 and 3.7 respectively. Using the notation of Shaw, these are

RB = net rate of reaction of n-butane

RP2 = net rate of reaction of propane

RE2 = net rate of reaction of ethane

Units: g moles/unit volume emulsion phase-sec

The net rate of reaction of n-butane, RB, gives directly the rate of the reaction summarized by Equation 3.33. Propane, however is formed by Equation 3.33 and depleted by Equation 3.3:

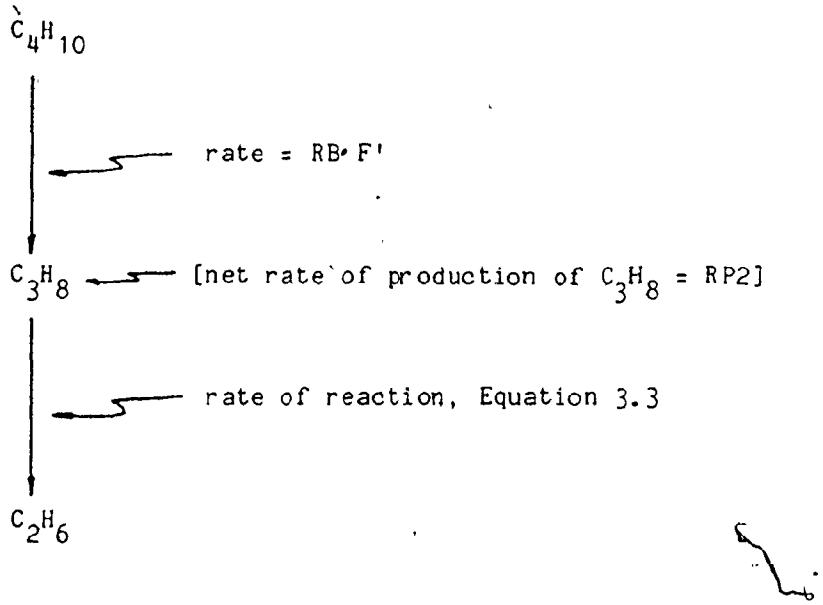

Define the rate of reaction of Equation 3.3, RP (g moles propane reacted/unit volume·emulsion phase–sec).

$$RP = (RB \cdot F') - RP2 \qquad 3.34$$

Similarly, for ethane

$$RE = RP + 2(1-F')RB - RE2 \qquad 3.35$$

where RE = rate of reaction, Equation 3.4 (g moles ethane reacted/unit volume emulsion phase sec).

Summarizing, the rates of reaction for reactions expressed by Equations 3.3, 3.4 and 3.33 are given by RP, RE and RB, respectively.

These rates are expressed as g moles hydrocarbon reacted/unit volume emulsion phase–sec. Equation 3.25 requires rates in units

g moles/g catalyst-sec. Each of the rates RB, RP and RE are multiplied by $1/\rho_s(1 - \varepsilon_{mf})$, to achieve the required conversion.

Heats of reaction for Equations 3.3, 3.4 and 3.33 are calculated using heats of formation of the product and reactant species, evaluated from polynomial expressions in temperature as given by Kjaer (13).

3.2.5 Circulating Oil Heating Tank and Air Cooler

Circulating Oil Heating Tank

Assuming negligible heat loss and perfect mixing, an enthalpy balance on the circulating oil heating tank is written:

$$\rho_{oil} V_{tank} \frac{dT_{tank}}{dt} = w_{oil} C_{p_{oil}} (T_{oil} - T_{tank}) + Q_e \qquad 3.36$$

The heat input to the tank from electrical immersion heaters in continuously variable from 0 to 2031 cal/sec.

Air Cooler

Since air at 20°C is used as the cooling medium in this heat exchanger, a large temperature driving force exists between this air and the oil entering the exchanger (= 250°C). It is expected that the time constant of the oil outlet temperature response to changes in air flowrate is small compared to the time constant of the reactor wall and therefore the dynamic response of the oil in the heat exchanger is ignored. A steady state model based on effectiveness factor is written. An effectiveness factor in this case is defined

$$\varepsilon = \frac{T_{air,out} - T_{air,in}}{T_{tank} - T_{air,in}} \qquad 3.37$$

which, for a countercurrent exchanger is given by Equation 3.27

$$\varepsilon = \frac{1 - \exp[-(NTU)(1 - R)]}{1 - R \exp[-NTU(1 - R)]} \qquad 3.27$$

where

$$R = \frac{(w\ C_p)_{air}}{(w\ C_p)_{oil}}$$

$$NTU = \frac{UA}{(w\ C_p)_{air}}$$

An enthalpy balance around the heat exchanger is written

$$(w\ C_p)_{oil}\ (T_{tank} - T_{oil,in}) = (w\ C_p)_{air}\ (T_{air,out} - T_{air,in}) \qquad 3.38$$

Using the definition of R above, this becomes, after rearrangement,

$$T_{oil,in} = T_{tank} - R(T_{air,out} - T_{air,in}) \qquad 3.39$$

The effectiveness factor ε is first calculated using Equation 3.27. This is used in Equation 3.37, knowing $T_{air,in}$ and T_{tank}, to give $T_{air,out}$. Equation 3.39 then gives $T_{oil,in}$, the temperature of the oil exiting the air cooler and entering the reactor heating/cooling coil.

3.3 DEVELOPMENT OF THE DYNSYS SIMULATION

In the previous sections the mass and energy balances for the

reactor, oil heater and air cooler were developed. In Section 3.3.1 these equations are programmed into the framework of DYNSYS modules. DYNSYS is an executive system which has been developed by Bobrow (14) to allow convenient dynamic simulation of chemical processes using a modular approach. Each processing unit requires a dynamic or steady state model, which forms the basis for a DYNSYS module. Dynamic modules must be written in terms of first order ordinary differential equations. A third order predictor corrector routine within DYNSYS, based on the Adams-Moulton-Shell formulations, is used to integrate the differential equations in all modules simultaneously. The Fortran programming of modules must conform to the particular requirements of the predictor-corrector integration method and to the overall organization of the modular approach to integration of the system equations adopted by DYNSYS. In the following sections it is assumed that the reader is familiar with programming of modules within the DYNSYS environment, and with computational procedures of the DYNSYS executive main program and subroutines. As reference, the reader is referred to Bobrow (14).

After some experience with testing of the modules it was decided that closed-loop simulation would not be convenient if the controller was programmed into a DYNSYS module and executed as part of a complete DYNSYS simulation. Furthermore, inlet stream variables which are forced externally (of the overall simulation) to change with time, cannot be programmed conveniently with the existing DYNSYS stream structure, without creating additional modules. Therefore, for this simulation study, the control function, including definition of inputs, setpoint

changes and load disturbances etc, was performed in a program external to DYNSYS. The DYNSYS executive main program was restructured into a subroutine, Model1. When provided with updated inputs, Model1 integrates the appropriate modules over one time interval and returns the one step ahead predictions of the system outputs to the calling program. Subroutine Model1 and a description of its use in a closed loop simulation, is described in Section 3.3.2.

3.3.1 System Modules: REAC01, OILHEAT, AIRCOOL

The fluidized bed reactor system consists of 3 processing units, for which the following modules have been written:

1. REAC01 - the reactor, including the wall and heating/cooling coil
2. OILHEAT - the circulating oil heating tank
3. AIRCOOL - the air cooler in the circulating oil system

An information flow diagram for the system is shown in Figure 3.3. All units which operate at a constant level, such as pumps and the feedpreheater need not be included in the information flow diagram. Each of the units in Figure 3.3 is described separately below.

The stream list has been defined as:

1. Stream number
2. Flag
3. Total flow (g/sec)

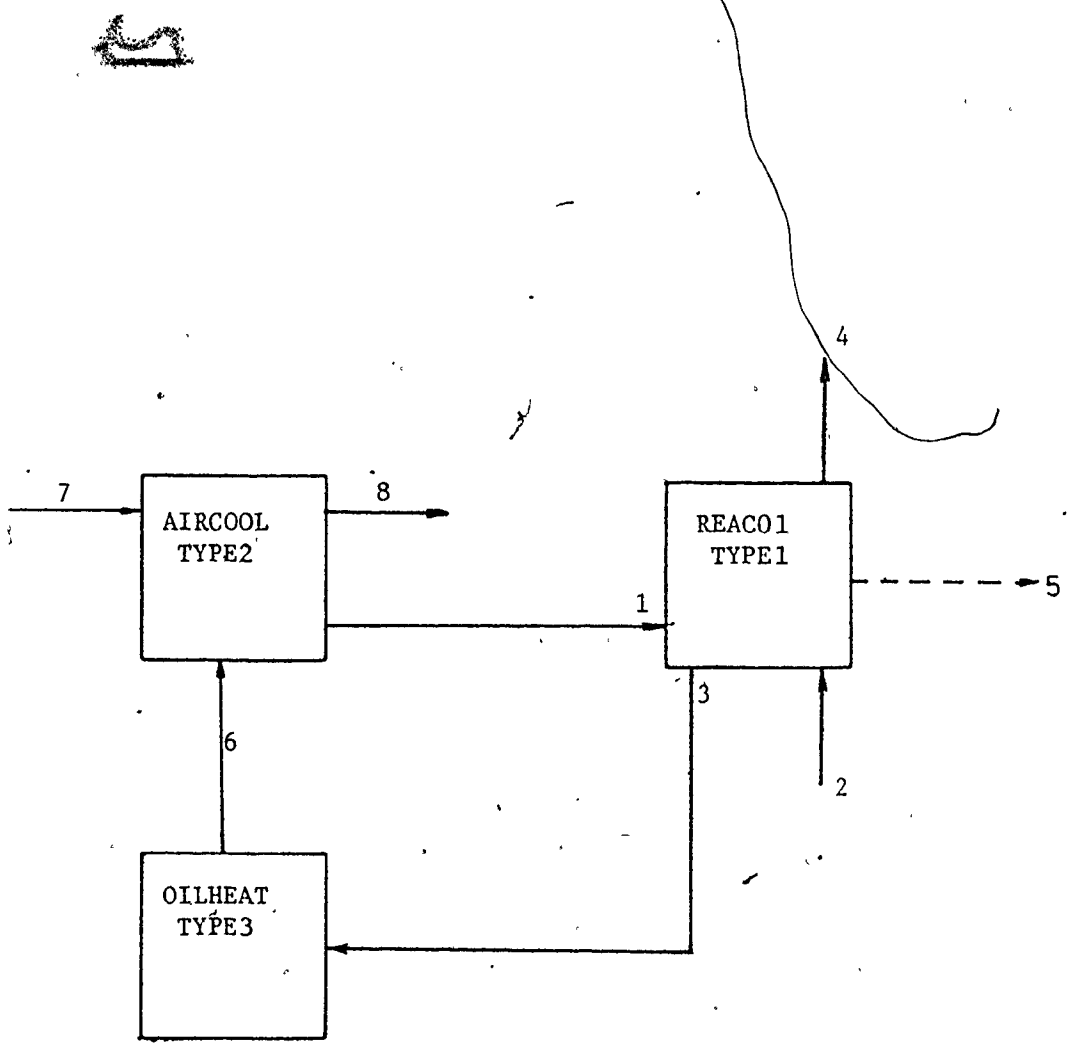

Streams
1 oil inlet to reactor heating/cooling coil
2 reactor feed
3 oil exiting reactor heating/cooling coil
4 reactor product gas
5 reactor information stream
6 oil line between oil heating tank and air cooler
7 cooling air to air cooler
8 exhaust air from air cooler

FIGURE 3.3 Information Flow Diagram for DYNSYS Simulation

4. Temperature (^{o}C)
5. Pressure (atm)
6. CH_4 flowrate
7. C_2H_6 flowrate
8. C_3H_8 flowrate
9. C_4H_{10} flowrate
10. H_2 flowrate
11. Circulating oil flowrate
12. Air flowrate

flowrates in g/sec.

REAC01 - TYPE 1

The reactor module consists of four separate mathematical descriptions, two which are differential and two which are algebraic:

1. algebraic equation describing the pseudo-steady state reactor mass balances (Equation 3.30)
2. differential equation describing temperature dynamics of reactor contents (Equation 3.25)
3. differential equation describing temperature dynamics of wall (Equation 3.26)
4. algebraic equations describing enthalpy balance on oil in heating/cooling coil (Equations 3.27 to 3.29)

The sequence of solution of these components within the module is shown with a flowchart in Figure 3.4.

A solution to the steady state mass balance based on the

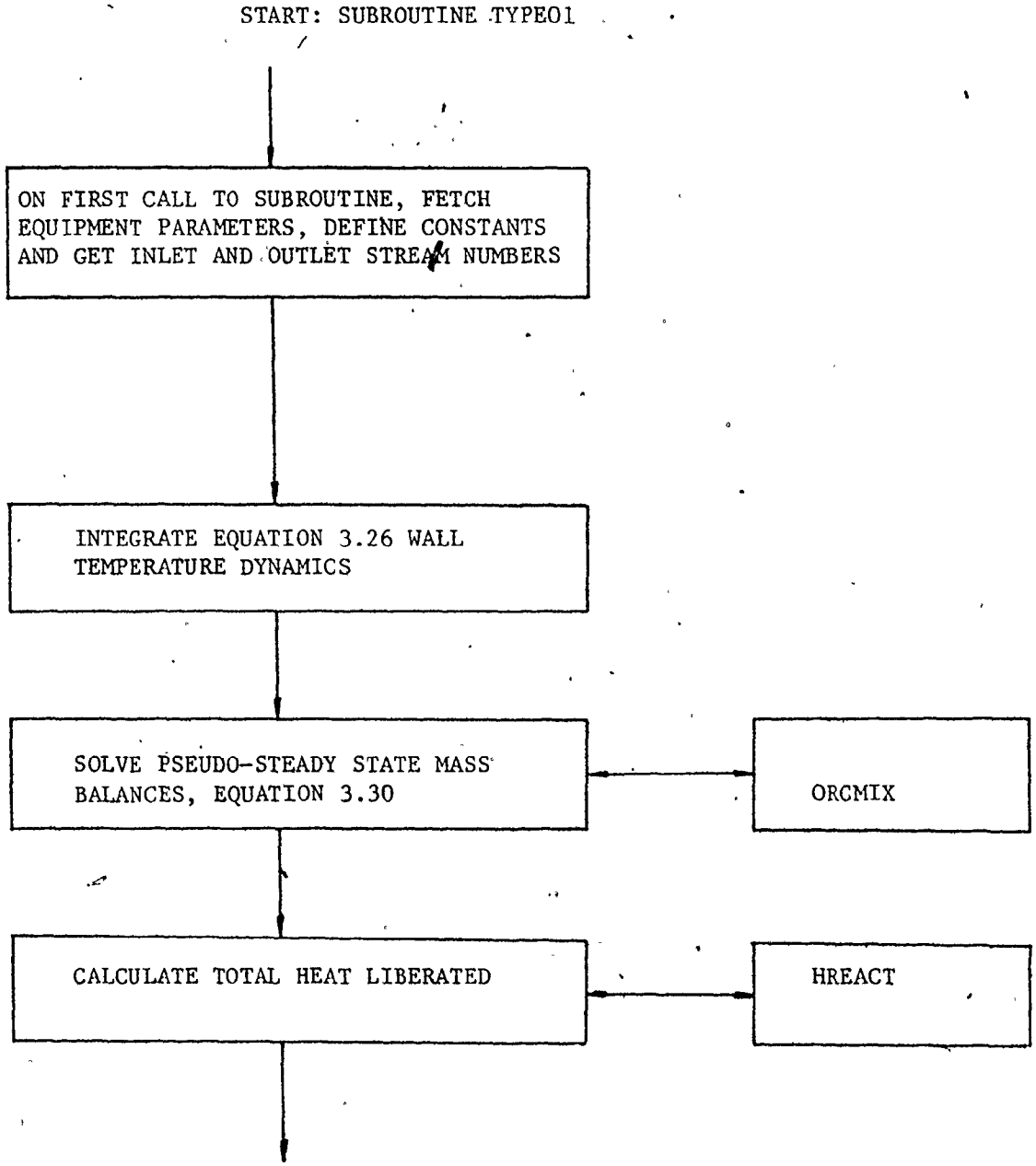

FIGURE 3.4 Flowchart of Subroutine TYPE1 (REAC01)

Figure 3.4 (cont'd)

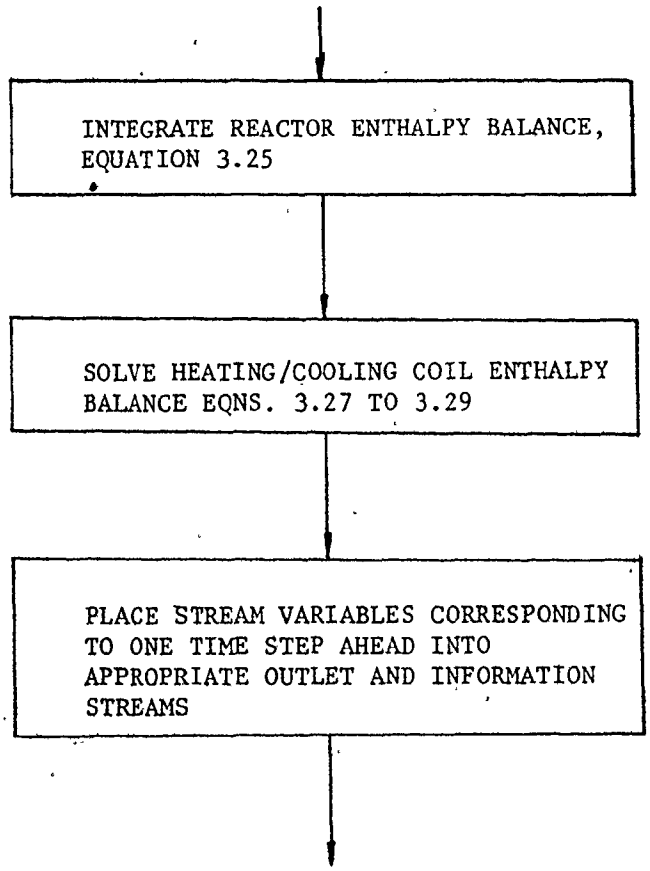

perfectly mixed emulsion phase model of Orcutt et al, is provided by Shaw(1) in the form of Fortran subroutine ORCMIX. This subroutine incorporates the reaction rate expressions Equations 3.5 to 3.9 and solves the (pseudo) steady state mass balance Equation 3.30 for each component. The calling argument for ORCMIX is defined as follows:

SUBROUTINE ORCMIX (CACT, FEED, FLOW, T, OUT, RB, RP2, RE2, S1, S2, S3, CONV)

inputs: CACT: catalyst activity (dimensionless)

FEED(I): inlet partial pressure of component I, atm

I=1 methane

2 ethane

3 propane

4 n-butane

5 hydrogen

FLOW; total volumetric feedrate to reactor, a.c.f.m.

T : reaction temperature °F

outputs:

OUT(I), outlet partial pressure of component I, atm

I defined as in FEED(I)

RB reaction rate of n-butane, propane

RP2 and ethane respectively

RE2 (g moles/unit volume emulsion phase-sec)

S1	outlet selectivities of methane,
S2	ethane and propane, respectively
S3	(g moles component produced/g moles n-butane reacted)
CONV	conversion of n-butane

Outlet partial pressures, selectivities and conversion returned from ORCMIX, refer to the product gas as it leaves the catalyst bed. As described in Section 3.2.4 the reaction rates of individual species given by RB, RP2 and RE2 require conversion to rates in terms of heat producing reactions, (Equations 3.3, 3.4 and 3.33) for use in the reactor enthalpy balance. The conversion is made on return from ORCMIX. Heats of reaction are calculated in subroutine HREACT:

SUBROUTINE HREACT (TREACT, HEAT)

input : TREACT, reaction temperature, ^{o}C

output: HEAT(I), heat of reaction for

I=1 Equation 3.33

I=2 Equation 3.3

I=3 Equation 3.4

(cal/g mole hydrocarbon reacted)

The parameters in the polynomials for the heat of formation variation with temperature for each component are placed in the data set immediately after the DYNSYS input data.

Listings of subroutines TYPE 1 (REAC01), ORCMIX and HREACT are

given in Appendix A 3.1. Equipment and extra list definitions are given below.

Equipment List:

EP(IM, 1)* : W_B = 7000 g.

EP(IM, 2)# : k/k_o = 1.87 (dimensionless)

EP(IM, 3)# : $h_w A_w$ = 21.41 cal/sec-^oC

EP(IM, 4)# : $h_c A_c$ = 17.36 cal/sec-^oC

EP(IM, 5)# : Q_L' = .0165 ^oC/sec (see Equation 4.4)

Extra List:

EX(1)# : $m_w C_{pw}$ = 3000 cal/^oC

EX(2) : $\bar{C}_{pg}$ = 0.64 cal/g - ^oC

EX(3) : C_{pB} = 0.25 cal/g - ^oC

EX(4) : MPRINT = 0 bypass printing in module

≠ 0 print module information not available in outlet stream lists.

EX(5) : IPASS = 0 bypass ORCMIX and calculations within module involving chemical reaction

≠ 0 proceed through module normally

---

* from direct measurement of catalyst mass; catalyst was removed from reactor for weighing, bed height = 47.6 cm

\# the numerical values reported here are a result of the parameter estimation from Chapter 4.

The parameter IPASS was included into the module to bypass ORCMIX and calculations involving chemical reaction. In Chapter 4, some parameter estimates for the enthalpy balance equations were obtained using dynamic temperature data collected under non-reaction conditions, i.e., hydrogen, but no butane was flowing into the bed. Computational difficulties within subroutines ORCMIX occur if the partial pressure of butane in the feed is zero, so this calculation and others involving chemical reaction were bypassed for these data.

OILHEAT: TYPE 3

The dynamics of the oil heater are described by the differential equation, Equation 3.36. The module has one inlet stream and one outlet stream. The inlet stream to the module is the oil line exiting the reactor heating/cooling coil and the outlet stream is the exit line of the heating tank. The stream list is defined as before, but only the positions for total flow and oil flowrate are used with this module. The equipment list is defined as follows:

EP(IM,1) : $C_{p,oil}$ = .78 cal/g-^{o}C

EP(IM,2) : $\rho_{oil} V_{tank}$ = 31,400 g

EP(IM,3) :+ Q_e = 2031 cal/sec

EP(IM,4) :* Q_L = 0 cal/sec (see Equation 4.1)

EP(IM,5) :* w_{oil} = 565.7 g/sec

+ the heat input from electrical heaters is continuously variable from 0 to 2031 cal/sec

* numerical values reported here are the result of parameter estimation from Chapter 4.

A listing of OILHEAT is given in Appendix A3.2.

AIRCOOL TYPE 2

The air cooler module is an algebraic one described by Equations 3.37 to 3.39. A listing of the module is given in Appendix A3.3. Algebraic modules should be executed after dynamic modules in the calculation order list. It is sufficient, therefore to program the module to operate on predicted stream variables, i.e., those stored in S(IG, -, -), IG = 1. The equipment list for the module is defined:

EP(IM,1): UA#

EP(IM,2): $C_{p_{air}}$ = .238 cal/g-°C

EP(IM,3): $C_{p_{oil}}$ = 0.78 cal/g-°C

3.3.2 Open and Closed Loop Simulations using Subroutine Model1

For the purpose of simulating the open and closed behaviour of the reactor, it was assumed that the temperature of the oil entering the reactor heating/cooling coil was freely adjustable as an input to the reactor. The manipulation of oil inlet temperature is accomplished in the physical system by adjusting the cooling air flowrate to the air cooler. The air cooler could not be included in the simulation at this point however, because an estimate of the overall heat transfer coefficient was not available. Manipulation of the oil inlet

an estimate of this parameter is not available, see Section 3.3.2

temperature in the simulation is performed asssuming that the same adjustment would be possible by manipulating air flowrate to the air cooler.

To facilitate open and closed loop testing on the reactor module REAC01, the DYNSYS executive main program was restructured into a subroutine, MODEL1. Given input information at the current time t_n, and one time-step ahead t_{n+1},# MODEL1 directs integration of REAC01 over the time interval t_n to t_{n+1}. A calling program, provided by the user, defines all inputs and controller functions, and calls MODEL1 when the dynamic response of the reactor over one time interval is required. The calling argument of MODEL1 is defined below.

SUBROUTINE MODEL1 (TR1, TW1, TOIL1, TFEED1, TFEED2, TOILIN1, TOILIN2, H2SCFM1, H2SCFM2, C4SCFM1, C4SCFM2, TRP, TWP, TOILP)

inputs TR1, TW1, TOIL1 : initial values of T_R, T_w, and T_{oil}, respectively (^oC). These require definition for the first call to MODEL1 only.

The remaining inputs require definition on each call to MODEL1:

The accuracy of integration using a predictor-corrector method is increased if inputs at t_{n+1} are available, when integrating from t_n to t_{n+1}. If inputs at t_{n+1} are not available, they must be set equal to the corresponding t_n inputs.

TFEED2, TFEED1 : feed temperature at times t_n and t_{n+1} respectively (^oC)

TOILIN2, TOILIN1: oil inlet temperature at times t_n and t_{n+1} respectively (^oC)

H2SCFM2, H2SCFM1: volumetric feedrate of hydrogen at times t_n and t_{n+1} respectively (scfm)

C4SCFM2, C4SCFM1: Volumetric feedrate of n-butane at times t_n and t_{n+1} respectively (scfm)

outputs returned to the calling program at the completion of the integration step

TRP, TWP, TOILP; t_{n+1} predictions of T_R, T_w and T_{oil} respectively (^oC)

S1, S2, S3, CONV: t_{n+1} predictions of selectivities of methane, ethane and propane respectively, and conversion of n-butane

-these are put into COMMON/PRED/

In the calling program, it is convenient to create vectors#, the elements of which define in advance the desired conditions at each time step of the simulation. For instance, consider an open loop test in which a step increase to the butane feedrate is required at a specified time. The number of integration steps for the simulation is defined in

---

If a particular feedstream input is constant over the simulation time period then the first two inputs at t_0 and t_1 need only be defined, as stream updating in MODEL1 (as is performed normally in the DYNSYS executive) will maintain these inputs constant.

the calling program and a vector, the length corresponding to this number is created for each of the inputs listed in the calling argument of MODEL1. The vector of n-butane feedrates contains a step increase at the desired time. MODEL1 is called the specified number of times, applying the t_n and t_{n+1} inputs at each time step.

For a closed loop simulation, the control calculation is performed immediately after return from MODEL1. The controller adjusts the manipulated input to be applied on the next call to MODEL1. A typical flowchart of a calling program for a closed loop simulation is shown in Figure 3.5.

As an example, a main program which implements PI control of reaction temperature T_R using the ratio of hydrogen-to-n-butane feedrates as manipulated variable, is given in Appendix A2.4. Setpoint changes to the reaction temperature are made at specified times over the integration period. The input data set for this particular simulation is also appended. In creating the load file for this simulation the following are required:

Program ABC – the calling program provided by the user

Subroutines: MODEL1, TYPE 1(REACO1), ORCMIX, HREACT

The DYNSYS subroutines:

DYN1, DYN2, FUNCTION Y1, GET

FETCH, FETCHR, REAL FUNCTION PROPS,

OUTPUT

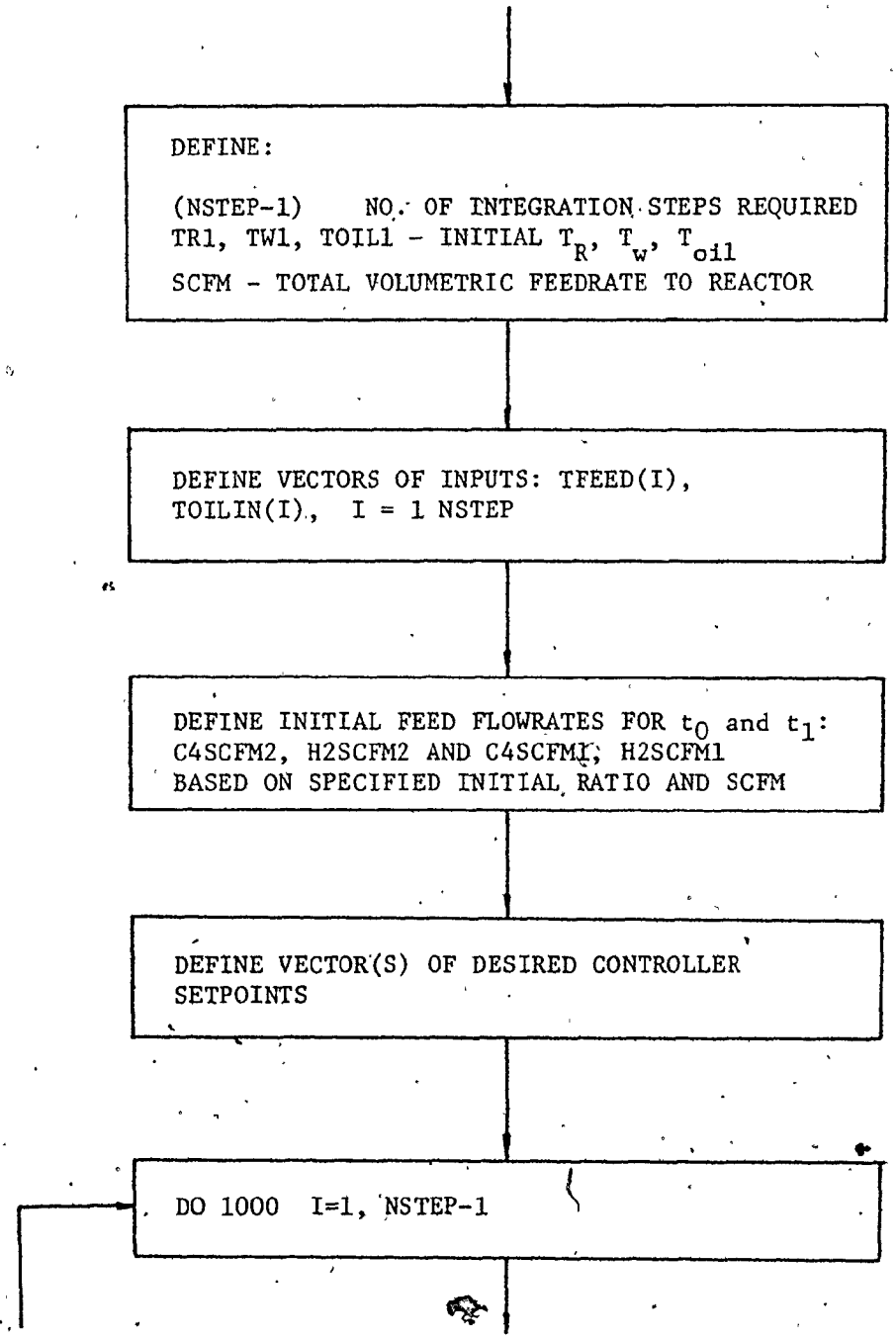

FIGURE 3.5 Flowchart of Closed Loop Simulation using MODEL1

Figure 3.5 (cont'd)

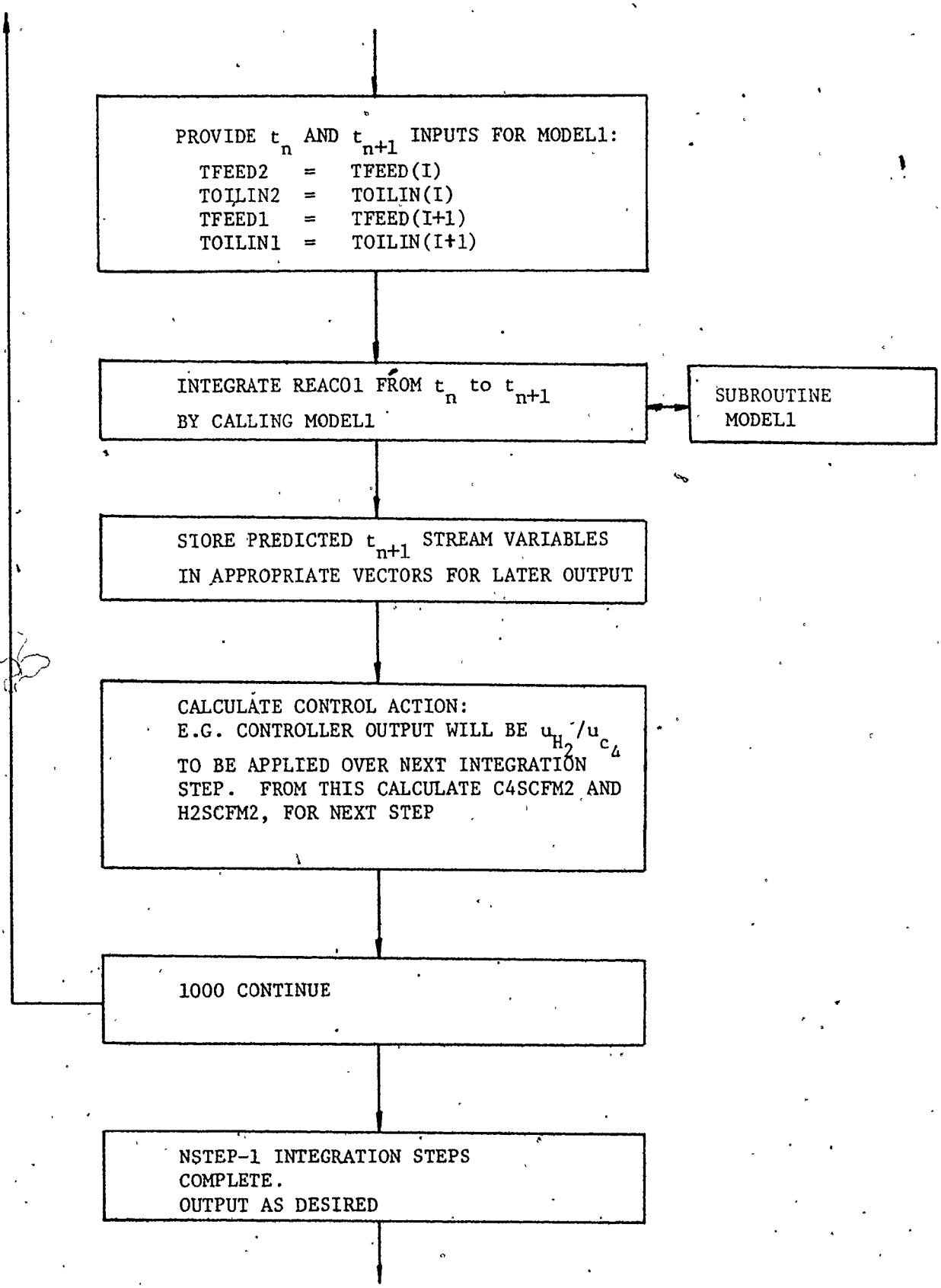

A listing of subroutine MODEL1 is given in Appendix A2.5. A flow chart is provided in Figure 3.6. As written, MODEL1 is specific to REAC01, since input and output stream information is transferred to and from the calling program only for REAC01. Other modules are easily added by including their equipment list in the DYNSYS input data set and by including the handling of appropriate stream information (i.e., flowrates of components in feedstreams and output streams that must be transferred to and from the calling program) in the calling program and MODEL1. MODEL1 is itself only a restructured version of the DYNSYS executive main program, the DYNSYS subroutines were unaltered.

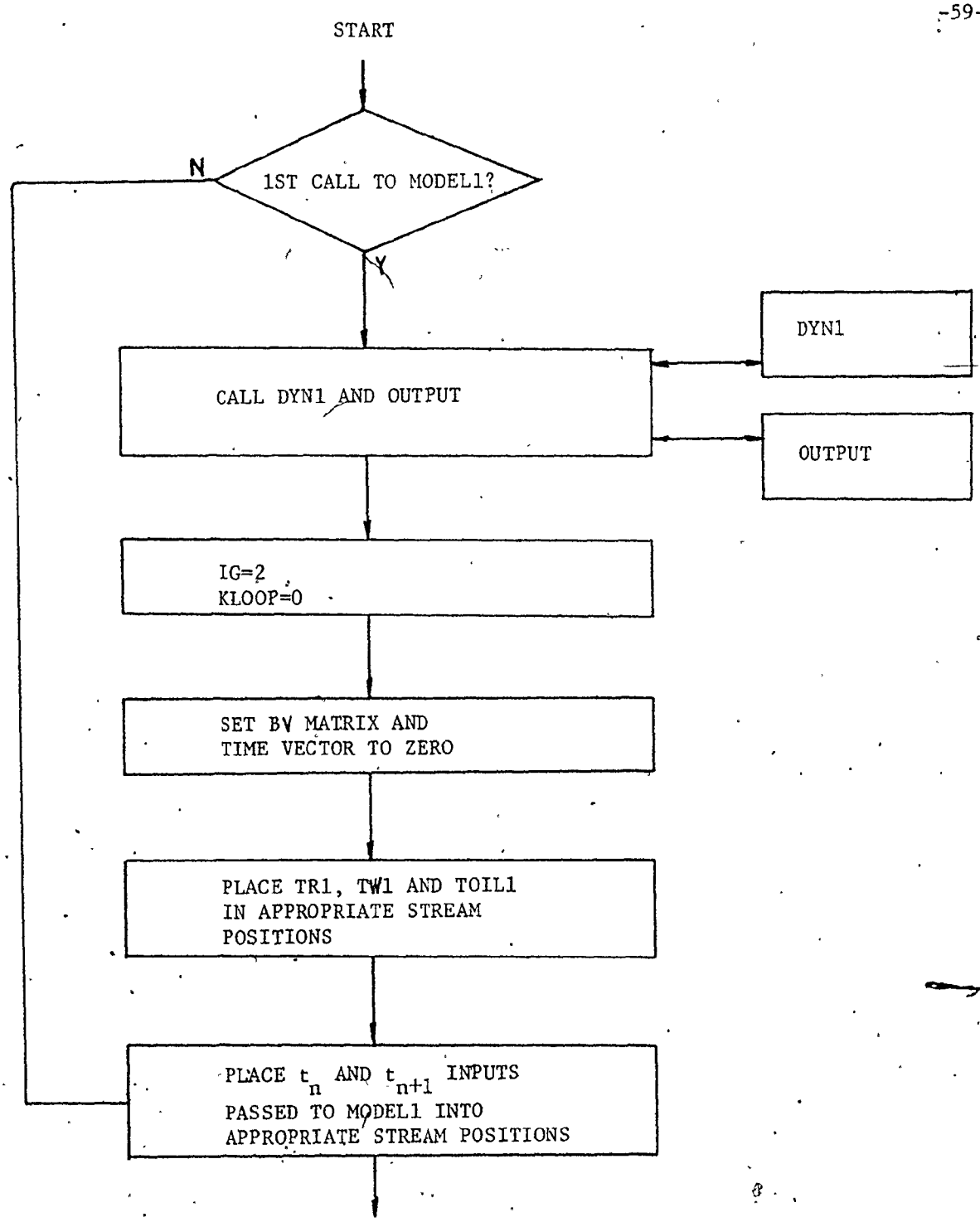

FIGURE 3.6 Flowchart of Subroutine MODEL1

Figure 3.6 (cont'd)

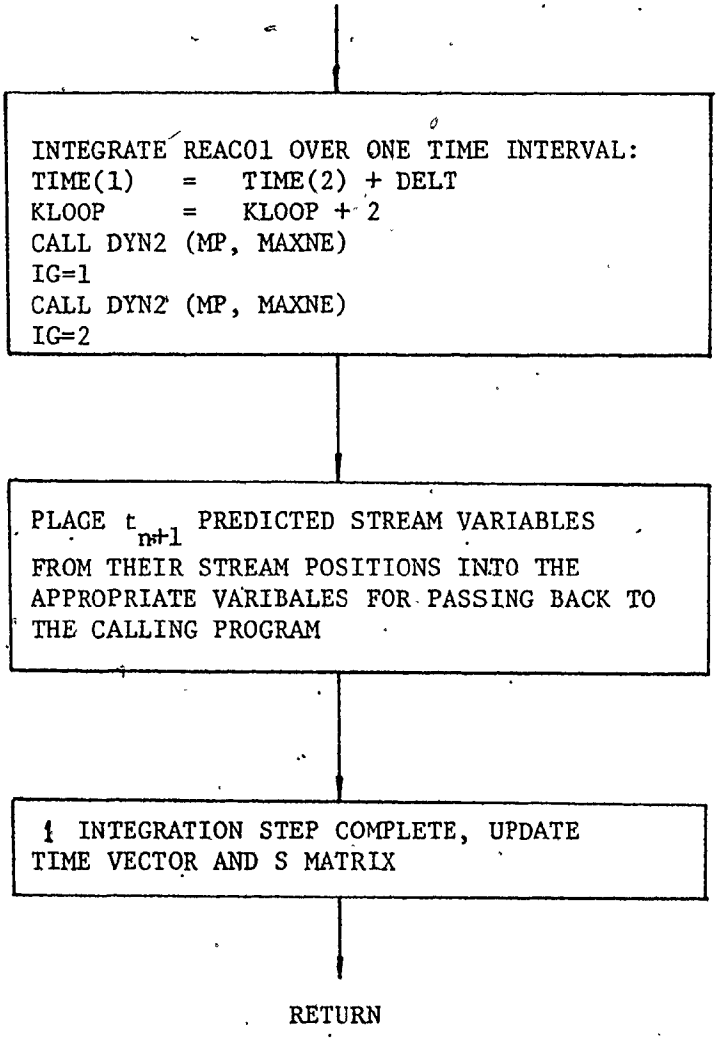

CHAPTER 4

PARAMETER ESTIMATION

4.1 INTRODUCTION

In this chapter, the estimation of the unknown parameters in the mass/energy balance equations is described. Estimates for all parameters in the kinetic expressions except catalyst activity were available from Shaw (1). The catalyst activity is expected to change from run to run, mainly due to variations in the level of activity achieved when the catalyst is regenerated prior to start-up of a run. It is anticipated that any on-line control strategy which utilizes the process model will require periodic on-line re-estimation of the catalyst activity. However, for the purpose of simulation studies, a fixed catalyst activity is estimated, using dynamic data collected around the expected operating conditions of the simulations. An estimate of the interchange parameter Q was also available from Shaw (1). The parameter had been estimated particularly for the perfectly mixed (emulsion phase) model of Orcutt et al, at the same bed depth as used for data collection in this study and therefore was expected not to require re-estimation.

The list of parameters requiring estimation is given in Table 4.1. The parameter w_{oil} is required in the enthalpy balance of the reactor heating/cooling coil. It also appears independently in the enthalpy balance for the circulating oil heating tank, and therefore it was possible to estimate it separately using dynamic temperature data

from the heating tank. For subsequent estmation of the remaining parameters, the estimate of w_{oil} was treated as a fixed known constant.

At the time of data collection, the Beckman Gas Chromatograph was not in service and so exit stream selectivities were not available. These data would have been valuable in the estimation, since they would reduce correlations between certain parameters. For instance, the catalyst activity CACT and the product of the heat transfer coefficient

TABLE 4.1 List of Parameters Requiring Estimation

	Computer Variable
$h_w A_w$	HAW
$m_w C_{pw}$	CPMW
$h_c A_c$	HAC
w_{oil}	WOIL
k/k_o	CACT

on the reactor inside wall and the area for heat transfer, HAW, were expected to be highly correlated. Referring to the reactor enthalpy balance Equation 3.25 and the kinetic rate expressions Equations 3.5 to 3.9, the catalyst activity appears as a multiplicative constant in the last term of Equation 3.25. The second last term contains the unknown parameter HAW. These two terms are large in magnitude and opposite in sign and therefore the estimates for CACT and HAW are expected to be highly correlated. In the absence of exit concentration data, this

problem was reduced by estimating CACT and HAW separately; first HAW (and CPMW and HAC) using dynamic temperature data collected under non-reaction conditions (i.e., butane feedrate reduced to zero), and then CACT using reaction data. Under non reaction conditions dynamic temperature data were generated by suddenly applying maximum cooling to the reactor wall. Since no reaction was occuring, the last term in equation 3.15 was zero for these conditions. With chemical reaction occurring, a number of step changes to the butane feedrate generated a dynamic response.

Details of the estimation procedure and a discussion of the results are given in the next section.

Parameter estimates were obtained by non-linear least squares, using an optimization algorithm due to Marquardt (15). At each parameter test point, the algorithm (subroutine UWHAUS) required the corresponding prediction vector for evaluation of the sum of squares. This required that the DYNSYS integration procedure be re-initialized, and the integration started with the new parameters passed to the appropriate modules. The DYNSYS executive was rewritten as subroutine DYN which performed these functions and created the prediction vector for return to the search algorithm. A listing of subroutine DYN (and the main program and subroutine MODEL used with UWHAUS), for the particular case of estimation of CACT, is given in Appendix A4.1.

4.2 RESULTS AND DISCUSSION

4.2.1 Estimation of WOIL

The parameter WOIL was estimated using dynamic temperature data from the circulating oil heating tank. The significance of heat loss from the tank was tested by adding a heat loss term Q_L to Equation 3.39:

$$\frac{dT_{tank}}{dt} = \frac{W_{oil}}{\rho_{oil} V_{tank}} (T_{oil,out} - T_{tank}) + \frac{Q_e}{\rho_{oil} V_{tank} C_{p_{oil}}} + Q_L \qquad 4.1$$

The circulating oil was heated to a high level using the immersion heaters fully on (2031 cal/sec) and with heat being generated by reaction (feedrates: C_4 = .36 s.c.f.m., H_2 = 3.37 s.c.f.m.). The air cooler was initially off (no cooling). At the beginning of the data collection run, the air cooler was turned fully on for maximum cooling of the circulating oil and the reaction was quenched by reducing the butane feedrate to zero. Five minutes and 51 seconds into the run the immersion heaters were turned fully off. Data were logged at a sampling interval of 20 seconds and were not filtered. This run was identified as DAT5, and was also used in the estimation of HAW, CPMW and HAC as described in the next section. Estimates of WOIL and Q_L were obtained by least squares according to

$$\min_{WOIL, Q_L} \underline{R}^T \underline{R} \qquad 4.2$$

where $\underline{R} = \underline{T}_{tank,obs} - \underline{T}_{tank,pred}$

$\underline{T}_{tank,obs}$ and $\underline{T}_{tank,pred}$ are the n-vectors of observed and predicted (by Equation 4.1) responses, respectively, of the heating tank temperature.

n is the number of observations, 70 for DAT5.

The 95% confidence interval on Q_L (the confidence intervals are calculated on a linear hypothesis and so are only approximate) includes zero, indicating that heat loss from the tank is not significant. The least squares estimate obtained for WOIL is

$$WOIL = 565.7 \quad g/sec$$

with 95% confidence interval (477.9, 653.6). The least squares prediction curve and observed tank temperatures are plotted in Figure 4.1 and show good agreement.

4.2.2 Estimation of HAW, CPMW, HAC and CACT

Estimation of HAW, CPMW, HAC and CACT proceeded in two steps. Under non-reaction conditions and maximum air cooling of the circulating oil (run DAT5 as described in the previous section) estimates of HAW, CPMW and HAC were obtained. These parameters were then treated as being perfectly known for the estimation of CACT. Separate data collected under reaction conditions were used to estimate CACT.

Both of these estimation problems are multiresponse where T_R, T_W and T_{oil} (in the absence of product concentration data) are the independent responses. However, a high level of precision in the

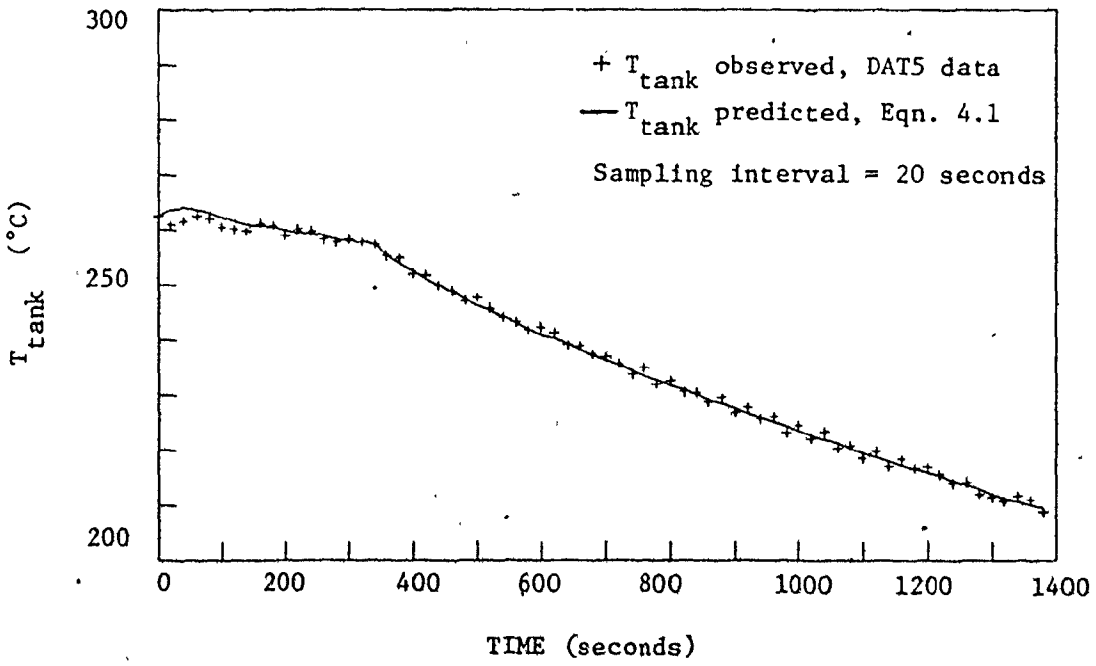

FIGURE 4.1 Prediction Curve for Dynamic Response of T_{tank}

estimates is not required at this stage of the investigation. The mechanistic model is providing at best only a rough approximation to the actual heat transfer phenomena occurring in the reactor. Furthermore, the estimates obtained will necessarily be of reduced quality, particularly catalyst activity, because of the absence of product concentration data. Better data will be available from the control runs to be performed later on the reactor. Therefore, the problem was simplified by concatenating the vectors of T_R, T_w and T_{oil} and finding the least squares estimates by

$$\begin{matrix}\min \\ \text{HAW} \\ \text{CPMW} \\ \text{HAC}\end{matrix} \quad \underline{Z}^T\underline{Z} \qquad 4.3$$

where $$\underline{Z} = \begin{bmatrix} \underline{T}_R \\ \hline \underline{T}_w \\ \hline \underline{T}_{oil} \end{bmatrix}_{\text{observed}} - \begin{bmatrix} \underline{T}_R \\ \hline \underline{T}_w \\ \hline \underline{T}_{oil} \end{bmatrix}_{\text{predicted}}$$

$\underline{T}_R$, $\underline{T}_w$ and $\underline{T}_{oil}$ are the n-vectors of observed or predicted responses of reactor, wall and oil temperatures respectively.

Estimates obtained in this manner will be identical to the ones obtained using multiresponse estimation if the responses T_R, T_w and T_{oil} are independent and their error variances are equal.

The observed responses of T_R, T_w and T_{oil} were calculated averages from several measurements. Reaction temperature was an average of thermocouple measurements at the center of the reaction chamber at heights of 1 ft, 2 ft and 3 ft from the distributor plate. Wall

temperature T_w was an average of temperatures measured on the outer surface or the wall at heights of 17 9/16" and 36 1/16" above the distributor plate. The observed average oil temperature in the heating/cooling coil T_{oil}, was an average of the inlet and outlet oil temperatures to the coil. Preliminary attempts at obtaining estimates for HAW, CPMW and HAC using Equation 4.3 indicated a high correlation between HAC and CPMW, and that a heat loss term was required in the enthalpy balance equations. Correlation between HAC and CPMW is expected since they appear in the numerator and denominator in the last term of Equation 3.29. HAC also appears in the enthalpy balance of the oil in the heating/cooling coil (Equation 3.32). The heat transfer effect associated with HAC in the oil enthalpy balance is much smaller than the magnitude of the term containing HAW and CPMW in Equation 3.29, and therefore the correlation is not reduced much with the information available from the dynamic response of the oil temperature. To overcome these problems, the following approach was adopted:

1. A heat loss term Q_L' was added to Equation 3.19:

$$\frac{dT_w}{dt} = \frac{h_w A_w}{m_w Cp_w}(T_R - T_w) + \frac{h_c A_c}{m_w Cp_w}(T_{oil} - T_w) + Q_L' \qquad 4.4$$

2. The objective function 4.3 was minimized by adjustment of HAC and HAW only. CPMW was treated as a fixed constant.
3. The converged sum of squares from step 2 was recorded for different values of CPMW over what was considered a reasonable range of values of CPMW.

Estimates of HAC, HAW, Q_L' and the converged sum of squares

obtained under this procedure are given in Table 4.2.

TABLE 4.2 Results of Estimation of HAW, HAC and Q_L' at Different Values of CPMW

CPMW	$\hat{HAW}$	$\hat{HAC}$	Q_L'	CONVERGED SUM OF SQUARES
500	20.18	19.12	7.4×10^{-10}	711
1000	21.73	7.60	4.5×10^{-2}	120
2000	21.66	12.47	2.3×10^{-2}	121
3000	21.41	17.36	1.65×10^{-2}	125
4000	21.16	21.833	1.4×10^{-2}	129
8000	20.31	35.25	1.5×10^{-2}	149

The high positive correlation between CPMW and HAC is clearly indicated in Table 4.2. Although the converged sum of squares is minimized in the vicinity of CPMW = 1000, increasing CPMW results in a different least squares estimate of HAC which does not greatly increase the converged sum of squares. An explanation for this high correlation is as follows. A higher heat transfer coefficient between the wall and the circulating oil results in greater heat transfer between the wall and the oil. To realize the observed dynamic temperature response of the wall, the predicted mass of the wall must be higher. By similar reasoning CPMW and Q_L' are negatively correlated. The estimate of HAW is insensitive to the value of CPMW and is well estimated with these data. No significant correlation between HAW and the other parameters was observed. It is apparent that the final estimate for CPMW should

not be chosen less than 1000 since the converged sum of squares begins to increase rapidly between CPMW = 500 and CPMW = 1000. Examination of residual plots for T_R, T_w and T_{oil} showed good fit in the range CPMW = 1000 and CPMW = 4000. No discernible difference between residual plots in this range was seen.

At this point in the estimation each of the sets of estimates in Table 4.2 was treated as fixed constants and each was used in a separate estimation of CACT. The final decision on which estimates were the best would be based not only on the converged sum of squares in Table 4.2, but also on which set of estimates when taken as known parameters in the estimation of CACT, gave the most acceptable estimate of CACT.

Dynamic reaction data for the estimation of CACT were generated as follows:

FIGURE 4.3	TIME(seconds)	CONDITIONS
	0	Qe: fully on
		C_4: .34 scfm
		H_2: 3.37 scfm
		air cooler: off(no cooling)
A	61	air cooler: fully on
B	654	C_4: .48 scfm
C	900	C_4: 0 scfm
D	1137	C_4: .35 scfm
		air cooler: off
	1380	end of run

This run is labelled DAT4, and consisted of 70 observations. Reaction temperature data generated under these conditions exhibited a considerable temperature gradient along the 3 measurement points in the reaction chamber. A gradient of 9-10 C^{o} was typically observed. Shaw (1) observed gradients of 7-10 C^{o} at flowrates five times minimum fluidization (minimum fluidization ≈ .3 s.c.f.m.) but these disappeared at flowrates above ten times minimum fluidization. Data collected here appear to contradict this observation as the gradient quoted above occurred at flowrates around 3.6 s.c.f.m., greater than ten times minimum fluidization. The large reaction temperature gradient resulted in a large gradient at the wall, as measured by the two wall thermocouples (a third wall thermocouple is in place but was not available at the time of the run)

Least squares estimates of CACT were obtained according to

$$\min_{CACT} \underline{Z}^{T}\underline{Z} \qquad 4.5$$

with $\underline{Z}$ defined as in Equation 4.3.

The results of this estimation for each set of parameters from Table 4.2, are given in Table 4.3. The converged sum of squares is minimized in the vicinity of CPMW = 4000, with an estimated catalyst activity of 2.91. However, considering the sum of squares from Table 4.2, the estimates obtained at CPMW = 3000 are chosen as being most reasonable. Furthermore, a catalyst activity of 2.91 was considered to

be high.

TABLE 4.3 Results of Estimation of CACT using RUN DAT4 Data (No. of Observations = 70)

From Table 4.2

CPMW	$\hat{HAW}$	$\hat{HAC}$	$\hat{Q_L}'$	$\hat{CACT}$	CONVERGED SUM OF SQUARES
1000	21.73	7.59	4.5×10^{-2}	.532	762
2000	21.66	12.47	2.3×10^{-2}	1.04	483
3000	21.41	17.36	1.65×10^{-2}	1.87	351
4000	21.16	21.83	1.4×10^{-2}	2.91	291
8000	20.31	35.25	1.5×10^{-2}	26.0	621

The observed responses of T_R, T_w and T_{oil} from DAT5 (non-reaction conditions) and the corresponding predicted responses using the estimates for HAW, HAC and Q_L' at CPMW = 3000 from Table 4.2, are shown in Figure 4.2. The prediction of general trends is quite good. Prediction curves for DAT4 reaction data using the parameter estimates at CPMW=3000 from Table 4.3, are shown in Figure 4.3. Predicted and observed responses of T_R and T_w show good agreement. However, due to the existence of significant gradients in the bed and at the wall, these predicitions are expected to contain some bias. Furthermore, the temperature reading at 3 ft. was actually above the top of the catalyst bed and was inadvertantly included into the calculation of average bed temperature, thus contributing to this bias. The prediction curve for T_{oil} was consistently higher than the observed response over the entire run. At t = 1137 seconds into the run, the air cooling was turned off

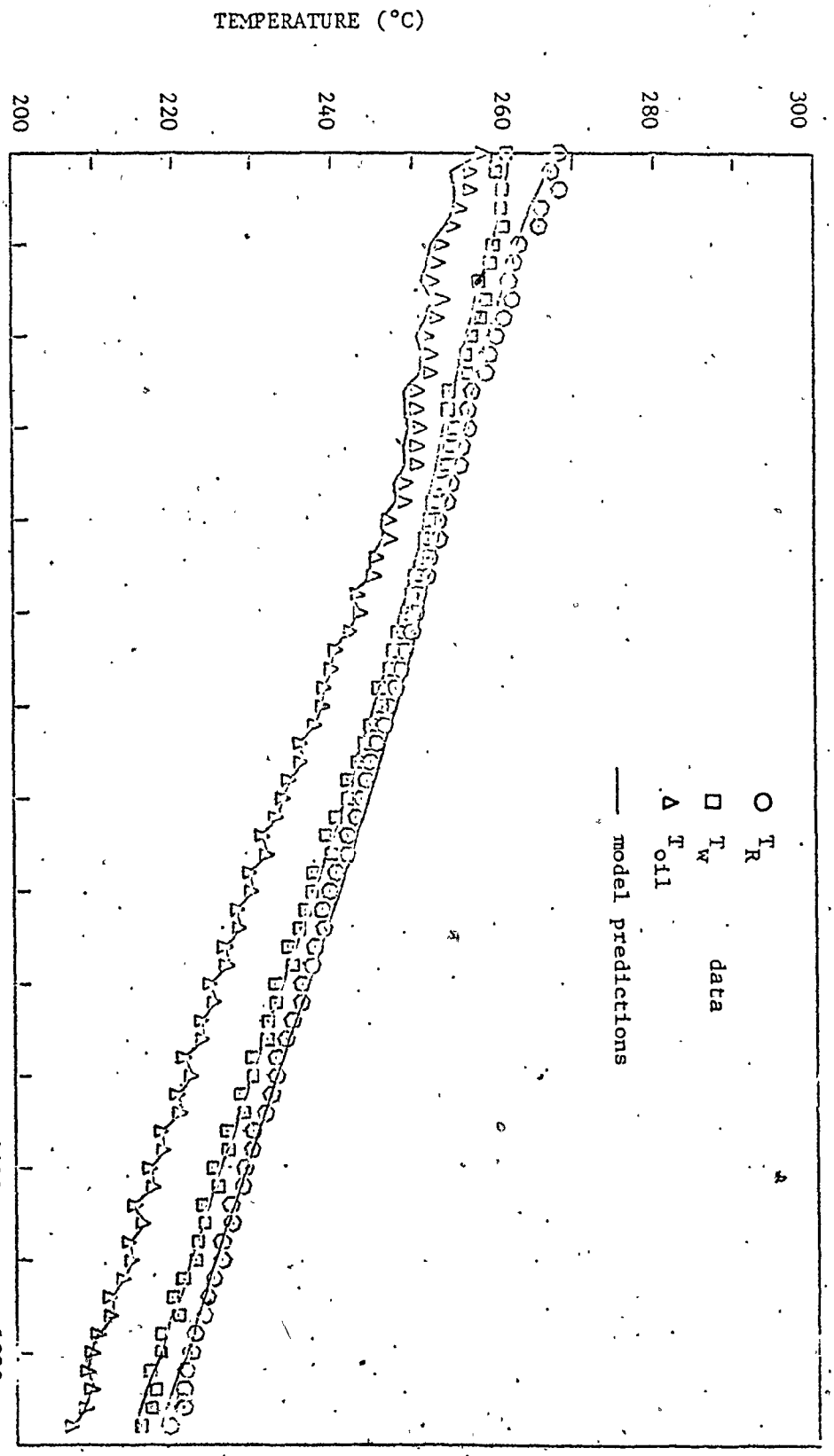

FIGURE 4.2 Prediction Curves for T_R, T_w and T_{oil} DAT5 NON-REACTION DATA

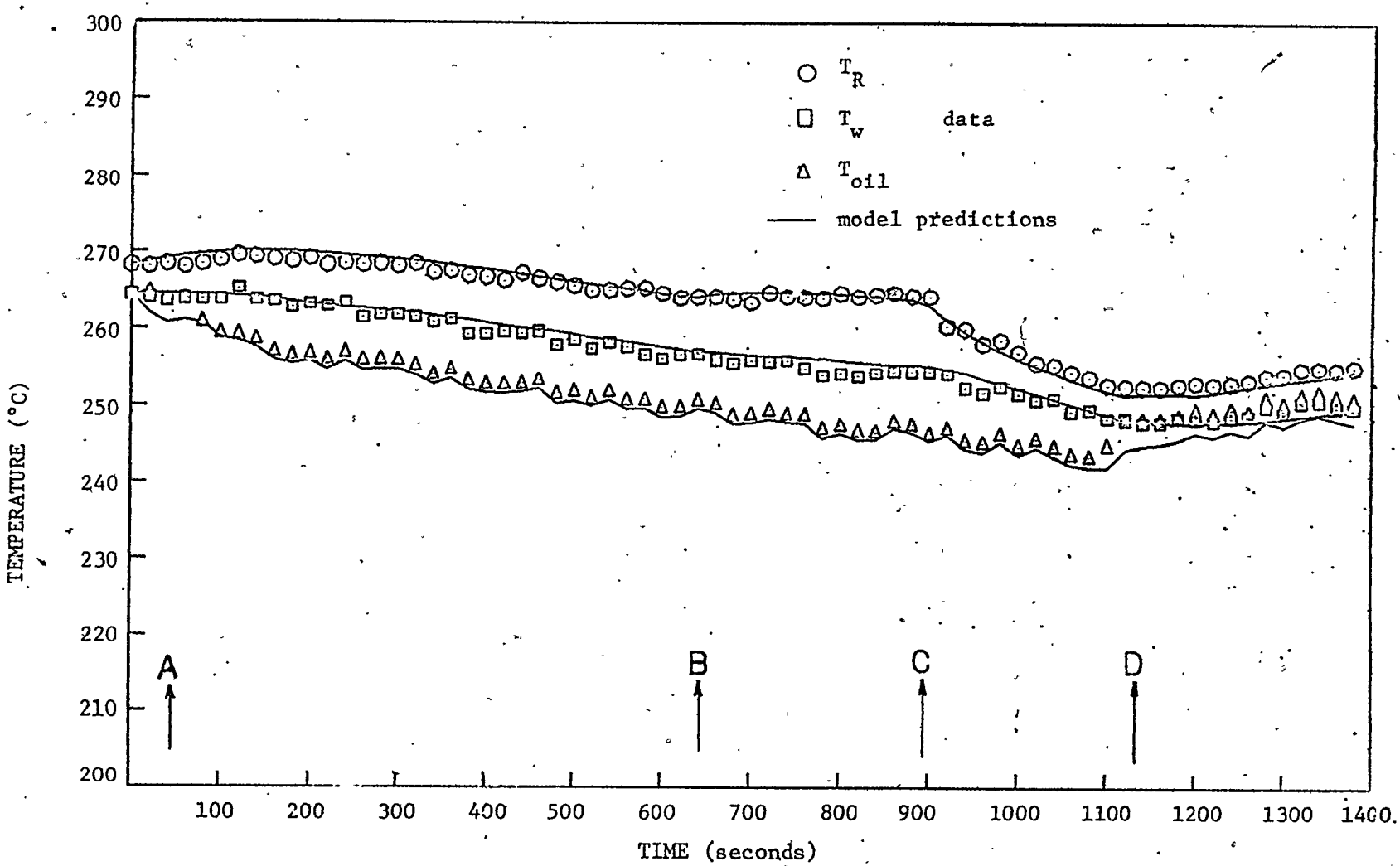

FIGURE 4.3 Prediction Curves for T_R, T_w and T_{oil} DAT4 Reaction Data

which caused an immediate increase in the temperature of the oil entering the heating/cooling coil. The model predicted an increase in T_{oil}, but failed to predict the magnitude of the change. The inability of the model to predict the average oil temperature is probably being contributed to by the existence of a significant gradient at the wall. Also, k/k_o alone was adjusted to minimize the sum of squares between observed and predicted responses of T_R, T_w and T_{oil}. Prediction of T_w and T_{oil} will be in error reflecting estimation error in the previously obtained estimates for HAW, HAC and Q_L'. Despite these difficulties, the estimates obtained are considered adequate for the planned simulation studies. Future runs are planned to improve these estimates by including concentration data in their estimation. A summary of the final estimtes which will be used in the simulation studies is given in Table 4.4.

TABLE 4.4 Final Estimates and Confidence Intervals for HAW, CPMW, HAC, Q_L' and CACT

PARAMETER	BEST ESTIMATE	95% CONFIDENCE INTERVAL (ON-LINEAR HYPOTHESIS)
HAW	21.41	(19.47, 23.35)
CPMW	3000.	not available
HAC	17.36	(14.35, 20.36)
Q_L'	1.65×10^{-2}	$(1.03 \times 10^{-2}, 2.27 \times 10^{-2})$
CACT	1.87	(1.70, 2.04)

CHAPTER 5

SIMULATION STUDIES

5.1 DISCUSSION OF CONTROL PROBLEM

Several factors contribute to the control problem on the fluidized bed reactor pilot plant. The temperature sensitivity of the reaction necessitates direct control of reaction temperature for stable and safe operation of the reactor. The response of reaction temperature to changes in oil temperature is too slow, due to heat transfer limitations, to have oil temperature as a manipulated variable for this purpose. For the control strategy to be proposed, reaction temperature will be controlled by manipulating the ratio of hydrogen to n-butane feedrates. However, maintaining stable reaction temperature is not the only control objective for this system. In chemical reaction systems where a number of products are formed, usually one or more of the products are of more importance than the others. For the control system to be suggested for the fluidized bed reactor the control objective has been specified as maintaining the selectivity of the intermediate product propane at a desired setpoint.

Another problem arises in the measurement of exit gas composition. Since the Beckman chromatograph has an analysis time of 360 seconds, product selectivities become available at intervals of 360 seconds, and are delayed by this same time. This interval is too long to use these measurements alone to control product selectivities.

The responses of the fludized bed reactor are highly non-linear, due primarily to the reaction system. Furthermore, the reactor is a 'changing plant'; catalyst activity is observed to be different from run to run and can possibly decay during a run.

A cascade control system has been implemented which is intended to provide a base-case for comparison with future studies anticipated to incorporate more sophisticated multivariable and adaptive control theory. The inner loop of the cascade system is a feedback controller which holds the reaction temperature T_R at a specified setpoint by manipulating the ratio of hydrogen to butane feedrates u_{H_2}/u_{C_4}. The scheme is shown in block diagram form in Figure 5.1. This inner loop controller will initially be a conventional proportional-integral type. The dynamic response of T_R to changes in u_{H_2}/u_{C_4} is represented by two separate transfer functions: $G_4^H(s)$ describes the dynamic response of T_R when it is increasing due to a decrease in u_{H_2}/u_{C_4} and $G_4^C(s)$ is the cooling response of T_R to increases in u_{H_2}/u_{C_4}. The time constant of the heating response is expected to be smaller than that for the cooling response. The cooling response of T_R is dominated by the heat transfer rate to the wall, whereas the heating response is additionally affected by the increased heat generated by reaction.

The temperature setpoint to the inner loop is provided by the output of the controller $G_1(s)$ on the outer loop. This outer loop has the purpose of maintaining the selectivity of a selected product intermediate at a desired setpoint. Propane was selected as the

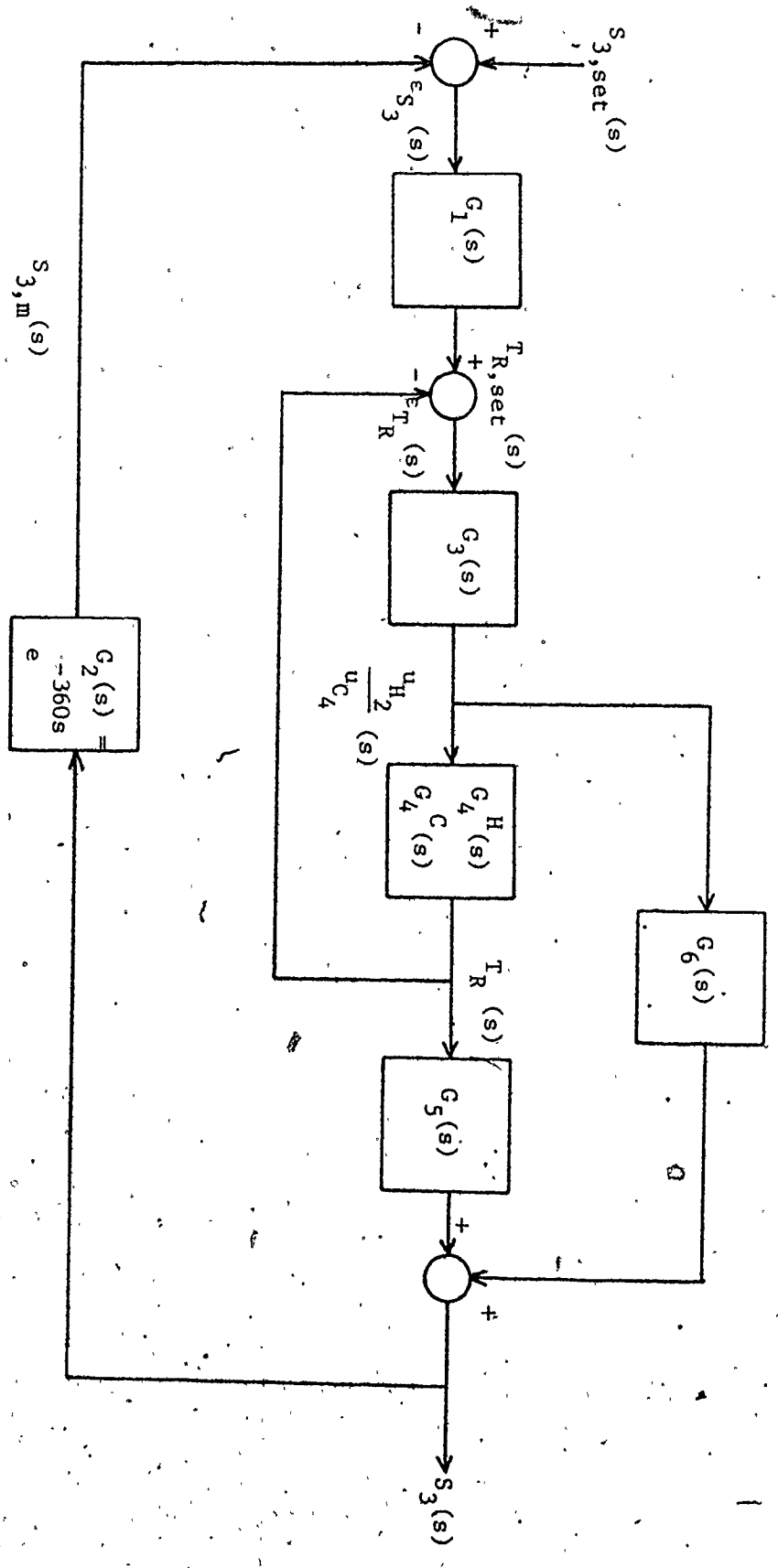

FIGURE 5.1 Block diagram of cascade control system.

component to be controlled since it is most sensitive to changes in operating levels, and thus is more controllable when only one system output is being considered in the control strategy. In Figure 5.1, the dynamic response of the selectivity of propane S_3 to changes in u_{H_2}/u_{C_4} is represented by the transfer function $G_6(s)$, and to changes in T_R by the transfer function $G_5(s)$. In applying the pseudo-steady state assumption (Section 3.2.3) to the mass balance equations, however, it is assumed that the time constants of these responses are small compared to the time constants of the thermal responses of the system, and can be ignored. In this case the transfer functions $G_6(s)$ and $G_5(s)$ consist of gains only:

$$G_6(s) = \frac{S_3(s)}{\frac{u_{H_2}}{u_{C_4}}(s)} = K_1 \qquad 5.1$$

$$G_5(s) = \frac{S_3(s)}{T_R(s)} = K_2 \qquad 5.2$$

Manipulations in u_{H_2}/u_{C_4} required to regulate T_R will result in a corresponding amount of variation in S_3, due to transfer function $G_6(s)$. A tuning method for the temperature loop is described below which effectively constrains the manipulations to u_{H_2}/u_{C_4}.

The measurement delay in S_3 caused by the chromatograph analysis is represented by the transfer function $G_2(s)$:

$$G_2(s) = \frac{S_{3,m}(s)}{S_3(s)} = e^{-360s} \qquad 5.3$$

where $S_{3,m}$ is the measured selectivity of propane as obtained from the chromatograph analysis data and S_3 is the selectivity of propane at the top of the catalyst bed. To be discussed in more detail later, the dynamic effect of the open volume of the disengaging section has not been modelled. For these simulation studies it is therefore assumed that the chromatograph sample is taken at the top of the catalyst bed, and the effect of the disengaging section is ignored.

The outer loop controller $G_1(s)$ was designed based on Dahlin's algorithm for setpoint changes in S_3, with control interval 360 seconds.

The cascade control strategy was tested in the simulations for setpoint changes in S_3, catalyst decay, and load disturbances in the oil inlet temperature.

Tuning of the temperature loop

The inner loop PI controller was tuned on the simulation model to minimize a weighted sum of squares of the deviations of T_R and S_3 from their respective setpoints. This turning procedure is described in Section 5.3.

Design of S_3 controller based on Dahlin's algorithm

Having selected suitable PI parameters for the temperature loop from section 5.3, a controller based on Dahlin's algorithm was designed and tested on the simulation model. This is described in Section 5.4.

Open loop testing

Before proceeding with the control tests described above, the open loop behaviour of the reactor simulation was examined by step testing. This testing is described in the next section. Approximate

transfer functions are identified, some components of which are used later in the design of the Dahlin's algorithm controller.

5.2 OPEN LOOP STEP TESTING

Identification of $G_4^H(s)$, $G_4^C(s)$, $G_5(s)$ and $G_6(s)$

The dynamic response of T_R to changes in u_{H_2}/u_{C_4} under heating and cooling conditions is approximated by first order transfer functions

$$G_4^H(s) = \frac{K_3}{\tau_1^H s + 1} \qquad 5.4$$

$$G_4^C(s) = \frac{K_3}{\tau_1^C s + 1} \qquad 5.5$$

Time constant τ_1^H was determined by observing the response of T_R to a step decrease in u_{H_2}/u_{C_4} from 8.0 to 6.0 (Figure 5.2); T_1^C was determined from the response of T_R to a step increase to u_{H_2}/u_{C_4} from 8.0 to 10.0 (Figure 5.3). For these tests, total volumetric feedrate was held constant at 3.5 s.c.f.m. Oil inlet temperature was held constant at 247°C, which was found to stabilize T_R at around 260°C.

The dynamic response of S_3 in Figures 5.2 and 5.3 demonstrates the dramatic effect of changes in u_{H_2}/u_{C_4} on S_3. The initial jumps in S_3 resulting from step changes in u_{H_2}/u_{C_4} are described by the transfer function $G_6(s) = K_1$. The non-linearity of this effect is clear in the different magnitudes of the jumps resulting from up and down step changes in u_{H_2}/u_{C_4}.

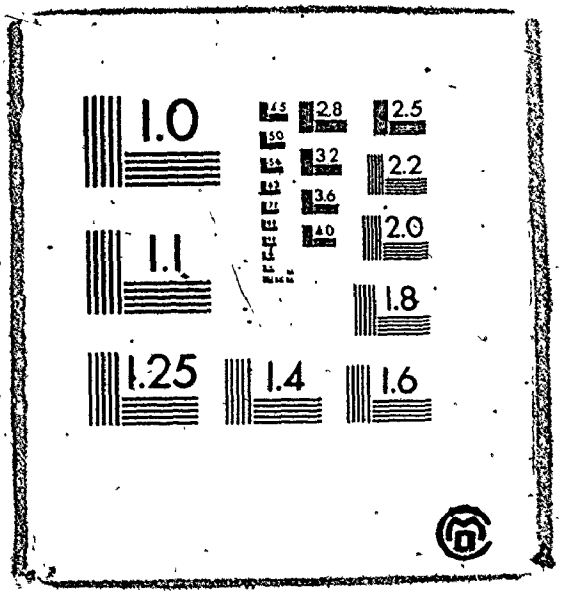
1.0
1.1
1.25
1.4
1.6
1.8
2.0
2.2
2.5
2.8
3.2
3.6
4.0
4.5
5.0

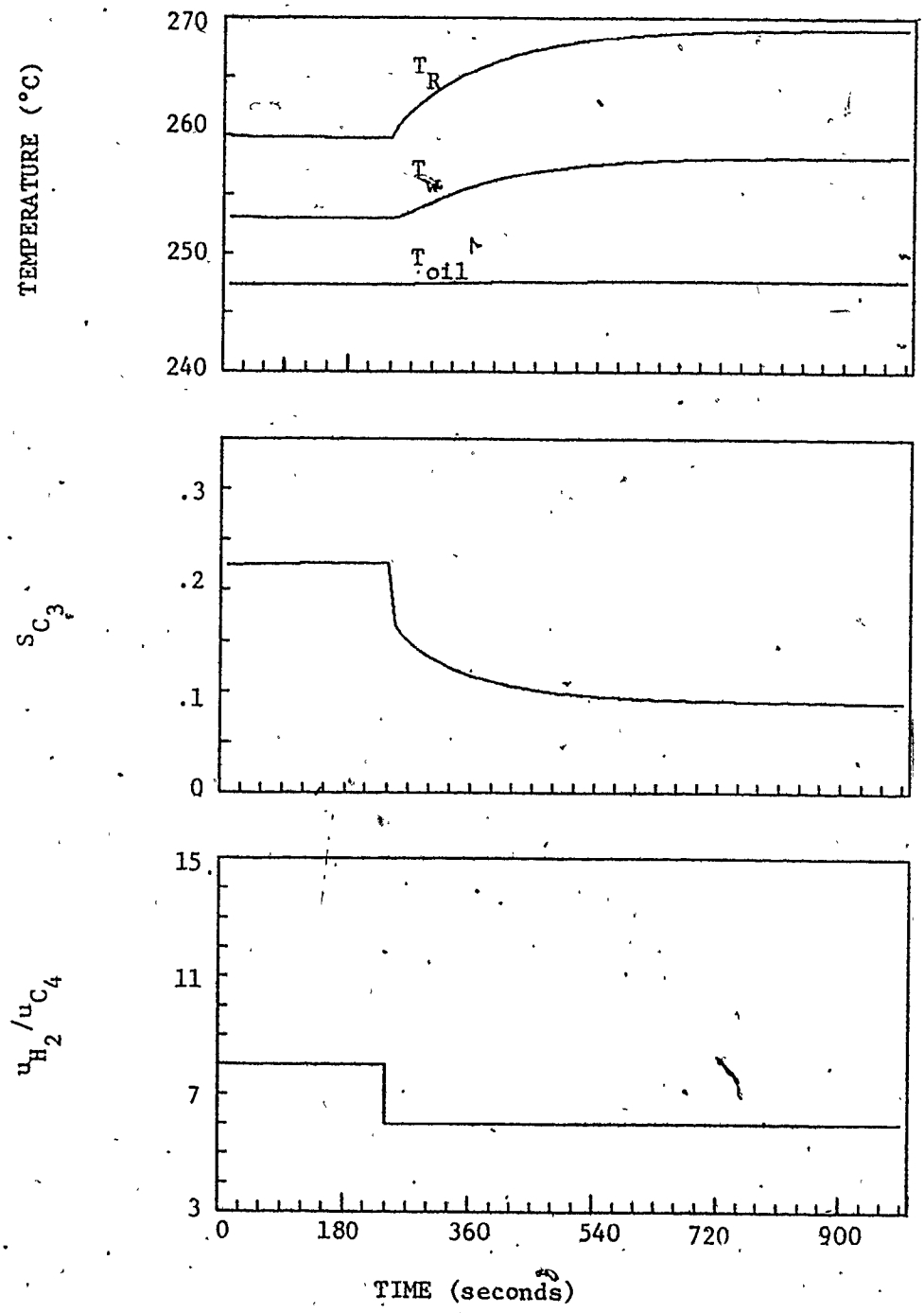

FIGURE 5.2 Open loop response to step down in in u_{H_2}/u_{C_4} from 8.0 to 6.0

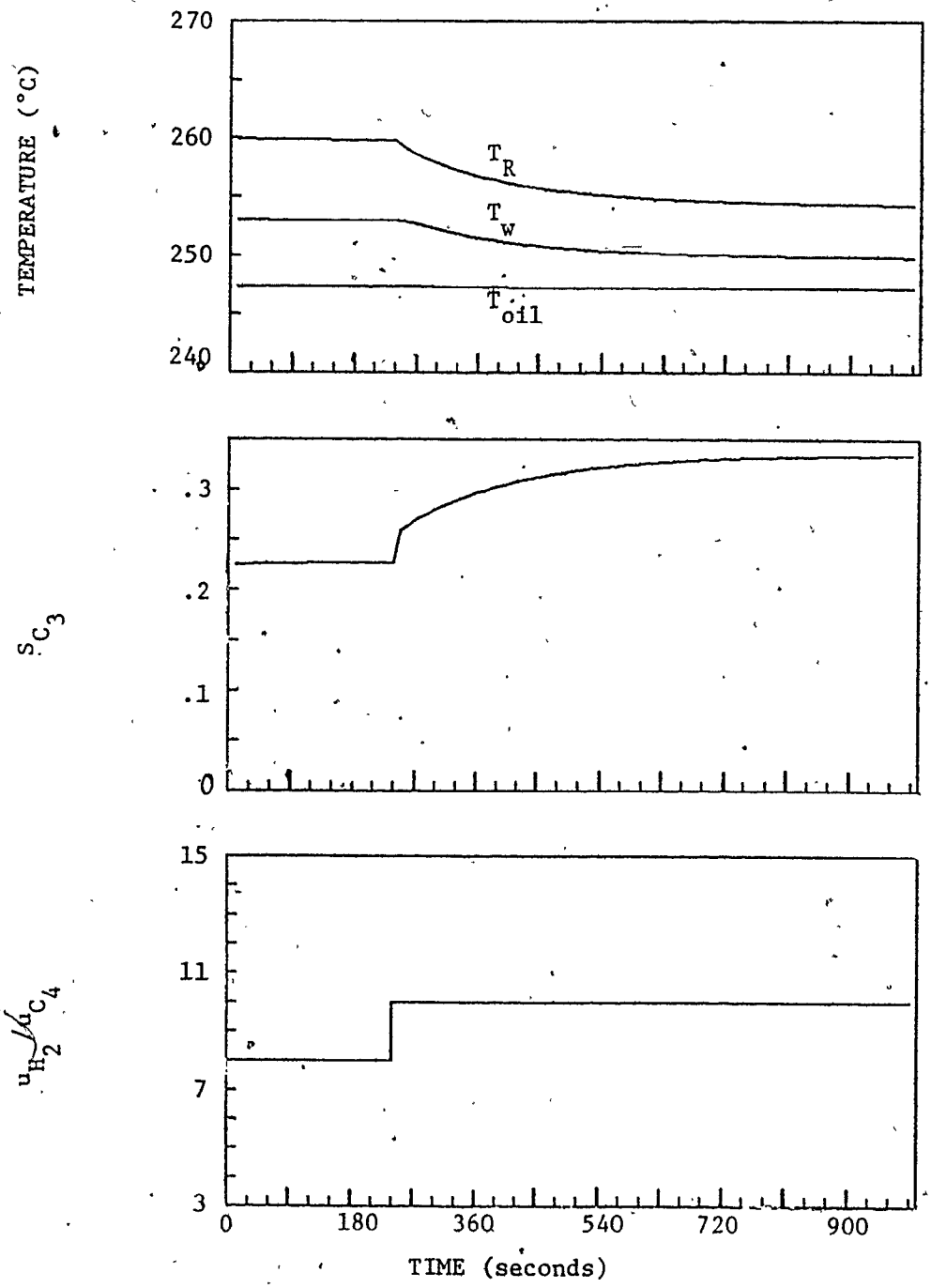

FIGURE 5.3 Open loop response to step up in u_{H_2}/u_{C_4} from 8.0 to 10.0.

The gains and time constants associated with the transfer functions $G_4^H(s)$, $G_4^C(s)$, $G_5(s)$ and $G_6(s)$ were estimated from the data used to plot Figures 5.2 and 5.3 and are tabulated in Table 5.1. The non-linearity of the gain terms is apparent. The difference in magnitude of τ_1^C and τ_1^H is 75 seconds, which is smaller than expected. However, this depends on the oil inlet temperature, which in this case was chosen to stabilize reaction temperature. With less cooling the difference would be greater.

TABLE 5.1 Transfer Function Parameters from u_{H_2}/u_{C_4} Step Testing

	K_1 (Dimensionless)	K_2 $(^oC)^{-1}$	K_3 (^oC)	τ_1 (seconds)
FIGURE 5.2: step down in u_{H_2}/u_{C_4} from 8.0 to 6.0	.0312	-.0148	-4.51	τ_1^H = 375
FIGURE 5.3: step up in u_{H_2}/u_{C_4} from 8.0 TO 10.0	.0161	-.0197	-2.83	τ_1^C = 450
	K_1^{avg}=	K_2^{avg}=	K_3^{avg}=	τ_1^{avg}=
AVERAGE	.0237	-.0173	-3.67	413

5.3 LEAST SQUARES TUNING OF TEMPERATURE CONTROLLER

Reaction temperature control was simulated using a discrete

proportional integral controller in the velocity form

$$\left.\frac{u_{H_2}}{u_{C_4}}\right|_t = \left.\frac{u_{H_2}}{u_{C_4}}\right|_{t-1} + K_p\left[\epsilon_{T_R,t} - \epsilon_{T_R,t-1} + K_I\epsilon_{T_R,t}\right] \qquad 5.6$$

where $\epsilon_{T_R,t} = T_{R,t}^{\text{measured}} - T_{R,t}^{\text{setpoint}}$

K_p = proportional gain

K_I = integral gain = $\frac{T'}{T_i}$

T' is the control interval of the temperature loop and T_i is the reset time.

The controller parameters K_p and K_I were estimated by minimizing a weighted sum of squares of the deviations of T_R and S_3 from their respective setpoints:

$$\min_{K_p,K_I} \sum_{i=1}^{N}\left[\frac{T_{R,i} - T_{R_{set},i}}{T_{R_{set},i}}\right]^2 + w\sum_{j=1}^{N}\left[\frac{S_{3,i} - S_{3_{set},i}}{S_{3_{set},i}}\right]^2 \qquad 5.7$$

where N = 200, the number of integration steps (control intervals) over which the minimization was performed and

w is the relative weighting placed on the deviations of S_3 from the S_3 setpoint

A measurement error $\sim N(0, .35^2)$ was added to the predicted response of T_R, and to the response S_3 was added an error $\sim N(0, .008^2)$. The search algorithm employed in Chapter 4 was also used for this minimization problem. A weighting of w=0 produces estimates for K_p and K_I which will minimize, under PI control, the squared deviations of T_R

from its setpoint, irrespective of the variation this causes in S_3 from manipulations in u_{H_2}/u_{C_4}. Increasing w in the objective function 5.7 increases the emphasis placed on minimizing the variation of S_3 about its setpoint relative to the variations in T_R.

Three trials were made: at w=0, w=.000125 and w=1. A weighting of w=.000125 resulted in approximately equal weighting of S_3 and T_R in the sum of squares calculation. With w=1, the weighting is effectively entirely on minimizing the variation in S_3. For each trial, four consecutive first order setpoint changes were generated in $T_{R,set}$, alternating up and down 3 C° starting at $T_{R,set}$=260°C. Since the cooling rate was held constant for these trials (by fixing the oil inlet temperature) and the catalyst activity was fixed, a particular T_R and u_{H_2}/u_{C_4} resulted in a specific S_3. However, the desired setpoint trajectory of S_3 was specified by assuming that S_3 followed only the dynamic response of T_R as given by the T_R setpoint trajectory (i.e., the effect of changes on S_3 from u_{H_2}/u_{C_4} directly was ignored). This does not affect the minimization problem in any way, as any convenient reference trajectory could have been chosen for S_3.

The estimates obtained for K_p and K_I for the three trials are given in Table 5.2. The dynamic responses of the inner loop to the imposed T_R setpoint changes, with the PI parameters being the least squares estimates from Table 5.2, are shown in Figure 5.4 (w=0), Figure 5.5 (w=.000125) and Figure 5.6 (w=1). With the PI controller tuned to minimize only squared deviations of T_R from its setpoint (w=0, Figure 5.4) the response of T_R to setpoint changes is expectedly tight. The

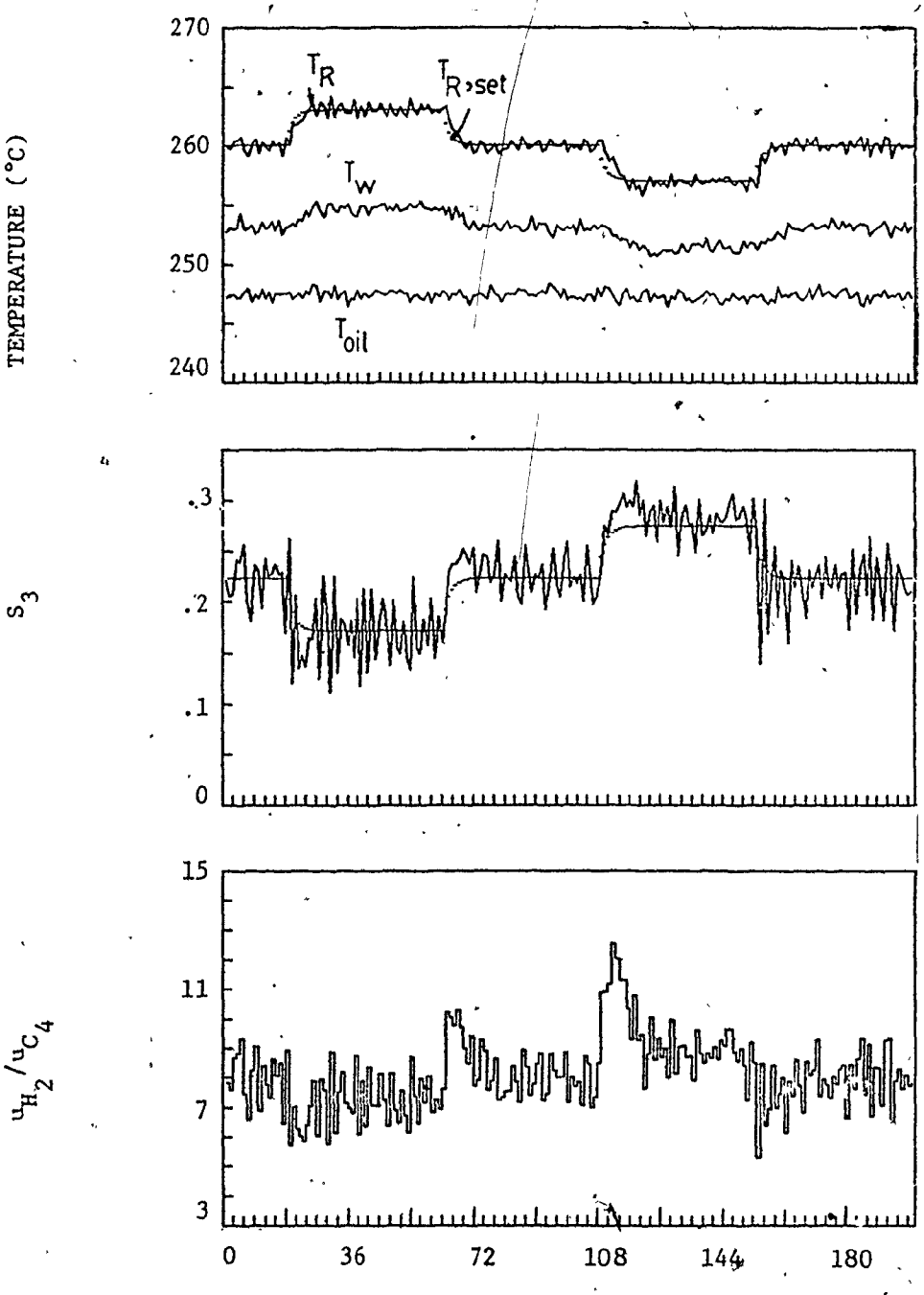

FIGURE 5.4 Temperature loop response to T_R setpoint changes, w=0 controller tuning.

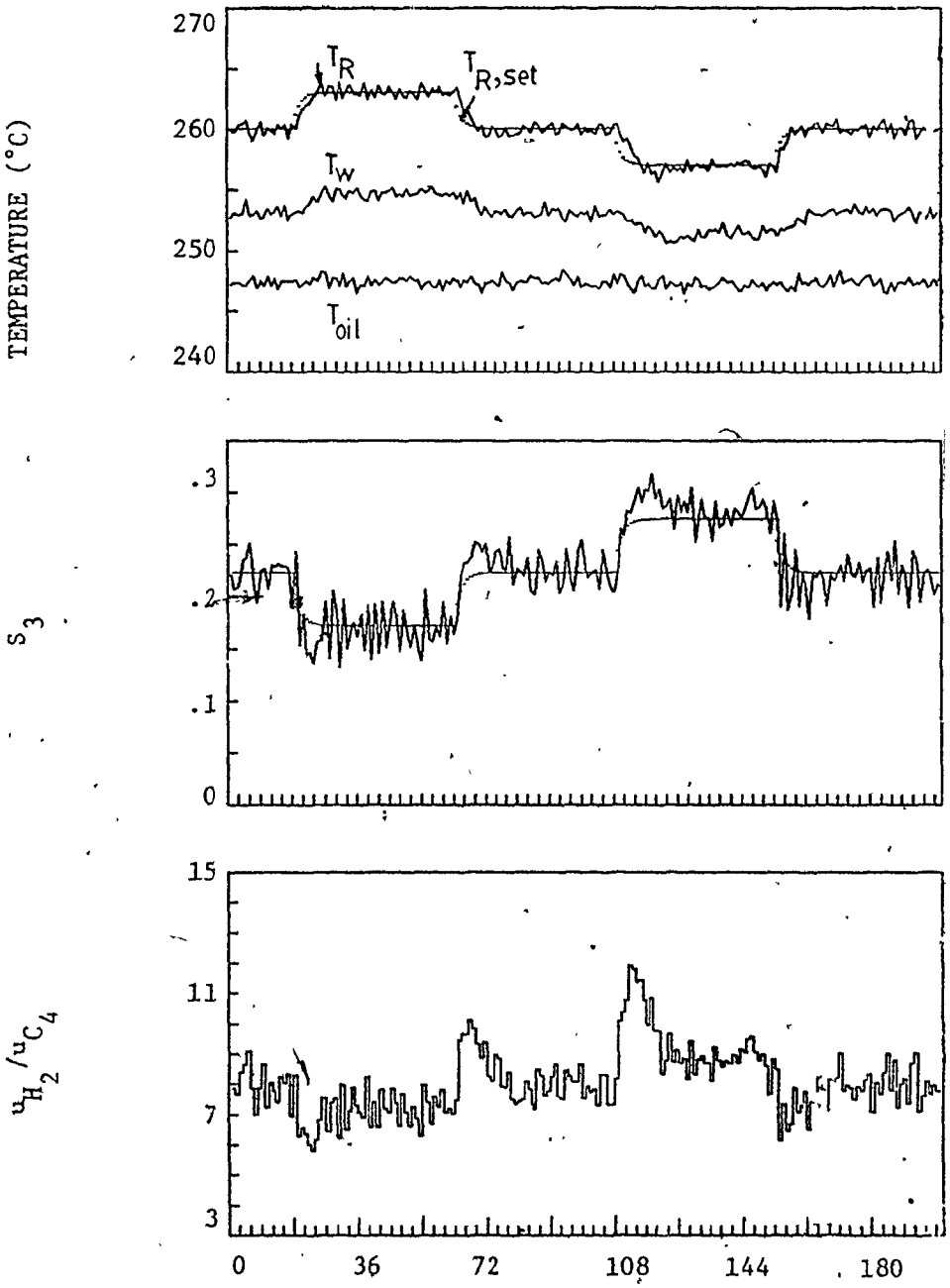

FIGURE 5.5 Temperature loop response to T_R setpoint changes, w=.000125 controller tuning.

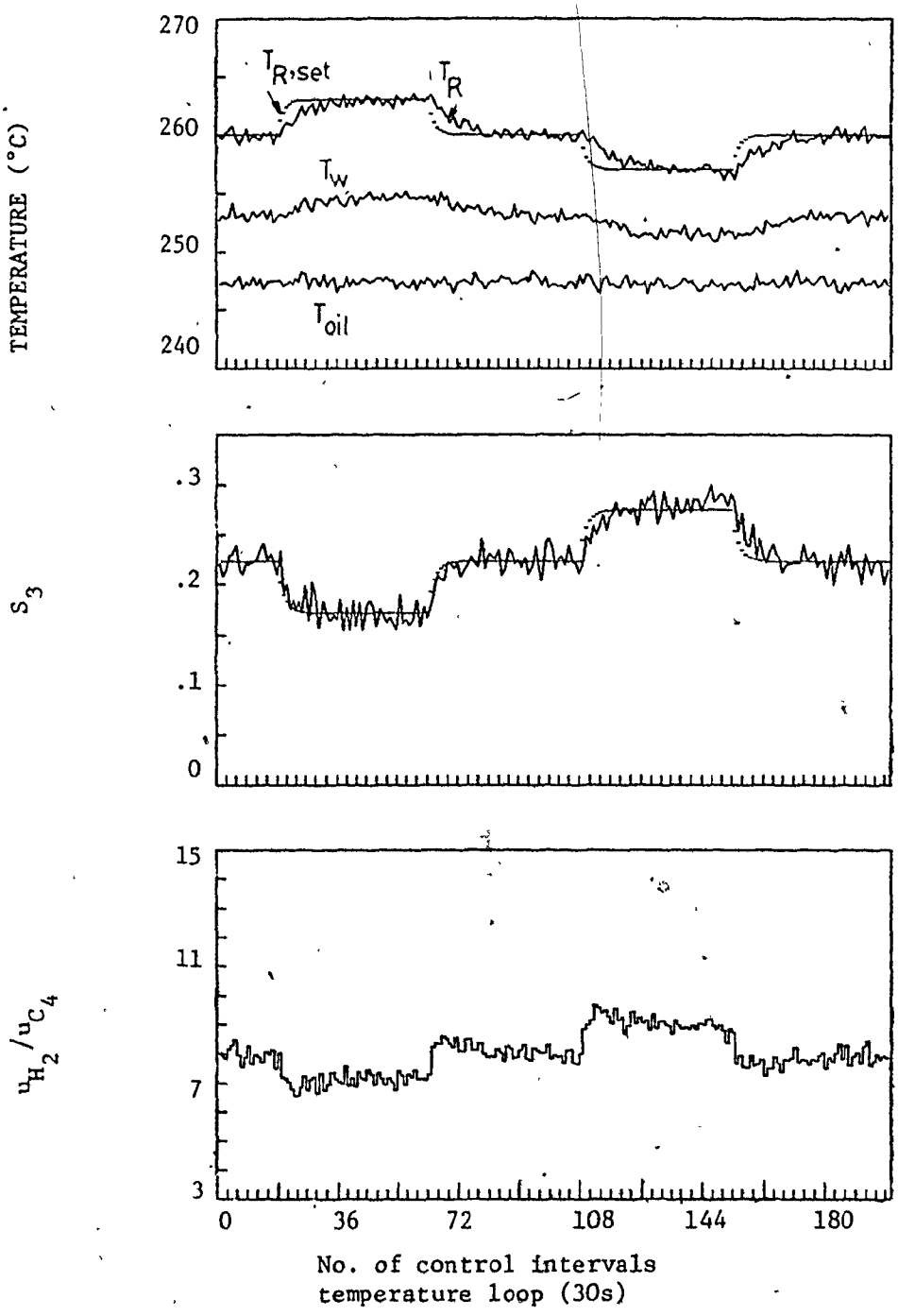

FIGURE 5.6 Temperature loop response to T_R setpoint changes, w=1 controller tuning.

proportional and integral gains are high (Table 5.2) which results in large adjustments to u_{H_2}/u_{C_4}. The penalty for this tight control of T_R is large variation in S_3 resulting directly from the manipulations in u_{H_2}/u_{C_4}. With the PI controller tuned to minimize equally variations in T_R and S_3 (w = .000125, Figure 5.5), the response of T_R to setpoint changes is much slower, but still adequate. The reduction in variation of S_3 is significant. The proportion gain is smaller (Table 5.2) resulting in smaller adjustments to u_{H_2} and u_{C_4}, and thus less variation in S_3. With the PI controller tuned to minimize only, the variation in S_3 was even further reduced. The response of T_R to setpoint changes is extremely sluggish, but once in the region of the steady state setpoint, the controller was successfully able to maintain T_R at the setpoint.

TABLE 5.2 Estimates Obtained for PI Parameters

w	$\hat{K}_p$ (95% confidence interval)	$\hat{K}_I$ (95% confidence interval)
0	1.508(1.29, 1.72)	.268(.180, .357)
.000125	1.03(.858, 1.204)	.34(.241, .442)
1	.573(.507, .640)	.073(.058, .088)

Referring to Figure 5.4, it is apparent that the response of T_R under PI control is different for positive and negative T_R setpoint changes. This is seen more clearly in the behaviour of u_{H_2}/u_{C_4} and in the response of S_3. This phenomenon was examined more closely by repeating the above tuning procedure with w=0, and with no added measurement noise on T_R and S_3. The least squares estimates for K_p and

K_I obtained in this case are given in the first row of Table 5.3.

The dynamic response of the temperature PI loop with these parameters is shown in Figure 5.7. The difference in responses for positive and negative T_R setpoint changes is very clear. An explanation lies in the non-linearity of the response of T_R. For all of the first order changes in T_R setpoint, the magnitude of the initial control action in u_{H_2}/u_{C_4} was the same. The second and subsequent control actions corresponding to positive and negative T_R setpoint changes were markedly different however. The reason for this is seen in the magnitude of the response of T_R to the initial control action in u_{H_2}/u_{C_4}, for the two cases. Examining the response of T_R to the first T_R setpoint change (positive), it is seen that the initial adjustment to u_{H_2}/u_{C_4} causes T_R to overshoot the setpoint trajectory. The controller responds by increasing u_{H_2}/u_{C_4}. This second control action causes T_R to fall below the setpoint trajectory, and this back and forth behaviour continues until the steady state setpoint is reached. The response of S_3 reflects these up and down adjustments in u_{H_2}/u_{C_4}. Contrast this behaviour of T_R to the second setpoint change in T_R (negative). The initial control action is approximately equal in magnitude, but opposite in direction, to the initial control action for the first T_R setpoint change. However, the magnitude of the response of T_R is not as large, and it does not overshoot the setpoint trajectory. The gains of the transfer functions $G_4^C(s)$ and $G_4^H(s)$ must be the same (approximately) for the response of T_R to these first two setpoint changes because the operating region is the same. The difference in magnitude of the

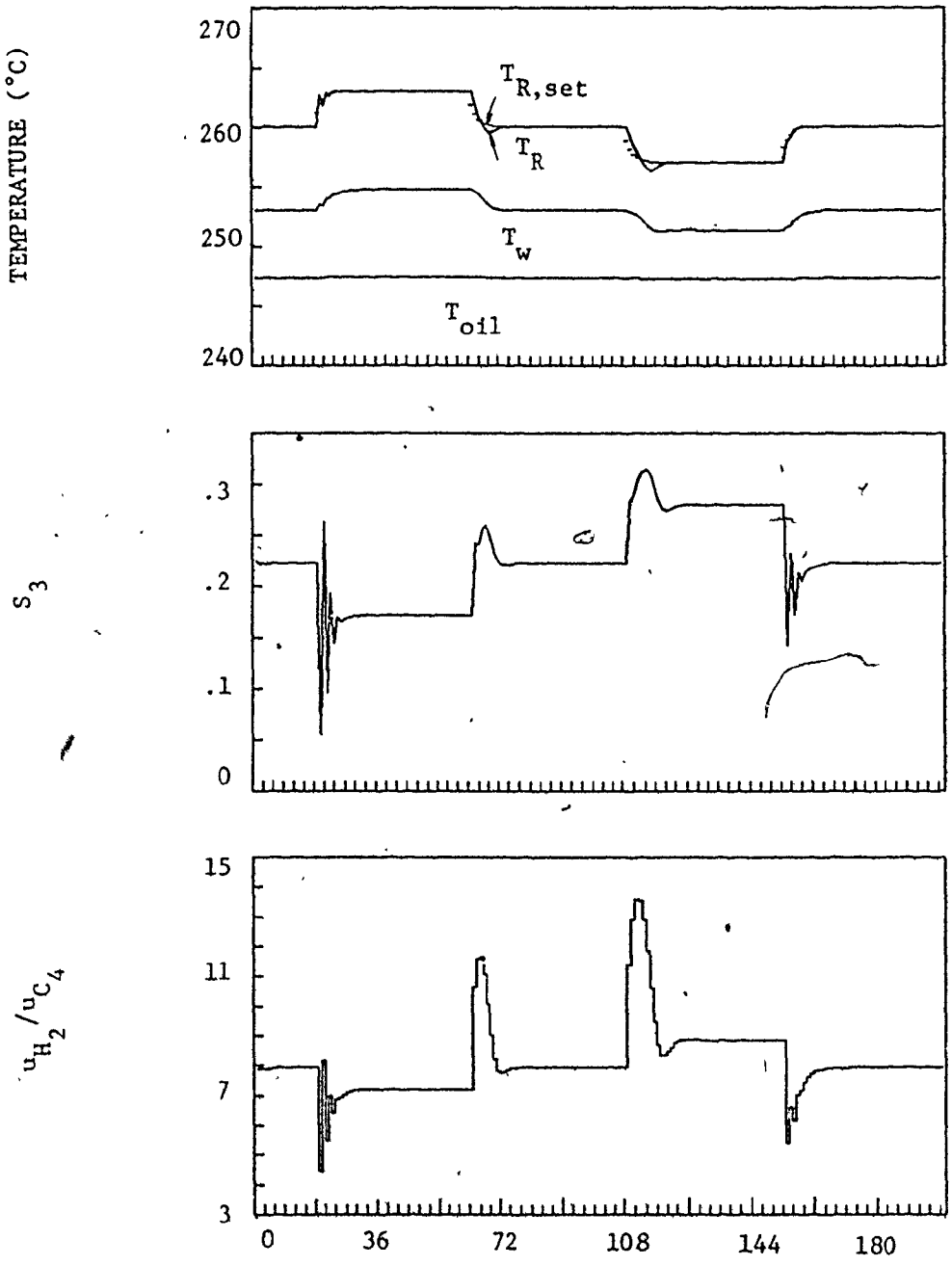

FIGURE 5.7 Temperature loop response to T_R setpoint changes, w = 0 controller tuning, no measurement noise added.

TABLE 5.3 Estimates obtained for PI parameters, (no measurement noise, multiple and single setpoint changes to T_R)

	$\hat{K}_p$ (95% confidence interval)	$\hat{K}_I$ (95% confidence interval)
FIGURE 5.7 -four consecutive up and down T_R setpoint changes	1.375(1.104, 1.647)	1.097(.7193, 1.474)
FIGURE 5.8 -single T_R setpoint change up	.7035(.4888, .9182)	2.548(1.388, 3.708)
FIGURE 5.9 -single T_R setpoint change down	3.236(2.919, 3.553)	.9414(.6582, 1.225)

These estimates are compared to the estimates obtained for the case of four setpoint changes. Slightly more integral gain is required (1.79 compared to 1.51; product of K_p and K_I), but significantly less proportional gain (.7035 compared to 1.375) was required. The result is less oscillatory response of T_R to this positive setpoint change (Figure 5.8 compared to the first setpoint change in Figure 5.7) and smoother transition of S_3 to the new steady state value.

The least squares response of T_R to a first order change down in T_R setpoint, from 260°C to 257°C, is shown in Figure 5.9. The estimates obtained for K_p and K_I in this case are given in the last row of Table 5.3. The integral gain is significantly greater than the two previous cases. The proportional gain is also much larger. These parameters resulted in oscillatory behaviour of T_R prior to the setpoint change (Figure 5.9), but still resulted in minimization of the sum of squares of the deviations of T_R from its setpoint. Of course, had the setpoint

TABLE 5.3 Estimates obtained for PI parameters, (no measurement noise, multiple and single setpoint changes to T_R)

	$\hat{K}_p$ (95% confidence interval)	$\hat{K}_I$ (95% confidence interval)
FIGURE 5.7 -four consecutive up and down T_R setpoint changes	1.375(1.104, 1.647)	1.097(.7193, 1.474)
FIGURE 5.8 -single T_R setpoint change up	.7035(.4888, .9182)	2.548(1.388, 3.708)
FIGURE 5.9 -single T_R setpoint change down	3.236(2.919, 3.553)	.9414(.6582, 1.225)

These estimates are compared to the estimates obtained for the case of four setpoint changes. Slightly more integral gain is required (1.79 compared to 1.51; product of K_p and K_I), but significantly less proportional gain (.7035 compared to 1.375) was required. The result is less oscillatory response of T_R to this positive setpoint change (Figure 5.8 compared to the first setpoint change in Figure 5.7) and smoother transition of S_3 to the new steady state value.

The least squares response of T_R to a first order change down in T_R setpoint, from 260°C to 257°C, is shown in Figure 5.9. The estimates obtained for K_p and K_I in this case are given in the last row of Table 5.3. The integral gain is significantly greater than the two previous cases. The proportional gain is also much larger. These parameters resulted in oscillatory behaviour of T_R prior to the setpoint change (Figure 5.9), but still resulted in minimization of the sum of squares of the deviations of T_R from its setpoint. Of course, had the setpoint

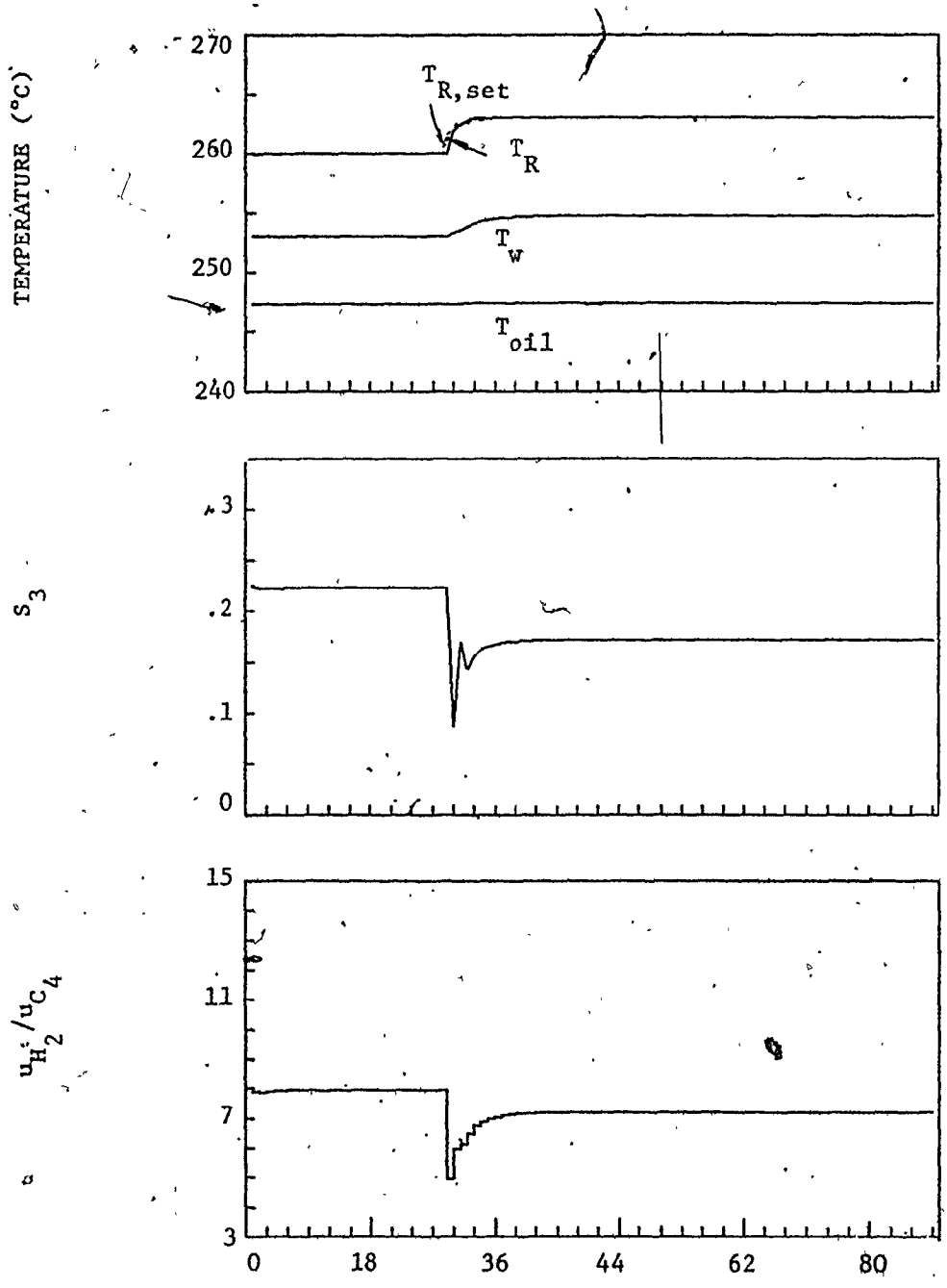

FIGURE 5.8 Temperature loop response to single first order change down to T_R setpoint, w=0 controller tuning.

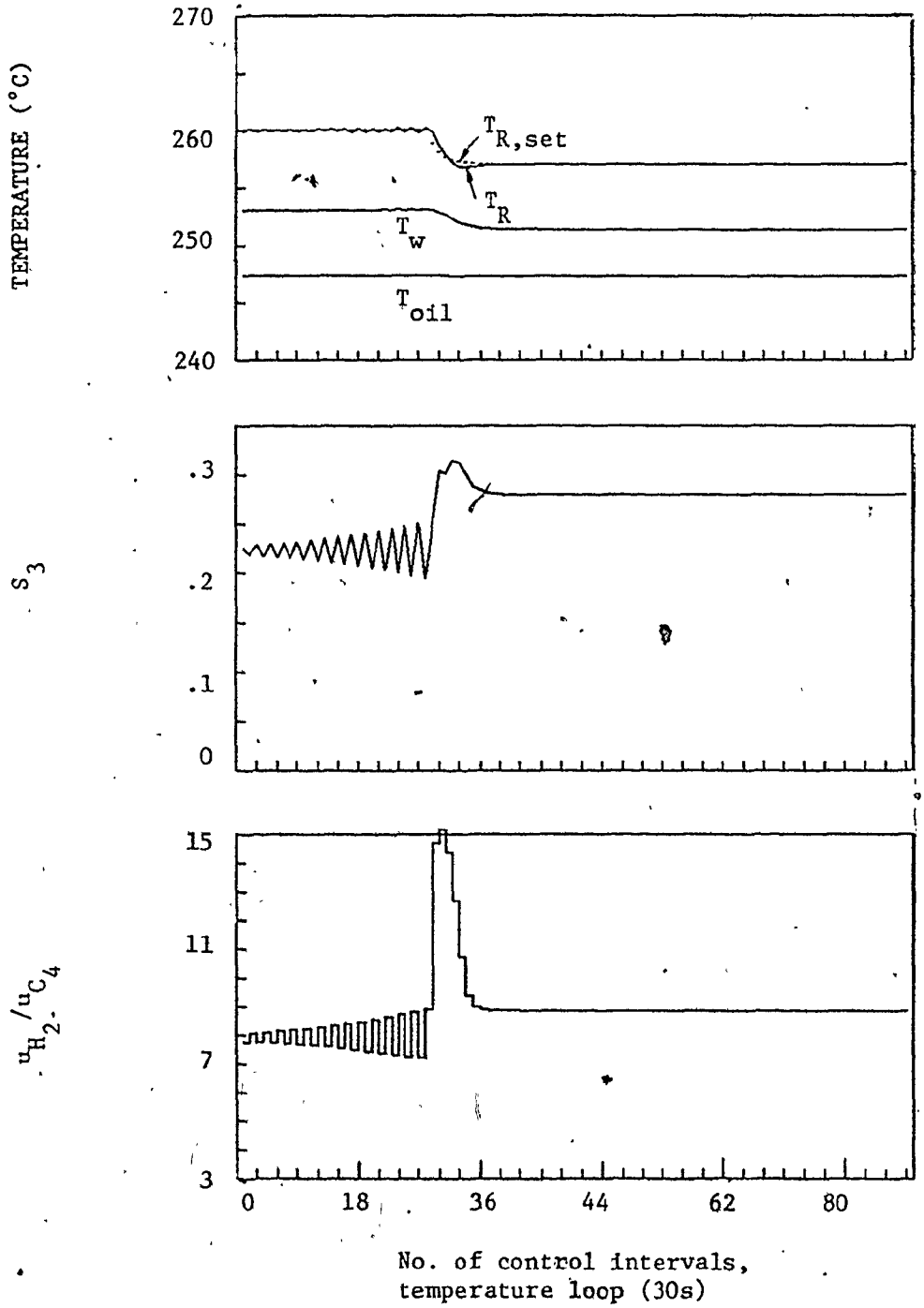

FIGURE 5.9 Temperature loop response to single first order change down to T_R setpoint, w=0 controller tuning.

change occurred at a later time, the oscillatory behaviour of T_R prior to the setpoint change would have become more significant in the sum of squares calculation, and the controller gains would have been adjusted down accordingly. The higher gains called for still did not produce a rapid response in T_R, because the cooling rate dominates this response.

It is apparent from observing the estimates of K_p and K_I for single positive and negative setpoint changes, that higher gains are required for the latter case. If estimates of K_p and K_I are obtained over a number of positive and negative setpoint changes, the estimates obtained will be too detuned for negative setpoint changes and too sensitive (i.e., too high gains) for positive setpoint changes.

5.4 SIMULATION OF CASCADE CONTROL STRATEGY

5.4.1 Design of Dahlin's algorithm controller for outer loop

The block diagram of the cascade control system in the s domain, Figure 5.1, is shown in the sampled data (z) domain in Figure 5.10. The transfer function $H_1(s)$ represents a zero order hold between the output of the discrete controller $G_1(z)$ and the continuous process G(s):

$$H_1(s) = \frac{1 - e^{-sT}}{s} \qquad 5.7$$

where T is the control interval, s.

G(s) describes closed loop dynamic response of S_3 (i.e., the model prediction of S_3 taken at the top of the catalyst bed) to changes in T_R setpoint. A first order dynamic lag with no dead time is assumed

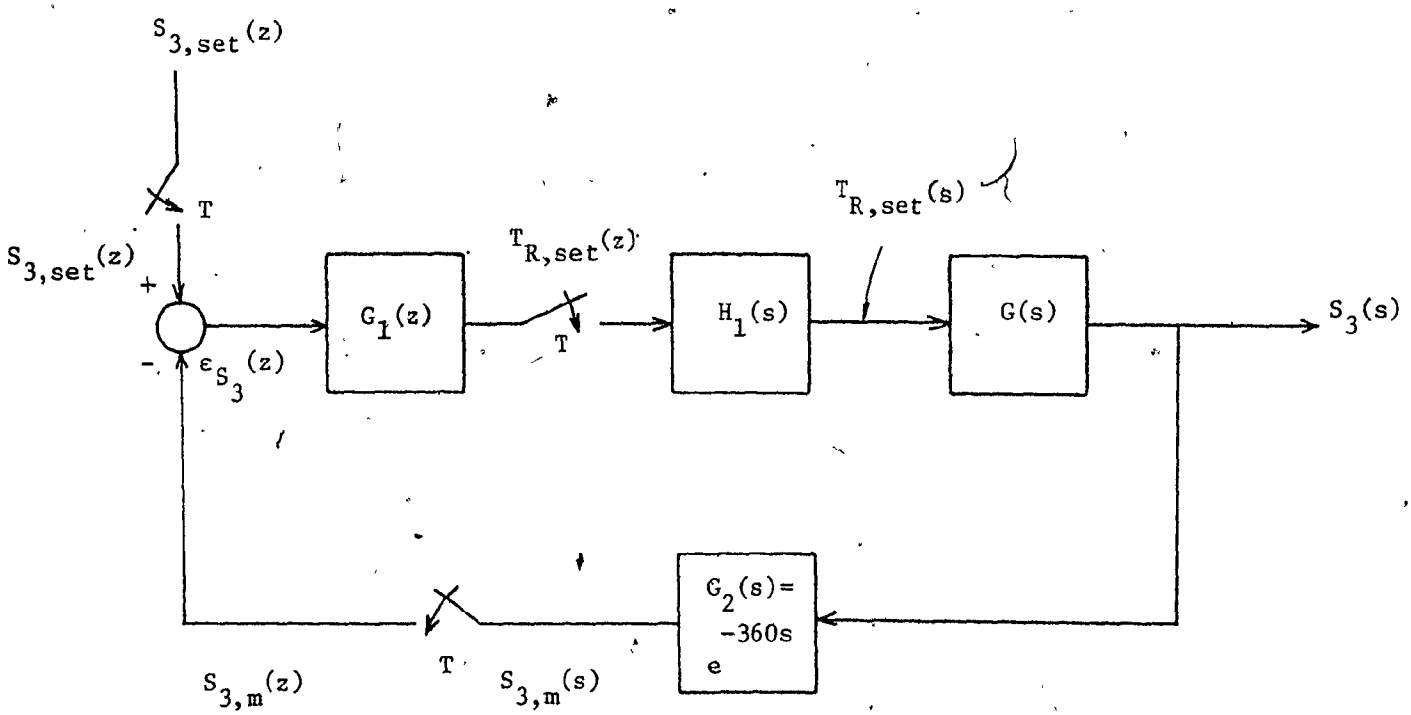

FIGURE 5.10 Block diagram of cascade control system in sampled-data domain

as an initial approximation:

$$G(s) = \frac{S_3(s)}{T_{R,set}(s)} = \frac{K}{\tau s + 1} \qquad 5.8$$

The value of the time constant τ is dependent on the performance of the inner temperature controller $G_3(s)$, shown in Figure 5.1.

Dahlin (18) suggests that the closed loop response of a system should behave like a process with first order dynamics plus deadtime. In our case

$$\frac{S_{3,m}(s)}{T_{R,set}(s)} = \frac{e^{-\theta' s}}{\lambda s + 1} \qquad 5.9$$

where λ is the time constant of the desired response of $S_{3,m}$ to changes in $T_{R,set}$ and θ' is the total deadtime in the process between $T_{R,set}$ and $S_{3,m}$.

In this case θ'=360 s, for the measurement delay of S_3. Transport delays in the reactor have been assumed to be negligible.

For a unit step change to $T_{R,set}$, and using θ' = 360, Equation 5.9 becomes

$$S_{3,m}(s) = \frac{1}{s} \cdot \frac{e^{-360s}}{\lambda s + 1} \qquad 5.10$$

Written in the z-domain this is

$$S_{3,m}(z) = \frac{(1 - e^{-T/\lambda})z^{-N-1}}{(1 - z^{-1})(1 - e^{-T/\lambda}z^{-1})} \qquad 5.11$$

where N is the nearest integer number of control intervals in θ'.

Since product selectivities from chromatograph data are available

at 360 second intervals, control action on the outer loop cannot be taken at intervals less than this, thus T=360 s and N=1. Using these values, and recognizing that a unit step in the z-domain is given by $1/1-z^{-1}$, Equation 5.11 becomes

$$\frac{S_{3,m}(z)}{S_{3,set}(z)} = \frac{(1 - e^{-360/\lambda})z^{-2}}{1 - e^{-360/\lambda}z^{-1}} \qquad 5.12$$

From Figure 5.2:

$$S_{3,m}(z) = H_1G_2G(z) \cdot G_1(Z)[S_{3,set}(z) - S_{3,m}(z)] \qquad 5.13$$

where $H_1G_2G(z)$ is the pulse transfer function given by

$$H_1G_2G(z) = z\{H_1(s)G_2(s)G(s)\}$$

Solving for $G_1(z)$ in Equation 5.12:

$$G_1(z) = \frac{1}{H_1G_2G(z)} \cdot \frac{S_{3,m}(z)/S_{3,set}(z)}{1 - S_{3,m}(z)/S_{3,set}(z)} \qquad 5.14$$

where $S_{3,m}(z)/S_{3,set}(z)$ is desired closed loop response of the outer loop, specified by Equation 5.12.

Solving the pulse transfer function, Equation 5.14, and using $G_1(z) = T_{R,set}(z)/\epsilon_{S_3}(z)$, the following form was found for Equation 5.14:

$$\frac{T_{R,set}(z)}{\epsilon_{S_3}(z)} = \frac{a_1 - a_1a_2z^{-1}}{a_3 - a_3(1-a_1)z^{-1} - a_1a_3z^{-2}} \qquad 5.15$$

where $a_1 = 1 - e^{-360/\lambda}$

$a_2 = e^{-360/\tau}$

$a_3 = K(1 - a_2)$

Converted to the discrete time domain, Equation 5.15 becomes after rearrangement

$$T_{R,set,t} = \frac{a_1}{a_3}(\varepsilon_{S_3,t} - a_2 \varepsilon_{S_3,t-1}) + (1-a_1)T_{R,set,t-1} + a_1 T_{R,set,t-2} \qquad 5.16$$

where $\varepsilon_{S_3} = S_{3,set} - S_{3,measured}$

Equation 5.16 is the final form of the Dahlin's algorithm which was implemented in the simulations of the cascade control system.

In implementing Equation 5.16 it is necessary to specify K and τ (Equation 5.8) and the desired time constant λ of the response of the outer S_3 loop (Equation 5.9). The gain K is given by $K_2^{avg} = -.0173$, from Table 5.1. The time constant τ is estimated by observing the inner closed loop response of S_3 to step setpoint changes in $T_{R,set}$.

The closed loop responses to 3 C^o steps up and down in $T_{R,set}$ are shown in Figure 5.11 (PI controller with parameters at w=1 from Table 5.1) and Figure 5.12 (PI controller with parameters at w=0 from Table 5.1). No measurement noise was added to the temperature responses or S_3 for these tests. The responses of S_3 in Figures 5.11 and 5.12 show again the range of behaviour to be expected in S_3 with differently tuned inner temperature loops. These plots differ slightly from Figures 5.7, 5.8 or 5.9, in that these plots show the deterministic behaviour of the inner loop, using PI parameters tuned from simulations where measurement

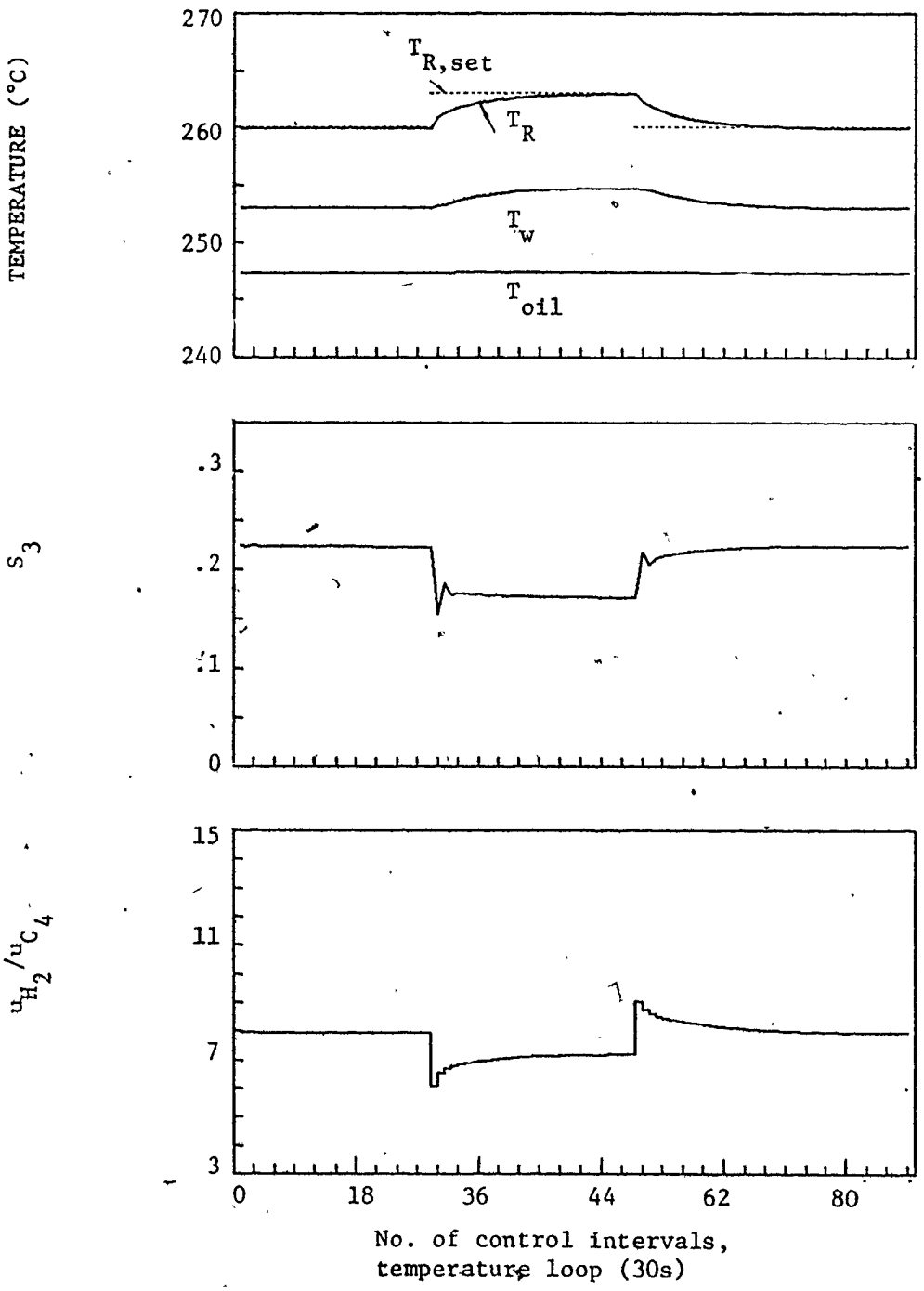

FIGURE 5.11 Temperature loop response to step setpoint changes to T_R, w=1 controller tuning

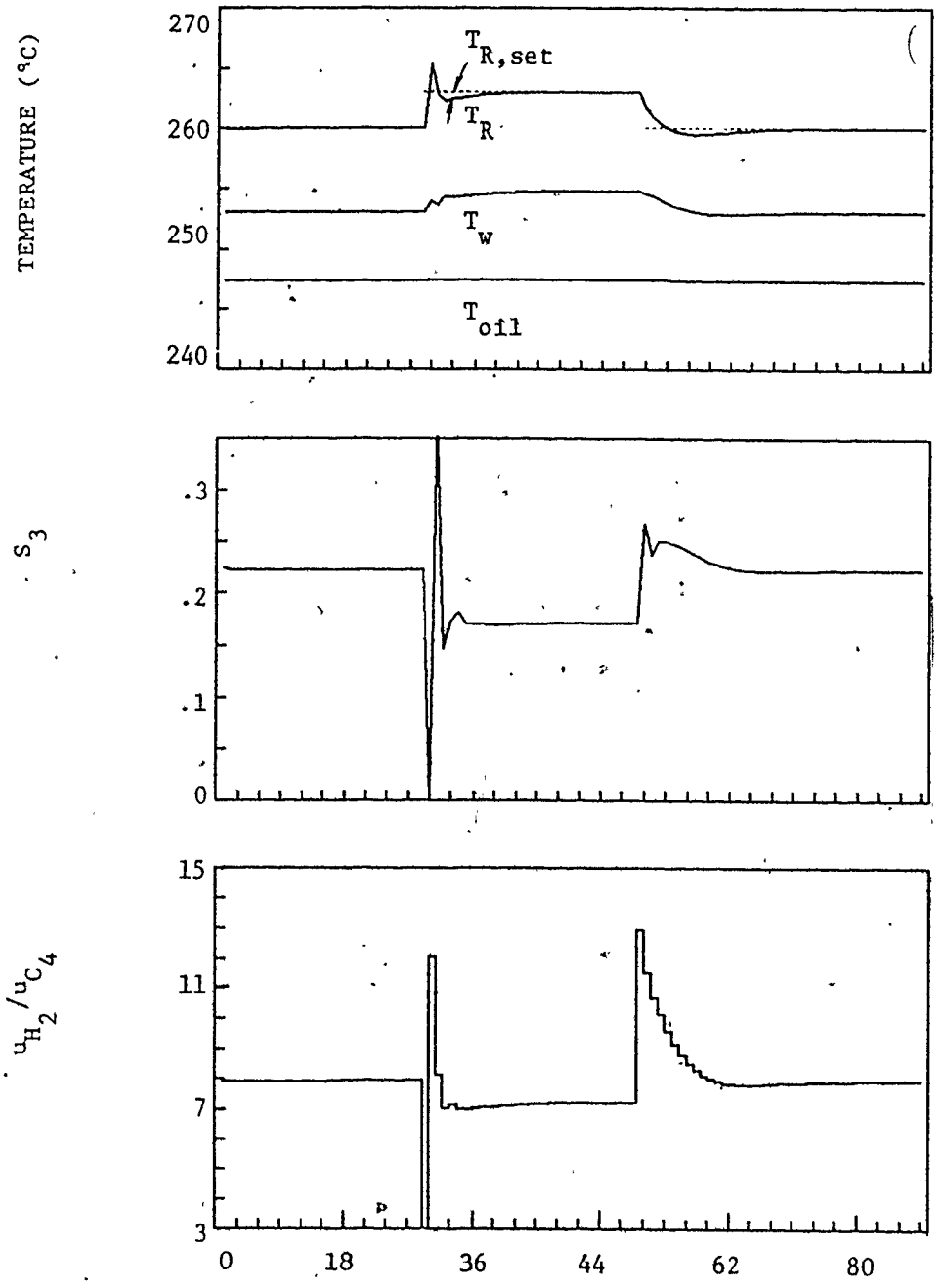

FIGURE 5.12 Temperature loop response to step setpoint changes to T_R, w=0 controller tuning.

noise was added to the temperature responses and S_3. The response of S_3 in Figure 5.11 more closely resembles a first order response than the S_3 response in Figure 5.12. Furthermore, the variation is S_3 is less when T_R setpoint changes are made. For simulation testing of the cascade control system therefore, PI parameters tuned with w=1 (i.e., K_p = .573, K_I = .073) will be used. It is difficult to estimate a time constant from the S_3 response in Figure 5.11; for the simulations a range of values of τ will be tested.

5.4.2 Testing of the Cascade Control System.

The Dahlin's controller Equation 5.16 was tested for a step setpoint change in S_3 from .22 to .26, for each of the levels of τ: 30, 70 and 140 s. The time constant λ was specified λ = 150 s for these tests. No measurement noise was added to the temperature or S_3 responses for these tests. As with previous simulations, total volumetric feedrate and oil inlet temperature were constant at 3.5 s.c.f.m. and 247 ^{o}C, respectively. Inner loop tuning was K_p = .573 and K_I = .073.

The control system performed adequately; very little difference in behaviour was observed over the levels of τ tested. A representative plot of the system responses is shown in Figure 5.13. The T_R setpoints shown in the upper plot of Figure 5.13 are the outputs from the Dahlin's controller. It should be noted that $S_{3,m}$ is plotted in this figure, as opposed to S_3 in all previous figures, showing the 360 s measurement delay in $S_{3,m}$.

Examining the behaviour of $T_{R,set}$ in Figure 5.13 it is seen that the first adjustment to $T_{R,set}$ in response to the setpoint change in S_3, is large. This first $T_{R,set}$ is approximately at the level required to bring S_3 to its new setpoint. It was recognized later (after the reactor control runs) that this large adjustment to $T_{R,set}$ results from setting λ too small relative to the control interval on the S_3 loop (360 s). The result of these initial simulations of the cascade control system suggest that the Dahlin's controller is insensitive to τ. Recall that the dynamic response of S_3 to changes in $T_{R,set}$ has been approximated by a first order transfer function, Equation 5.8. The Dahlin's controller was designed on the basis of this assumed response for the inner loop. With the detuned PI parameters used, the response of S_3 to a step change to $TR_{,set}$, is in fact not far from first order (Figure 5.13). The initial jump in S_3 can be accounted for in the transfer function by specifying a smaller τ. However inaccurate specification of τ is not likely to cause a problem with this particular design of the Dahlin's controller for the following reason. The Dahlin's controller works on a control interval of 360 s. The actual response (Figure 5.13) of $S_{3,m}$ to a step change in $T_{R,set}$ is essentially complete in this time (including 360 s measurement delay). If τ is specified incorrectly, the error will not be apparent to the Dahlin's controller; it takes control actions on what are essentially steady state responses of S_3. Correct specification of the gain in Equation 5.8 is more important. This gain was estimated by step testing using the simulation model (Section 5.2) in the same operating region as these

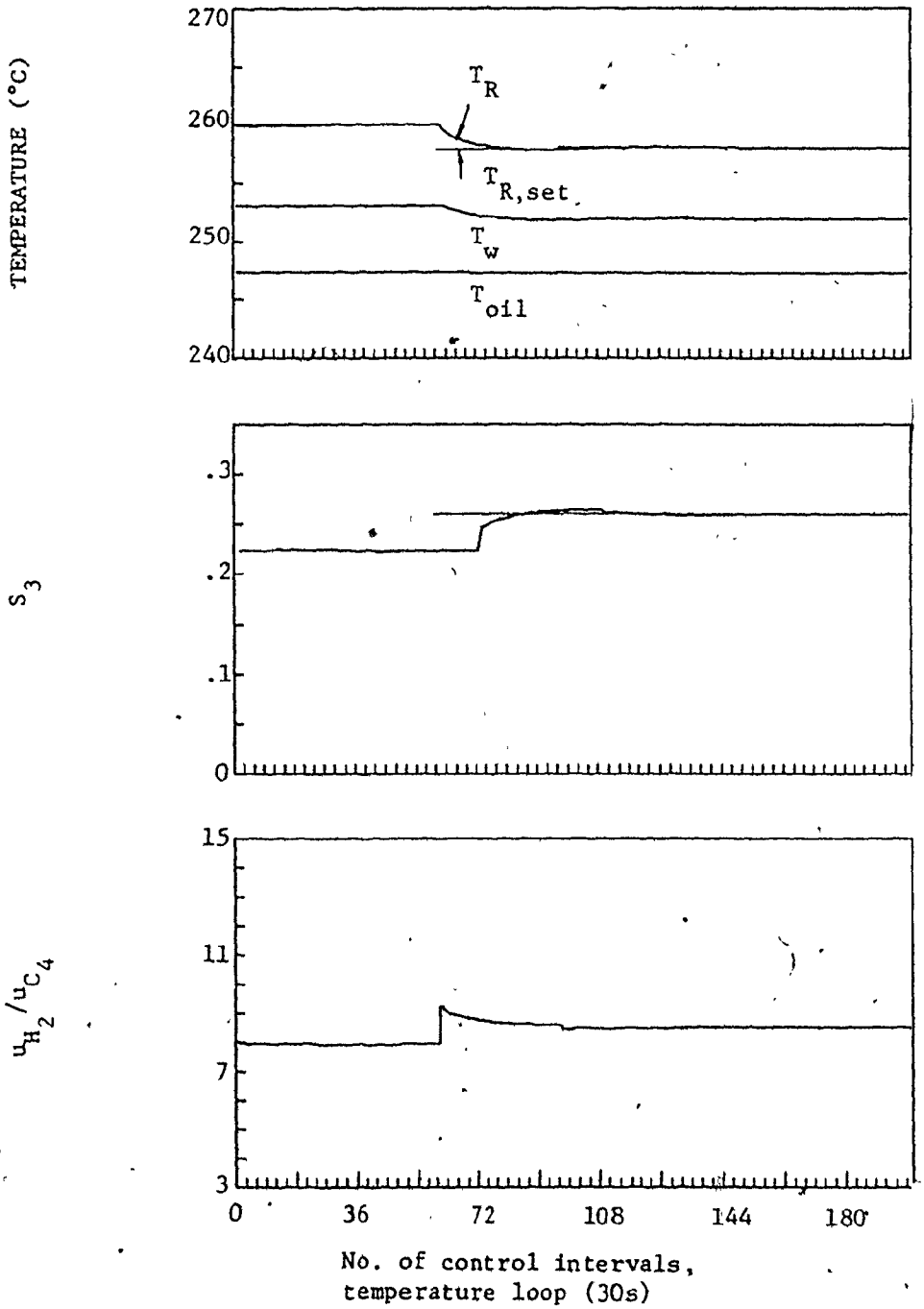

FIGURE 5.13 Response of cascade control system to step up in S_3 setpoint from .22 to .26, temperature loop: w=1 tuning, S_3 loop: τ=70, λ=150

simulations and therefore can be considered accurate.

For subsequent simulations, τ=70 s and λ=150 s, (with K_p=.573, K_I=.073) were used.

Figure 5.14 shows the performance of the control system to a ramp down in $T_{oil,in}$ from 247°C at t=0 to 242°C at 200 control intervals. S_3 setpoint was constant at .22. The performance of the control system is excellent; S_3 is held at the setpoint over the entire test interval. As the wall temperature drops in response to the decreasing oil inlet temperature, the rate of heat transfer to the wall from the catalyst bed increases. A greater heat generation from reaction is required to maintain reaction temperature; the temperature controller calls for decreasing u_{H_2}/u_{C_4}. The Dahlin's controller in striving to maintain S_3 at its setpoint, slowly adjusts $T_{R,set}$ down, so that the combination of reaction temperature and u_{H_2}/u_{C_4} is correct to keep S_3 constant at the desired setpoint.

Figure 5.15 shows the performance of the control system to a ramp down in catalyst activity from 1.87 at t=0 to 1.13 at 100 control intervals, after which it was held constant at 1.13. This represents a severe decay in catalyst activity (and would be unlikely to occur in a real system unless the catalyst was poisoned). Over the period when the catalyst decay is occuring, the Dahlin's controller is always 'behind'. That is, control action taken is never sufficient to bring S_3 back to its setpoint, because an additional amount of catalyst decay has occured over the control interval. As the catalyst activity decays, a higher reaction temperature is called for by the Dahlin's controller to

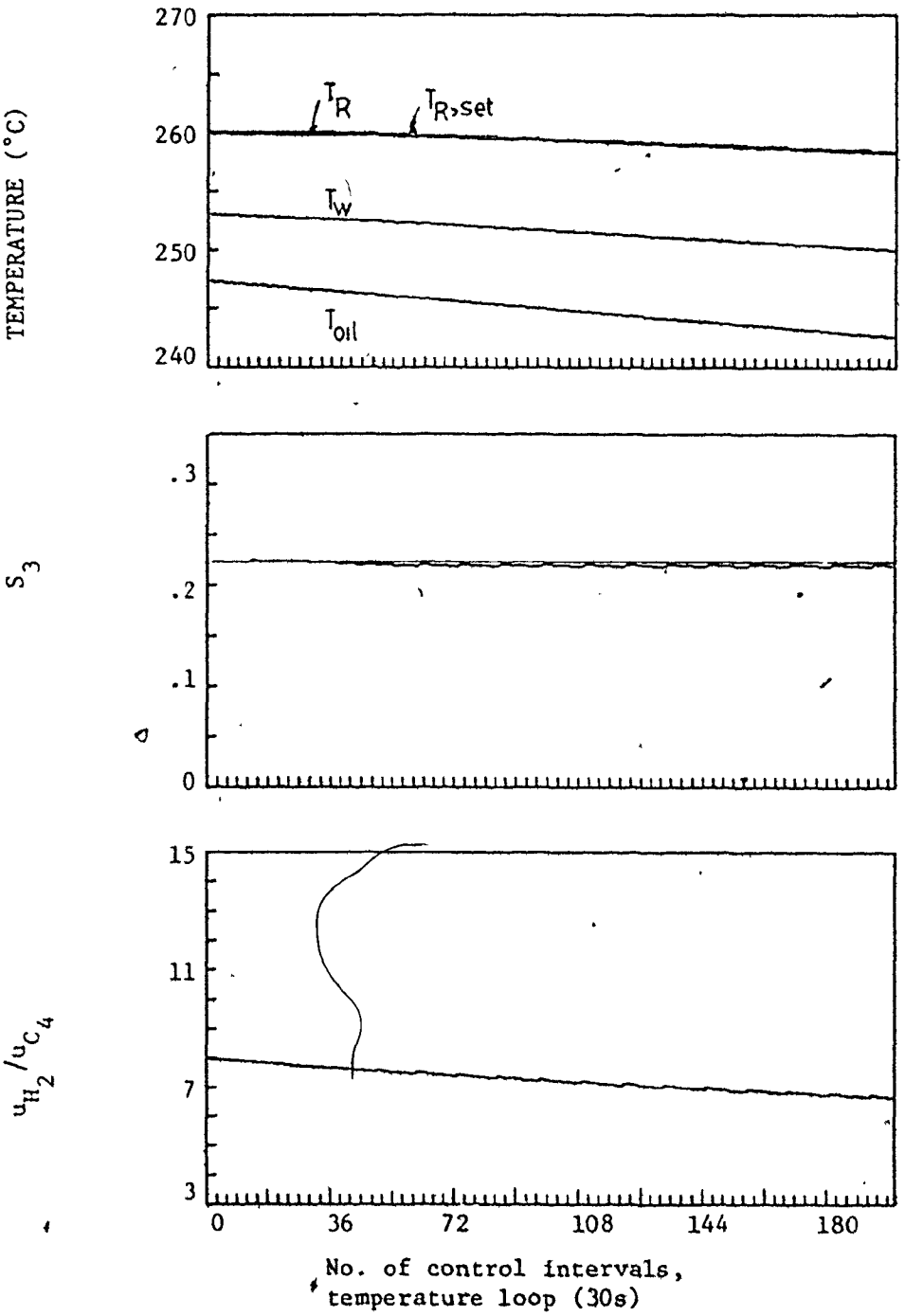

FIGURE 5.14 Response of cascade control system to ramp down in $T_{oil,in}$ (247 °C to 242 °C over 200 control intervals) temperature loop: w=1 tuning, S_3 loop: τ=70, λ=150

achieve the desired level of S_3. The inner loop responds by progressively lowering u_{H_2}/u_{C_4}.

In summary, the performance of the cascade control system on the simulation model is satisfactory. The tuning parameters τ=70, λ=150, K_p=.573 and K_I=.073 were considered to be adequate for initial testing of the control system on the fluidized bed reactor.

The simulations also uncovered interesting dynamic behaviour in T_R; its response to u_{H_2}/u_{C_4}, the manipulated variable for the temperature loop, is asymmetric.

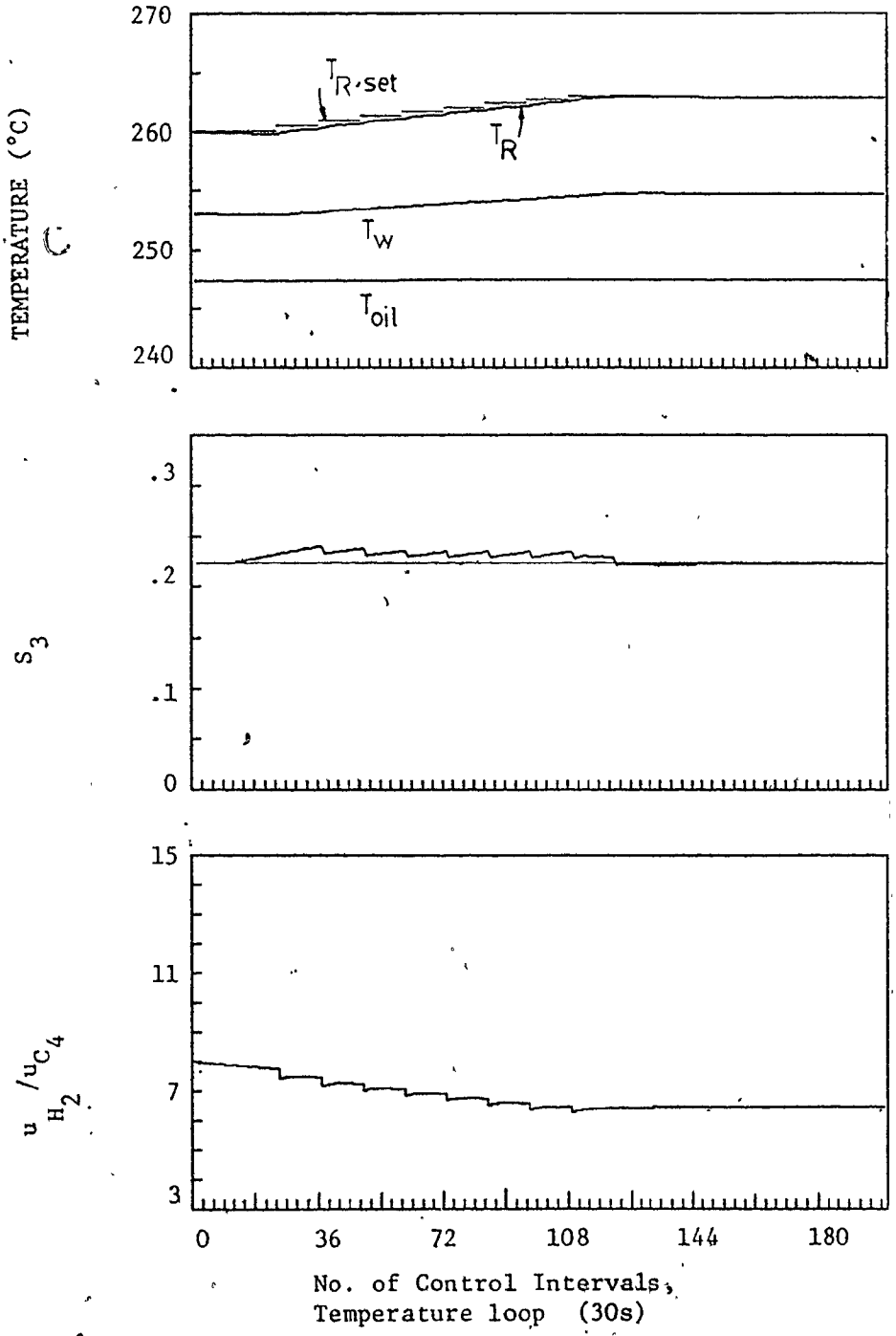

FIGURE 5.15 Response of cascade control system to ramp down in catalyst activity from $k/k_o = 1.87$ (t=0) to $k/k_o = 1.13$ ($t \geq 3000$, 100 control intervals) temperature loop: w=1 tuning, S_3 loop: τ=70, λ=150

CHAPTER 6

REACTOR CONTROL RUNS

6.1 INTRODUCTION

This chapter describes the on-line implementation on the fluidized bed reactor of the cascade control strategy developed and tested on the simulation model in Chapter 5. The results of the simulation tests suggested reasonable values for the PI parameters on the temperature loop and for the parameters in the Dahlin's algorithm controller, τ and λ. These parameters were used as a starting point in implementing the control system on the reactor.

A third level of cascade control is required for on-line implementation of this control system. This level manipulates the stem positions of the n-butane and hydrogen control valves to maintain the feed flowrates at setpoints specified by the temperature controller.

The testing of the control system proceeded as follows. The temperature loop was evaluated first (RUNS 1 and 2, Section 6.2), by applying a number of step changes to T_R setpoint. The setpoints were entered on-line at the computer console. The outer S_3 loop was not active for these tests. At the completion of these runs, the S_3 loop was activated, with S_3 setpoint and desired controller parameters entered on-line at the console. The control system was evaluated for step changes to S_3 setpoint and for a step disturbance in oil inlet temperature (RUNS 3, 4 and 5, Section 6.3).

Section 6.4 provides a summary and discussion of the results from Chapters 5 and 6.

6.2 TEMPERATURE LOOP TESTING

Testing of the temperature loop was performed with PI parameters estimated at w=1 from Section 5.3 (i.e., K_p = .573, K_I = .073). These parameters represented a detuned PI controller, and the resulting tracking response of temperature in simulation tests was sluggish. However, because less severe manipulation to u_{H_2}/u_{C_4} were required, the variation in the response of S_3 was minimized.

When implemented on the reactor system, a PI controller with these same tuning parameters resulted in a similar response. Figure 6.1 (RUN 1) shows the response of the temperature loop to a step decrease in T_R setpoint from 251.5°C to 249.0 °C. Total volumetric feedrate to the reactor was held constant at 3.3 s.c.f.m. for RUN 1 (and RUN 2). The oil inlet temperature was held constant around 248°C, by manual manipulation of the air flowrate to the air cooler. The tracking response of T_R is sluggish as expected, and is reflected by the relatively small maniuplations requested in u_{H_2}/u_{C_4}. The operating region of T_R for this run is not much higher than the oil inlet temperature, and the resulting low heat transfer rate to the wall contributes to the sluggish response of T_R to a decrease in setpoint. The response of S_3 is smooth in transition to its new level, and shows little variation with T_R controlled at a fixed setpoint. The selectivities and conversions plotted in Figure 6.1 (and in all subsequent figures in this chapter) are those corresponding to the times

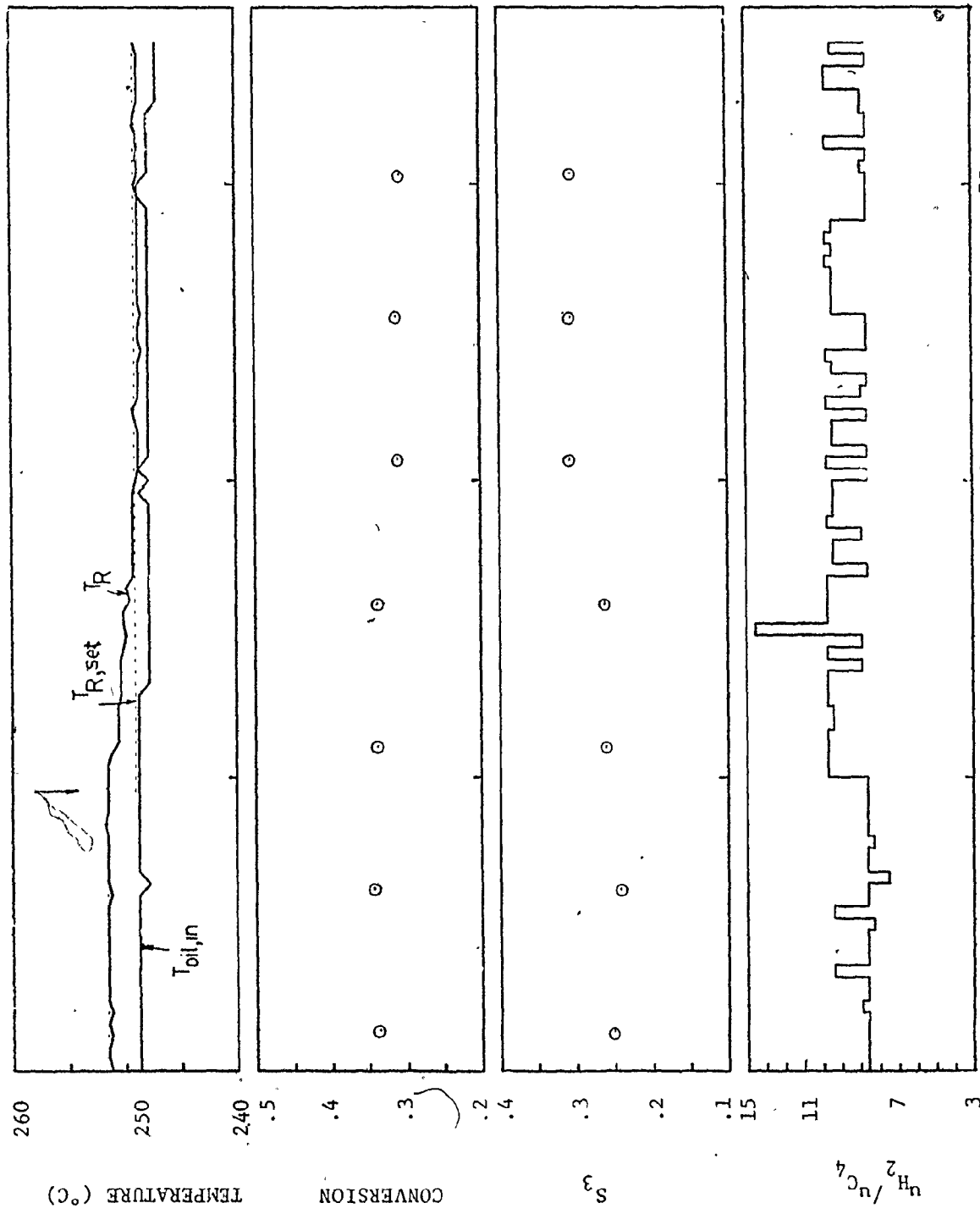

FIGURE 6.1 RUN 1: Step change to $T_{R,set}$ from 251.5°C to 249.0°C

at which the chromatograph samples were taken. The variation in S_3 is less than that observed in the simulation runs for several reasons. The noise in the response of T_R in the real system is less than that simulated resulting in less variation in the requested manipulations of u_{H_2}/u_{C_4}. In the simulations, the response of S_3 at the top of the catalyst bed was plotted at 30 s intervals, reflecting each manipulation to u_{H_2}/u_{C_4}. On the real system, the exit gas from the reactor is sampled at 360 s (approximately) intervals. This sampling frequency is low compared to the actual frequency content of the response of S_3; much of the dynamic character of this response is lost in sampling. Also, the dynamic responses at the top of the catalyst bed are damped by mixing as the product gas passes through the disengaging section of the reactor.

Figure 6.2 (RUN 2) shows the performance of the temperature loop to a step increase in T_R setpoint from 250.0 °C to 252.0 °C. Parameter tuning and reactor conditions were the same as those used in RUN 1. The tracking response of T_R is faster in this case (note the difference in time scales of Figure 6.1 and 6.2). The response of S_3 is smooth.

RUNS 1 and 2 showed that the objective of minimizing variation in S_3 was achieved on the real system with the PI parameters tested. Therefore, subsequent testing of the control system proceeded using these parameter values.

6.3 CASCADE CONTROL SYSTEM TESTING

In implementing the cascade control system on the reactor, it was

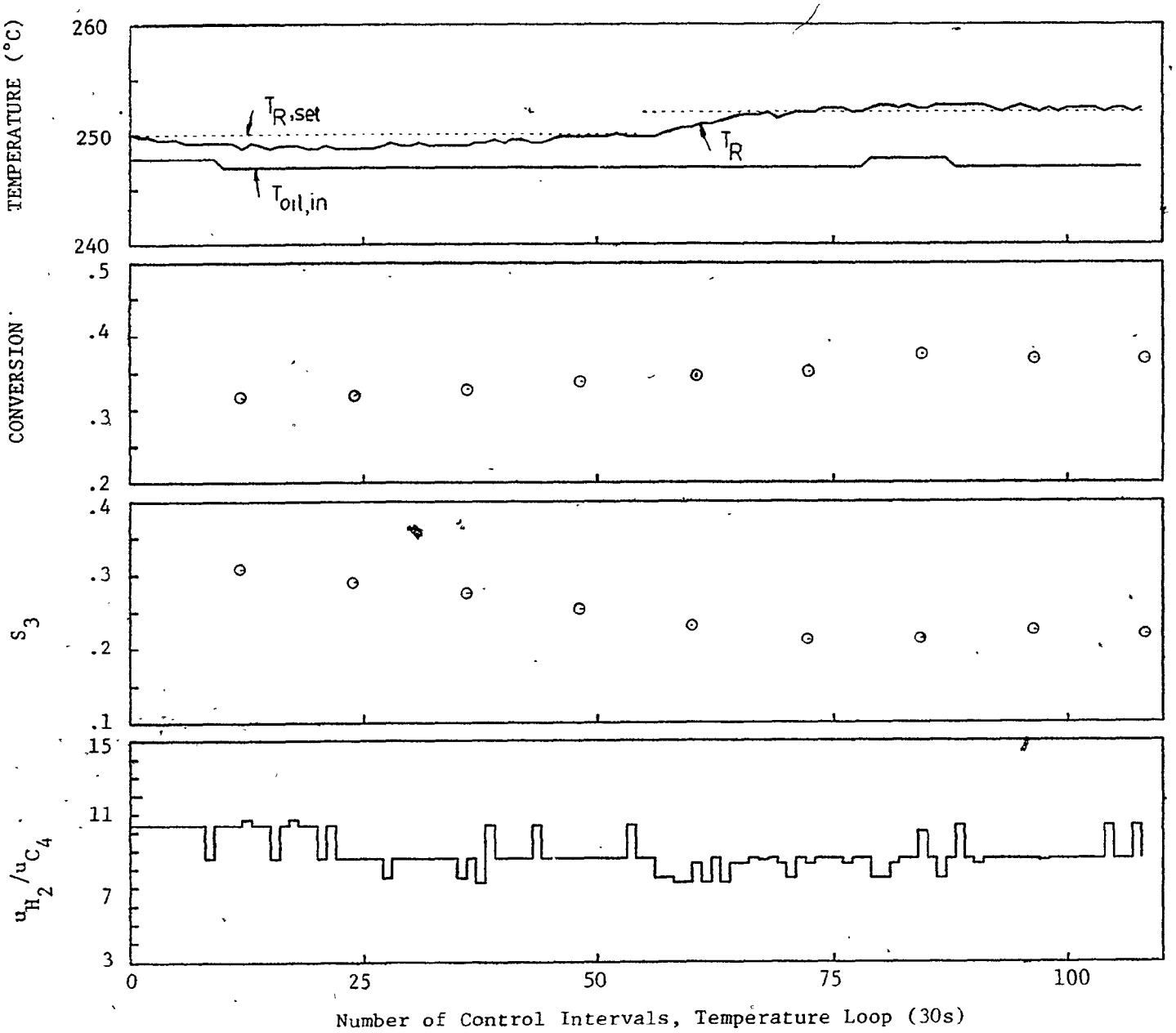

FIGURE 6.2 RUN 2: Step change to $T_{R,set}$ from 250.0 °C to 252.0 °C

recognized that the open volume of disengaging section would have a damping effect on the dynamic response of S_3 at the reactor exit. It was assumed that the disengaging section could be treated as a perfectly mixed tank and the dynamic effect on S_3 could be modelled with a first order transfer function with unity gain and time constant equal to the volume of the disengaging section (including the open volume in the reaction chamber above the catalyst bed) divided by the volumetric flowrate through the reactor. The design of the Dahlin's controller used in the simulation studies was modified to inlcude this transfer function, (i.e., in addition to the assumed first order transfer function for the dynamic response of S_3 at the top of the catalyst bed).

An initial run with this controller was unsuccessful as computational difficulties developed in the algorithm, the source of which was unresolved at the time of writing. This algorithm was abandoned and all subsequent runs used the algorithm from the simulation studies (Equation 5.16). The damping effect of the disengaging section was included into this algorithm by increasing the time constant τ, of the assumed first order transfer function for the dynamic response of S_3 at the top of the catalyst bed.

The first test of this algorithm on the reactor system was for a step setpoint in S_3 from .23 to .26: RUN 3, Figure 6.3. The time constant τ was increased to 100 s, with λ = 150 s, for this run. The temperature loop tuning remained at K_p = .573 and K_I = .073. Total volumetric feedrate was held constant at 3.3 s.c.f.m., and oil inlet temperature was held around 247^{o}C.

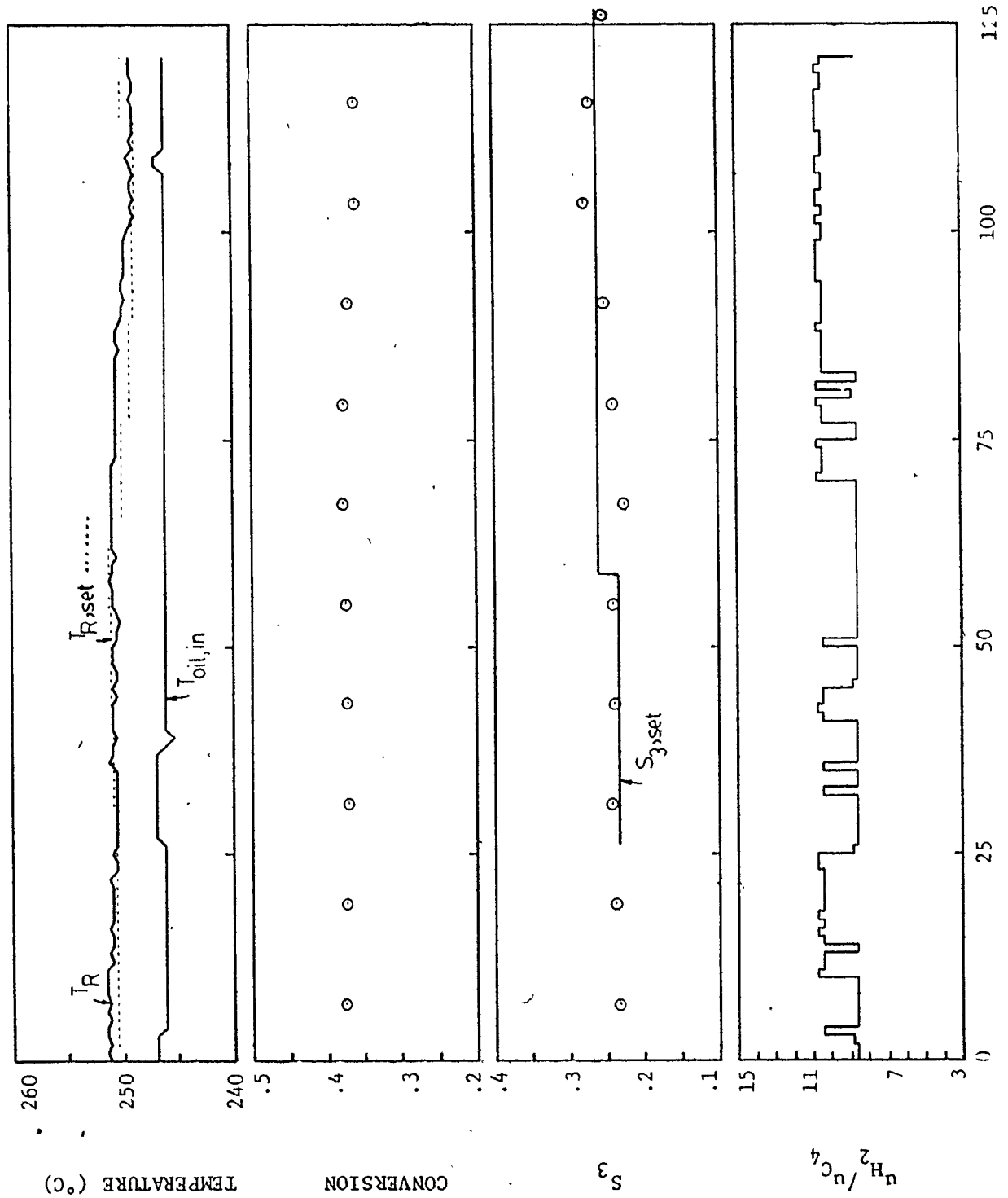

Number of Control Intervals, Temperature Loop (30s)

FIGURE 6.3 RUN 3: Step change in $S_{3,set}$ from .23 to .26

The performance of the control system is satisfactory; S_3 moves smoothly with some overshoot to the new setpoint. The run was cut short due to mechanical difficulties, but it appeared as though the response of S_3 was tending to settle out. Some oscillation would be expected, however, as the last T_R setpoint called for by the Dahlin's controller was increased near the end of the run. Considering the sluggish temperature response, the net result of small adjustments up and down in $T_{R,set}$ would not significantly effect the response of S_3.

RUN 4 (Figure 6.4) evaluated the performance of the control system to a step down in S_3 setpoint from .31 to .24. This run was performed the day after the previous runs. The catalyst had been kept hot overnight using the circulating oil system, and with hydrogen flowing (at a rate to maintain minimum fluidization) through the catalyst bed. On the second day the catalyst activity was observed to have increased significantly from the previous day, as indicated by the different operating conditions required to stabilize the reactor. On the first day (RUN 3) T_R was controlled around 251°C ($T_{oil,in}$ was at 246°C) with u_{H_2}/u_{C_4} manipulations in the region 8.5 to 10.5. The resulting S_3 responses were around .23. On the second day, T_R was controlled at 251°C ($T_{oil,in}$ remained at 246°C) with manipulations in u_{H_2}/u_{C_4} around 14, i.e., less butane was required at comparable cooling rates. The response of S_3 showed more variation, averaging .32. One explanation for this increased variation in S_3 is that it resulted from poor temperature control in this operating region. With u_{H_2}/u_{C_4} around 14 (total volumetric flowrate for this run was 3.2 s.c.f.m.), the butane

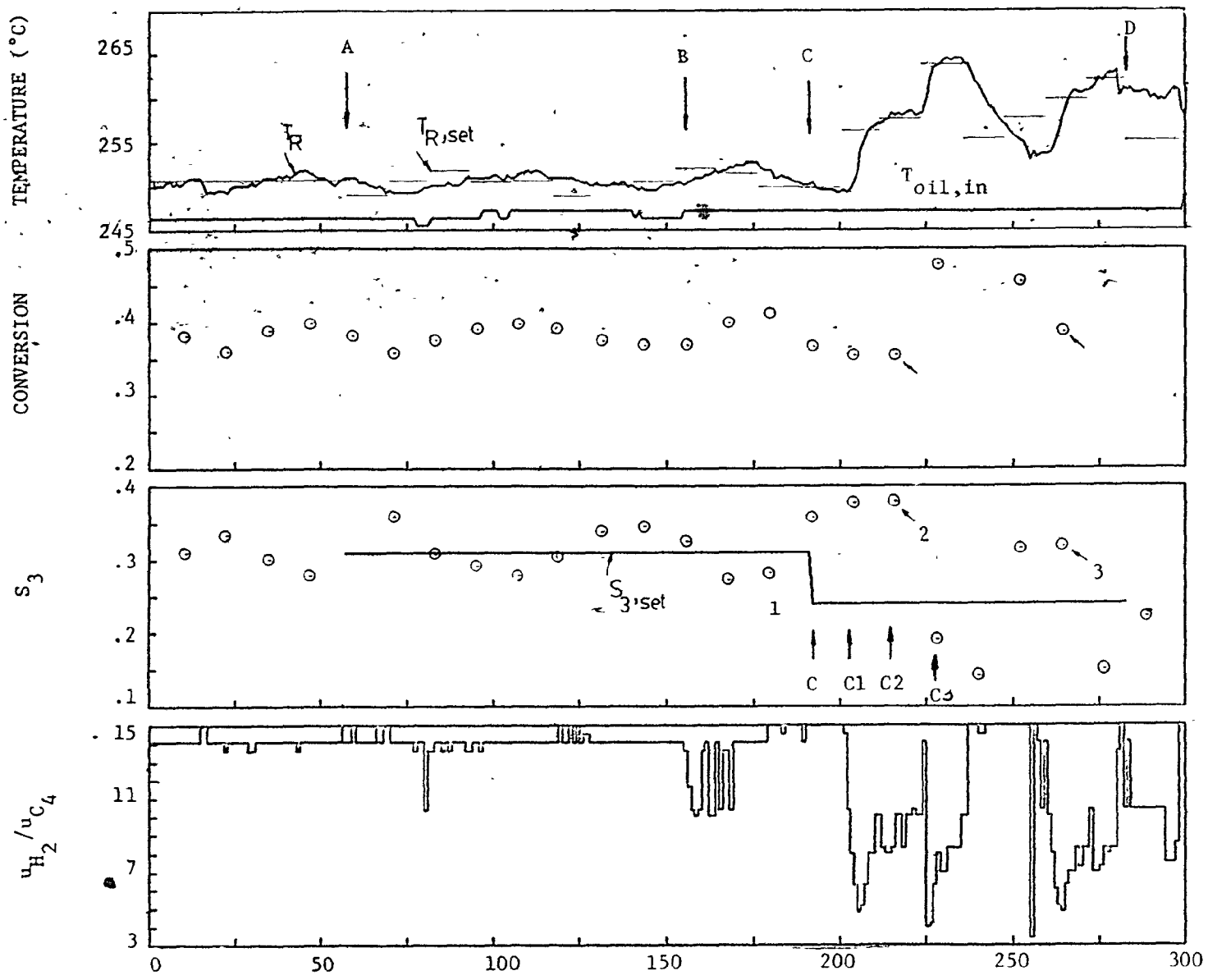

FIGURE 6.4 RUN 4: Step change in $S_{3,set}$ from .31 to .24

feedrate is around .23 s.c.f.m.. This is at the extreme low end of the calibration region for butane flow and the control valve is nearly closed; manipulation of butane flow is inaccurate in this region and results in poor temperature control. Furthermore, the process gain (between T_R and u_{H_2}/u_{C_4}) is lower in this region and a fixed control (tuned at different operating conditions) would be expected to regulate less efficiently. This is particularly true of the PI controller used in this case, since it was highly detuned.

At A (Figure 6.4) the Dahlin's controller was activated with $S_{3,set} = .31$, $\tau = 100$ s and $\lambda = 150$ s. The temperature loop parameters were the same as those used to begin the run. The variation of S_3 during the period A to B was not significantly less than before the Dahlin's controller was activated. The tracking response of T_R is extremely slow; it is not able to keep up with changes in setpoints called for by the Dahlin's controller. Little difference is seen in the dynamic behaviour of T_R during this period and before the Dahlin's controller was activated, which explains the behaviour of S_3. At B, the PI controller gains were increased to $K_p = 1.03$ and $K_I = .340$ ($w = .000125$ tuning parameters from Section 5.3), to speed up the tracking response of T_R. These PI parameters were in effect up to the end of the run. The temperature response with this higher gain controller was considerably faster but the performance of the overall controller system did not improve. At C it was decided to go ahead witha change in $S_{3,set}$ to .24. It shoud be pointed out again that the plotted S_3 responses in Figure 6.4 correspond to the time at which the chromatograph samples

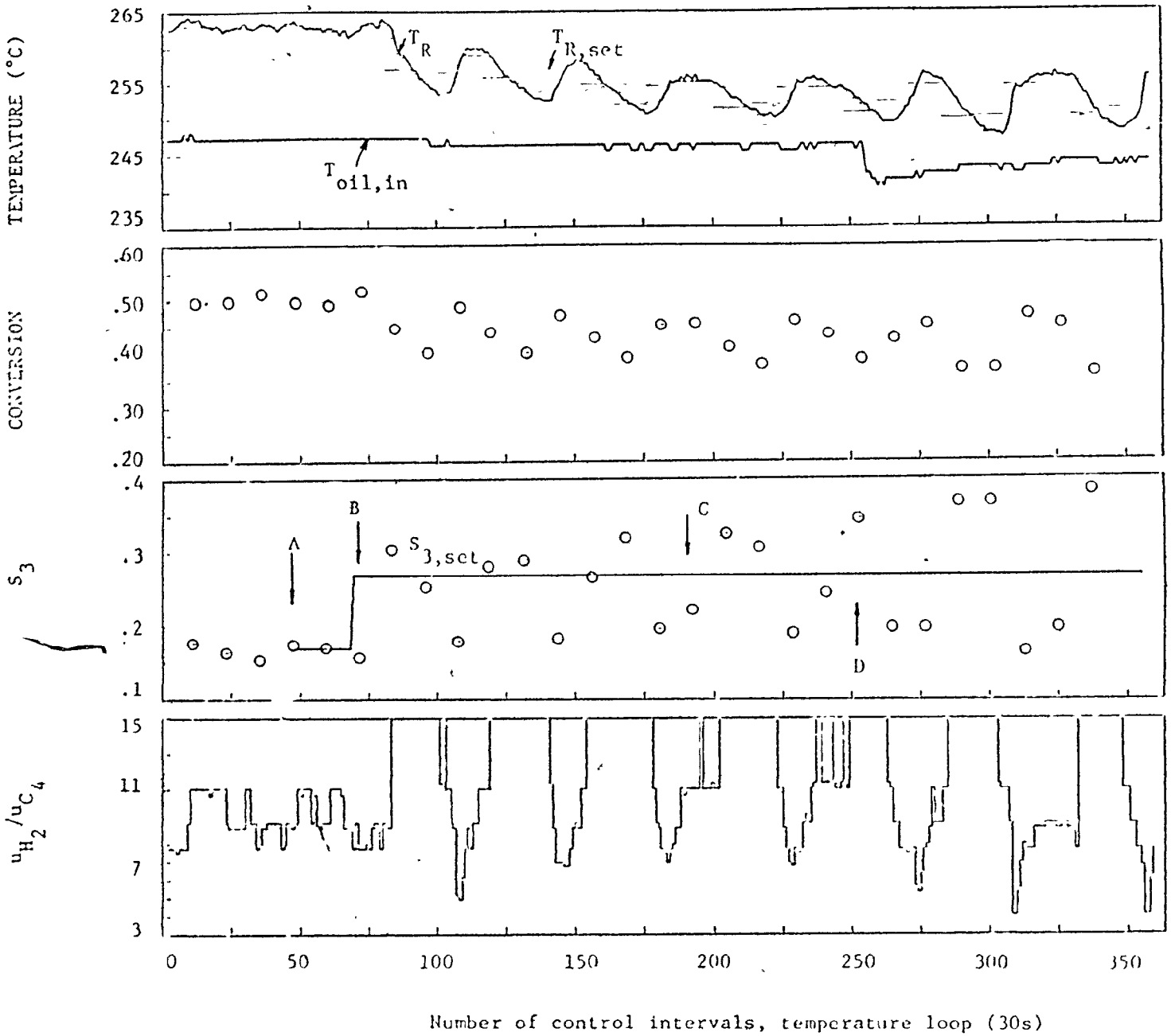

FIGURE 6.5 RUN 5: Step change to $S_{3,set}$ from .17 to .27. Load disturbance in $T_{oil,in}$

were taken. Thus, when the change to $S_{3,set}$ made at C, the calculated error corresponds to the S_3 datum marked '1' in Figure 6.4. Since this observed S_3 is not appreciably higher than the new S_3 setpoint, minimal adjustment is made to $T_{R,set}$ (the algorithm is also accounting for previous control actions). However, at the next control interval C1, the error is appreciable and a large adjustment up in $T_{R,set}$ is made. At C2, the error is still large, but the controller 'remembers' the previous adjustment to $T_{R,set}$, and only a small additional increase is made. At C3, the controller calcuates the error based on the S_3 observation marked '2'. This observation is in fact faulty, resulting from a failure of the chromatograph programmer to initiate an analysis cycle after the completion of the previous analysis. The reported S_3 is simply a repeat of the previously determined value. The Dahlin's controller interprets this observation as indicating that S_3 is not responding to the control actions previously taken, and a further large increase to $T_{R,set}$ is called for. This action injects a large disturbance into the orderly progress of the control actions, and it was anticipated that a number of control intervals would be required for the controller to recover. However, another faulty observation appeared to occur at '3' (although the corresponding conversion datum did not appear to be in error), and the run was terminated at D (S_3 loop de-activated). Had these errors occurred during a period of constant $S_{3,set}$ rather than during a period of transition, the consequences would not have been as severe. However, in evaluating the performance of this control system it must be concluded that the system is strongly dependent on having available reliable chromatograph data.

RUN 5 (Figure 6.5) tested the performance of the control system

to a step increase in $S_{3,set}$ from .17 to .27, and to a load disturbance in oil inlet temperature (an approximate step decrease of $5^{o}C$). From the start of the run to A the temperature loop alone was activated (K_p = 1.03, K_I = .340). However, in contrast to RUN 4, the starting T_R setpoint was $263^{o}C$ (compared to $251^{o}C$). Manipulations in u_{H_2}/u_{C_4} were in the range 8 to 11. Temperature control is tight in this region (up to A) and the resulting variation in S_3 is less than for the corresponding region in RUN 4. This is primarily a result of higher gain temperature controller parameters being used in RUN 5 than for initial region of RUN 4. Also, as pointed out before, temperature control up to C in RUN 4 was attempted in the region of $u_{H_2}/u_{C_4} \approx 14$, where manipulation of butane flow is innacurate, and where the controller gains were too highly detuned.

At A in RUN 5, the Dahlin's controller was activated with $S_{3,set}$ = .17, τ = 100 s and λ = 150 s. Subsequent control of S_3 at this setpoint is satisfactory and at B a step increase to $S_{3,set}$ from .17 to .27 was made (the setpoint change was entered at the console at the time indicated by the step in Figure 6.4, but the change was not actually recognized by the controller until the next control calculation was made, at B). The performance of the Dahlin's controller in the region B to C was oscillatory and unacceptable. At C the Dahlin's parameters were increased to τ = 150 s and λ = 350 s. The performance of the system did not improve and at D the planned load disturbance to the oil inlet temperature was made. The air flowrate to the air cooler was suddenly inoreased causing a rapid decrease in $T_{oil,in}$ as indicated in Figure 6.4. The subsequent behaviour of the manipulations to $T_{R,set}$ in this region did not change appreciably from the period before the load

disturbance was made. The resulting increase in cooling rate however, caused the temperature controller to call for lower u_{H_2}/u_{C_4} to increase the rate of heat generation by reaction. A chromatograph failure occured at datum '1', and the run was terminated shortly thereafter.

6.4 SUMMARY

The chromatograph failures in RUNS 4 and 5 make it difficult to evaluate the performance of the cascade control system under the conditions tested. However, by considering the performance of the control system for all the runs, a number of important observations can be made.

1. The response of the temperature loop is too slow with PI parameters obtained with w=1. The parameters obtained from tuning at w = .000125 gave faster response to setpoint changes and tighter control at the specified setpoint. With this higher gain controller an increase in variation in S_3 was not noticed (RUN 5); the manipulations in u_{H_2}/u_{C_4} did not cause S_3 to vary excessively, as suggested in the simulations. It is apparent that these variations are damped as a result of mixing of the product gas in the disengaging section. The variation in S_3 follows more closely the slower variation in reaction temperature. Much of the higher frequency ccontent of the dynamic response of S_3 at the reactor exit is also lost due to the low sampling frequency.

2. The mixing effect of the disengaging section is significant and must be included in the design of the Dahlin's controller for the S_3 loop. This can be done by modelling the disengaging section as a perfectly mixed tank, as described previously. Alternatively, the time constant τ of the response of S_3 (at the top of the catalyst bed) to T_R setpoint changes to the (closed) temperature loop, can be increased.

This is equivalent to assuming that the effect of the disengaging section is simply to slow the response of S_3. This latter approach was taken in implementing the control strategy on the reactor system.

3. The Dahlin's algorithm was implemented with λ too small. Since λ specifies the desired speed of response of measured S_3 (63.2% of the response of S_3 must be complete in λ s (plus 360 s for the measurement delay). The value of λ was increased to 350 s (RUN 5, C) but the oscillatory behaviour of the control system persisted, as this value was still too small.

Dahlin's algorithm works by cancelling the dynamics of the plant (in this case the dynamic response of S_3 at the reactor exit) by pole-zero cancellation. A desired dynamic response is substituted by pole placement (in this case specified by λ). The performance of the algorithm is dependent on having an accurate model of the plant. It has been assumed that the dynamic response of S_3 at the reactor exit can be modelled with a first order transfer function, as described previously. The sensitivity of Dahlin's algorithm to innacuracies in this plant model increases as λ is decreased. It is apparent (and expected) that some model innacuracy is present in this control system. The innapropriately small values of λ used accentuate the model inaccuracy and the result is the oscillatory behaviour that was observed. Observations made in Chapter 5 suggest that accurate specification of gain K is more important than τ, since the response of S_3 (at the top of catalyst bed for the simulations) is inherently fast. However, for the real reactor, this response is slowed considerably by the mixing effect of the disengaging section, and increases the relative importance of specifying τ correctly. Further runs should be performed with λ at

least 3 or 4 times greater than the outer loop control interval. A slower response in the outer loop is not undesireable, since the purpose of the outer loop is not primarily to provide for rapid setpoint tracking, but to regulate against slow disturbances entering the plant (i.e., catalyst decay or slow dirfts in inlet oil temperature). A detuned outer loop would still regulate against more rapid disturbances, but the system recovery would be slower.

4. It is difficult to ascertain the degree of sensitivity of the algorithm to changes in operating conditions (and plant characteristics) due to the many confounding factors which contributed to it's performance. However, RUN 3 was satisfactory (change in $S_{3,set}$ from .22 .23 to .26), while runs performed on the next day, after an increase in catalyst activity had occured overnight, showed poorer performance (RUNS 4 and 5). The previous suggestion is that a more highly detuned outer loop would perform more satisfactorily (in this case, at least not oscillate) when plant model innacuracy is present. In this particular plant the accuracy of a particular fixed linear model can be affected in many ways: from a change in operating conditions (due to the highly non-linear nature of the process), from a change in plant characteristics (typically catalyst decay or as observed in these runs, an increase in catalyst activity), or by the speed of the closed loop response of the temperature loop. Detuning of a control loop is a typical method for achieving acceptable (but in no sense optimal) control when these types of problems are present, and certainly points to the necessity of adaptive control algorithms. This same observation applies to the temperature loop. The reaction temperature response to changes in u_{H_2}/u_{C_4} is highly non-linear and exhibits asymmetric

behaviour.

5. The control system implemented is strongly dependent on reliable chromatograph information. A multivariable control strategy utilizing a state space model of the system and Kalman filtering would not be sensitive to chromatograph failures, as predicted selectivities could be used in the feedback controller.

CHAPTER 7

SUMMARY AND RECOMMENDATIONS

This thesis describes the modelling, simulation and direct digital computer control of the fluidized bed reactor in the Department of Chemical Engineering. It represents the first control study on this system, and has addressed the problems associated with the starting of control studies on a sophisticated pilot plant system. This thesis provides some of the necessary interfacing, modelling and simulation work on which future control studies on the fluidized bed reactor can be based.

A process interface has been installed between the pilot plant and the minicomputer system, providing the means for on-line datalogging and control implementation. The interface consists of instrumentation for the measurement and manipulation of feed flows, and for measurement of temperatures at selected points in the pilot plant. In addition, exit gas composition is measured with an on-line gas chromatograph.

The dynamic behaviour of the reactor system has been studied through the development and application of a dynamic simulation of the process. The simulation was based on a mechanistic description of the process and estimates for the unknown parameters in the mass/energy balance equations were obtained using dynamic temperature data from the reactor. This phase of the study (i.e., Chapters 3 and 4: dynamic modelling, development of the simulation, parameter estimation) provides

valuable insight into the dynamic behaviour of the system from a mechanistic viewpoint. Future studies should recognize the power of the simulation model in studying the open and closed behaviour of the process, and utilize the model accordingly.

In this study, the simulation model proved to be useful in testing of a control strategy before on-line implementation. This exercise was useful in defining the real-time programming requirements of the control system. Of greater importance however, was the analysis of the performance of the control system on the simulation model, which led to a better understanding and interpretation of the results from the on-line control runs.

The following specific conclusions and recommendations for future work pertain to specific phases of the study. By chapter:

3: The on-line control runs suggested that the open volume of the disengaging section (ie., including the open volume of the reaction barrel between the top of the catalyst bed and the disengaging section) has a significant damping effect on the dynamic responses of the exit gas compositions. It is suggested that this effect be modelled and included in the simulation as a separate DYNSYS module.

4: Estimates for the unknown parameters in the mass/energy balance equations were obtained using temperature data only. As a result, very high correlations existed among some of the parameter estimates. Better estimates will be obtained if composition data on

the reaction products are included in the estimation program. Moreover, the performance of this dynamic model in predicting temperature and composition responses should be evaluated against actual plant trials.

5 and 6: The performance of the cascade control system can be improved, as discussed in Section 6.4. This control system will provide a base case against which more sophisticated control systems may be evaluated and compared.

- The response of reaction temperature in the fluidized bed reactor to changes in feed composition is highly non-linear. Also, changes in catalyst activity were observed to occur during a run, as well as over periods of shut-down. Therefore, a fixed-parameter control system should not perform as well as adaptive type controllers when changes in operating levels are made or when changes in catalyst activity occur. It is suggested that future studies implement adaptive controllers on each of the loops of the cascade control system tested in this study.

- The overall control problem is a multivariable one in which three independent product gases require regulation. One possible approach to solving this problem would be to utilize a process model on-line in the form of an extended Kalman Filter to predict exit gas selectivities, and use this information in a feedback controller.

The controller can be designed using linear quadratic stochastic control theory by using local linearization of the non-linear process model. This approach then would be expected to provide satisfactory regulation when changes in operating conditions occur. The mechanistic model developed in this study would provide the basis for this approach.

APPENDIX A2.1 Relay box and multiplexer connections.

RELAY BOX CONNECTIONS

T.C. input	Pin designation	
1	–	A
	+	B
2	–	C
	+	D
3	–	J
	+	H
4	–	G
	+	F
5	–	E
	+	K
6	–	L
	+	M
7	–	N
	+	P
8	–	R
	+	Z
9	–	X
	+	W
10	–	V
	+	U
11	–	T
	+	S
12	–	a
	+	b
13	–	c
	+	d
14	–	e
	+	f
15	–	m
	+	k
16	–	j
	+	h

Pin connections for voltage from multiplexer :

+ 6v for Relay #	PIN (connector 3)
1	1
2	2
3	3
4	4
5	5
6	6
7	7
8	8

COMMON: PIN 3

Multiplexed outputs:

#1 :

+ Connector 1, Pin 2
– Connector 1, Pin 1

#2 :

+ Connector 1, Pin 4
– Connector 1, Pin 3

Multiplexer Connections

Manual Reset:

Connector 2, Pin 6
2, Pin 8
2, Pin 10

Minicomputer reset:

Connector 1, Pin 6
1, Pin 8
1, Pin 10

APPENDIX A2.2 Thermocouple locations

LOCATION	THERMOCOUPLE #
Reaction chamber, at distributor plate	*
Reaction chamber, 6 in. from distributor plate	*
Reaction chamber, 1 ft. from distributor plate	2
Reaction chamber, 2 ft. from distributor plate	4
Reaction chamber, 3 ft. from distributor plate	5
Reaction chamber, 4 ft. from distributor plate	*
Reaction chamber, at entrance to disengaging section	*
Reactor wall, 9 1/16 in. from distributor plate	*
Reactor wall, 17 9/16 in. from distributor plate	9
Reactor wall, 36 1/16 in. from distributor plate	10
Reactor feed line	8
Oil line entering heating/cooling coil	12
Oil line exiting heating/cooling coil	13
Oil line exiting circulating oil heating tank	14
Oil line entering feed preheater	*

* not in use

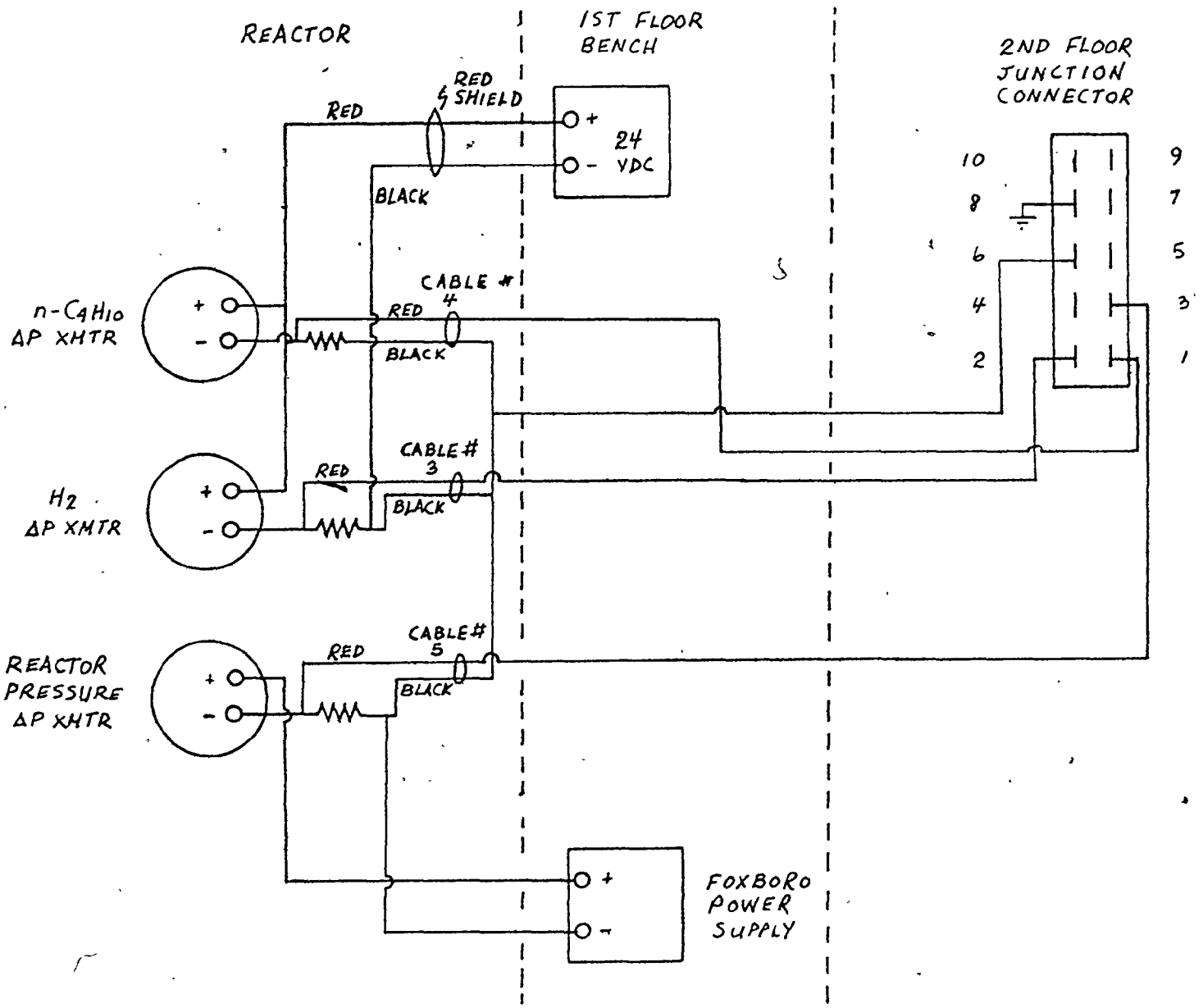

APPENDIX A2.3 Schematic of Flow Measurement Interface

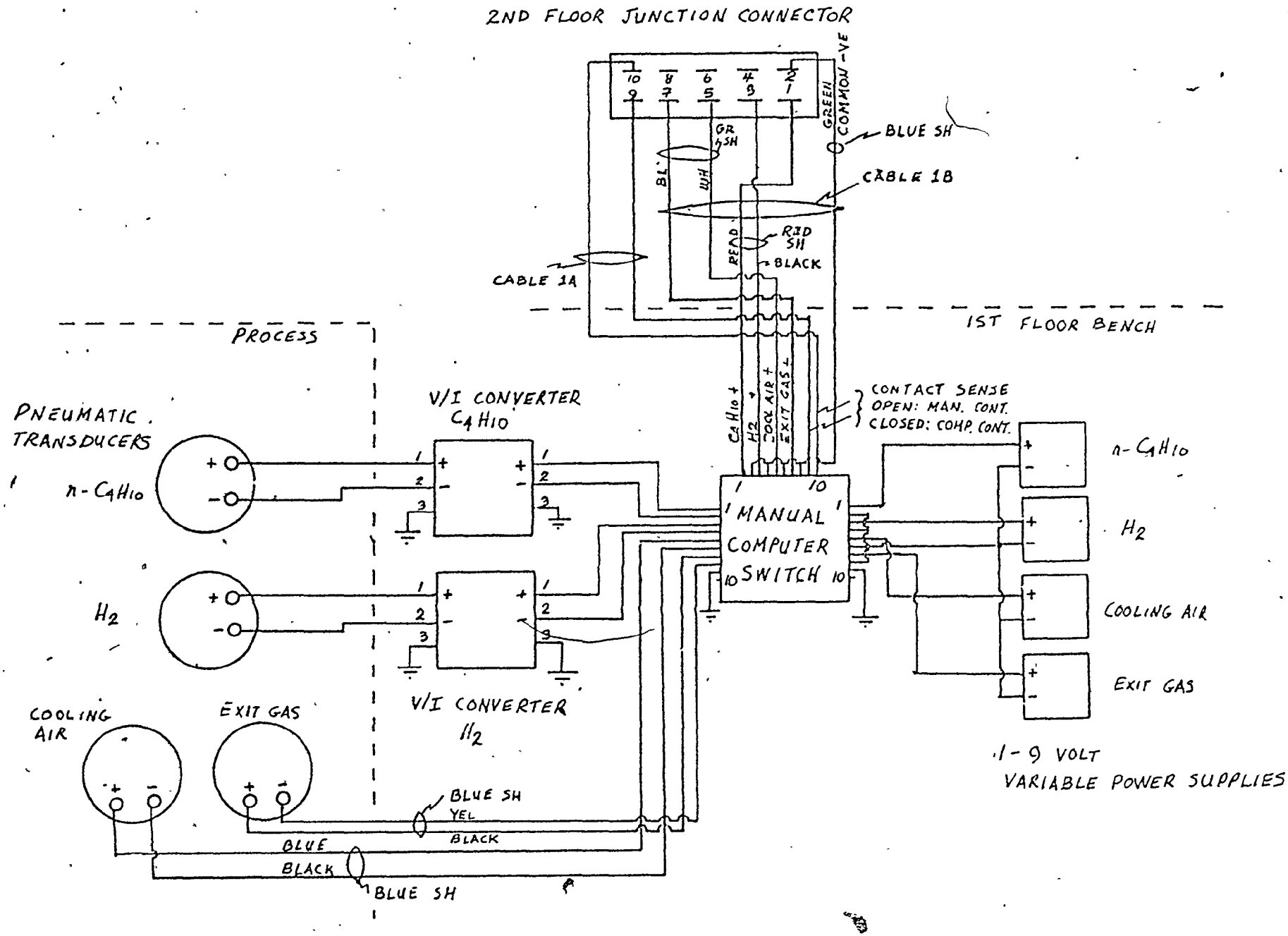

APPENDIX A2.4 Schematic of Control Valve Interface

APPENDIX A2.5 Pin connections for interface cable

1	+ C_4H_{10} valve	D/A ch 4000
2	+ H_2 valve	D/A ch 4001
3	+ air valve	D/A ch 5002
4	+ exit gas valve	D/A ch 5003
5	- ve common to above	
6		
7	contact sense ch. 12003 for 'MANUAL/AUTOMATIC' switch	
8		
9	N.O. Thermocouple multiplexer advance	
10	N.C. Relay ch 14002	
11.	common	
12	GROUND	
13	+ C_4H_{10} flow	A/D ch 3013
14	+ H_2 flow	A/D ch 3007
15	+ reactor pressure	A/D ch 3010
16		
17	- ve common to above	
18	N.O. Relay ch 14003	
19	common Nitrogen solenoid actuation	
20	- A/D ch 3012	
21	+ Thermocouple amplifier #2 signal	
22	+ A/D ch 3011	
23	- Thermocouple amplifier #1 signal	
24	No wire in transmission cable.	

APPENDIX A2.6 G.C. Cable #1 pin connections

1	+ CH_4	A/D ch 2005
2	+ C_2H_6	A/D ch 2006
3	+ C_3H_8	A/D ch 2007
4	+ C_4H_{10}	A/D ch 2010
5		
6		
7	- ve common to above	
8		
9	+	start of analysis contact sense#
10	-	
11	+	end of analysis contact sense#
12	-	
13		
14		
15		
16		
17	N.C.	single-cycle initiation
18		Relay output ch 14007
19	COMMON	
20		
21		
22		
23		
24	SHIELD	

These are wired at the programmer should they ever need to be used, but have not as yet been allocated contact sense channels at the DGDAC.

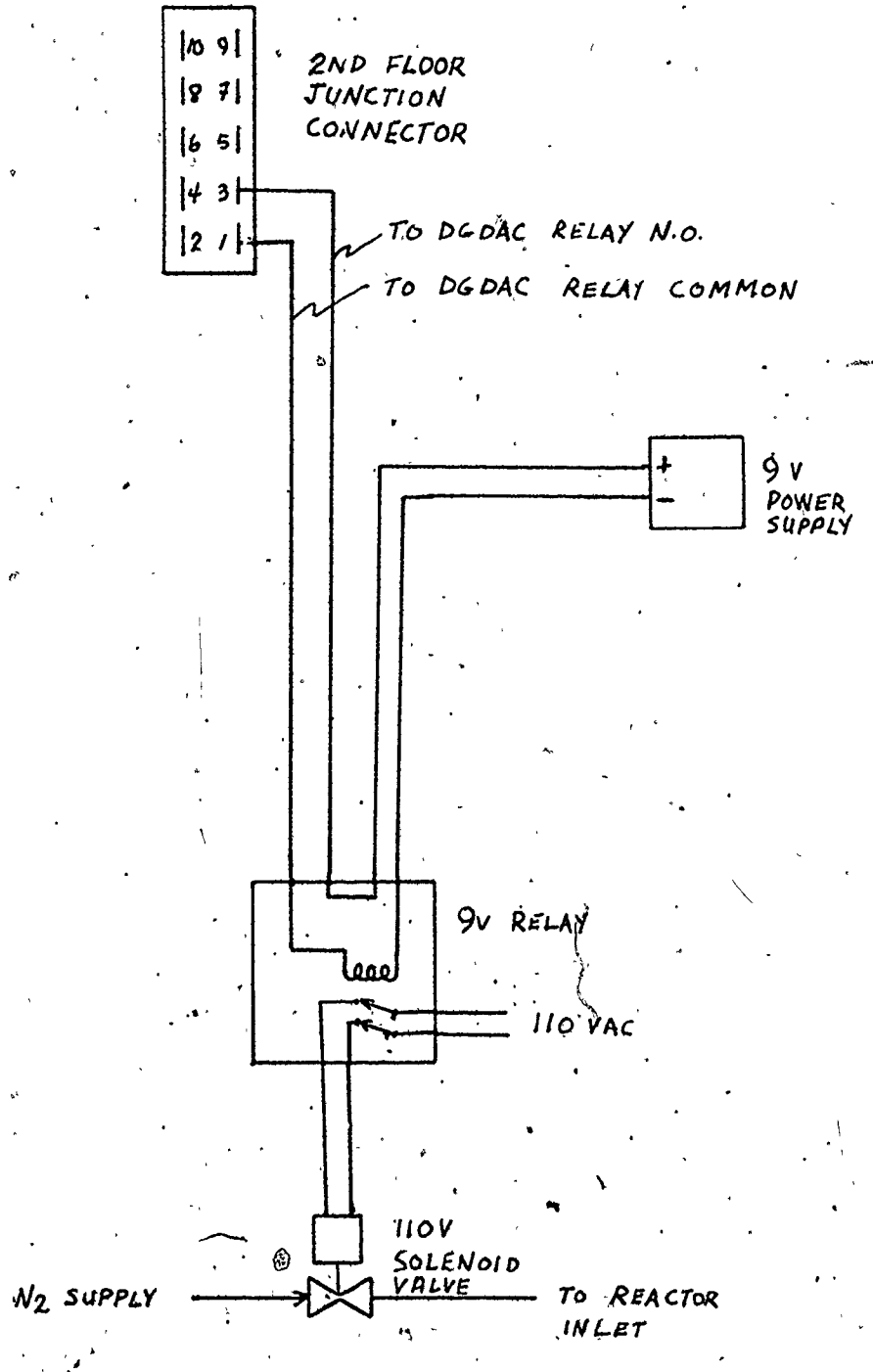

APPENDIX A2.7 Schematic of N_2 Solenoid Valve System

APPENDIX A2.8 Calibration procedure for n-butane and hydrogen flowrates

BUTANE CALIBRATION

The butane flow system was calibrated using a wet test meter (Precision Scientific Company). Butane exiting the wet test meter was exhausted to the exhaust fan on the south wall of the laboratory. Flowrates ranged from .3 s.c.f.m. to 1.3 s.c.f.m. The zero and span on the butane P transmitter was adjusted so that these flows produced approximately 1 and 9 volts respectively, across the dropping resistor on the output of the P transmmitter. A calibration curve was prepared for the rotameter and is shown in Figure A2.1. A straight line fit to the calibration data in Figure A2.2 gives the n-butane calibration equation for minicomputer software:

$$(C_4H_{10}\ \text{flow})^2 = \beta_0 + \beta_1\ (\text{ADC units})$$

$\beta_0 = -.49524$ S.E. = .73576

$\beta_1 = .58161 \times 10^{-3}$ S.E. = $.32783 \times 10^{-5}$

where C_4H_{10} flow is in s.c.f.m.

ADC units 0 - 4095 integer corresponding to 0 - 10 volts at the A/D input

For the n-butane and hydrogen calibrations, backpressure on the rotameters was maintained at 4.0 p.s.i.g. using the backpressure regulator.

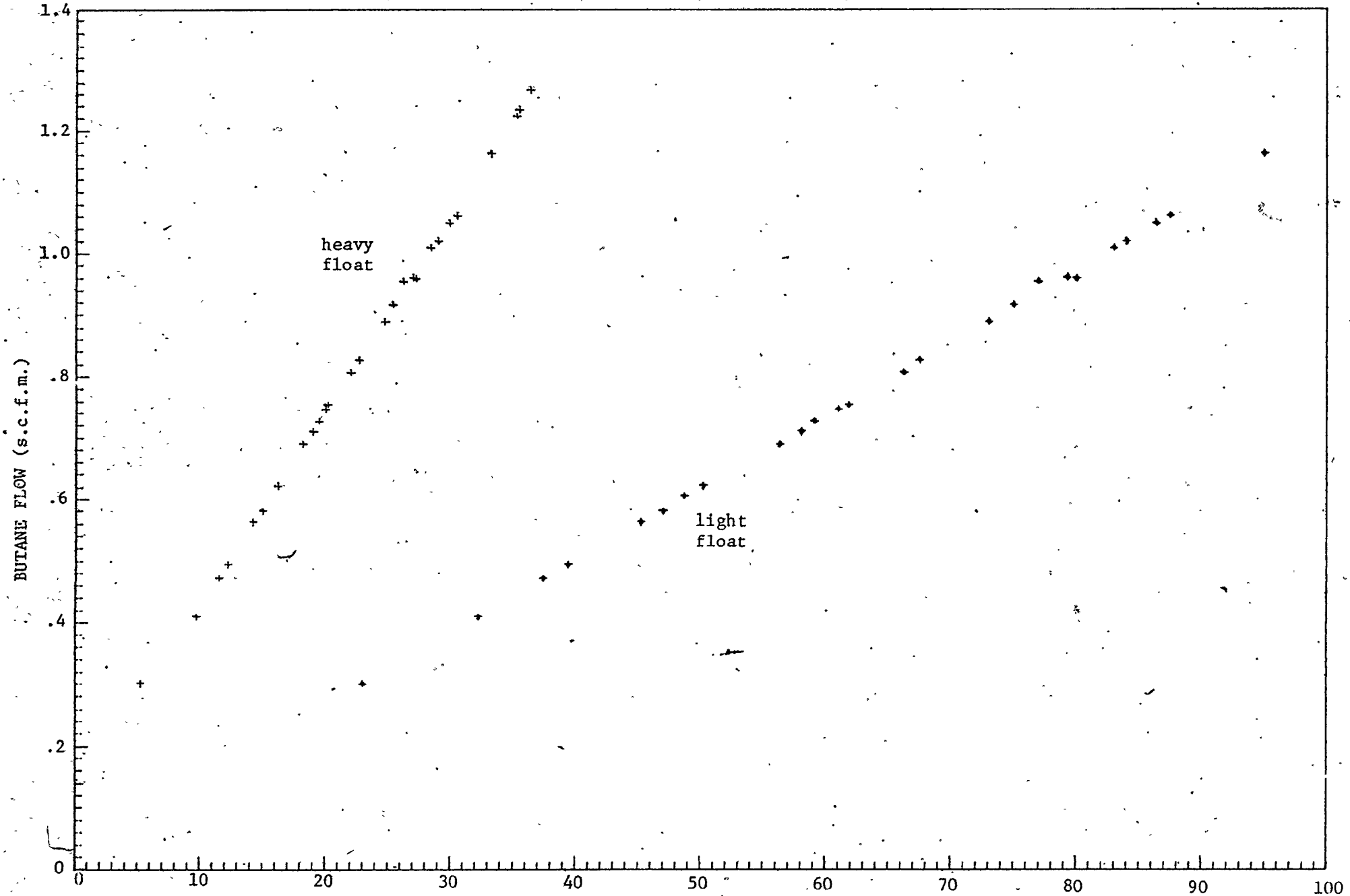

FIGURE A2.1 Rotameter Calibration for n-butane flow

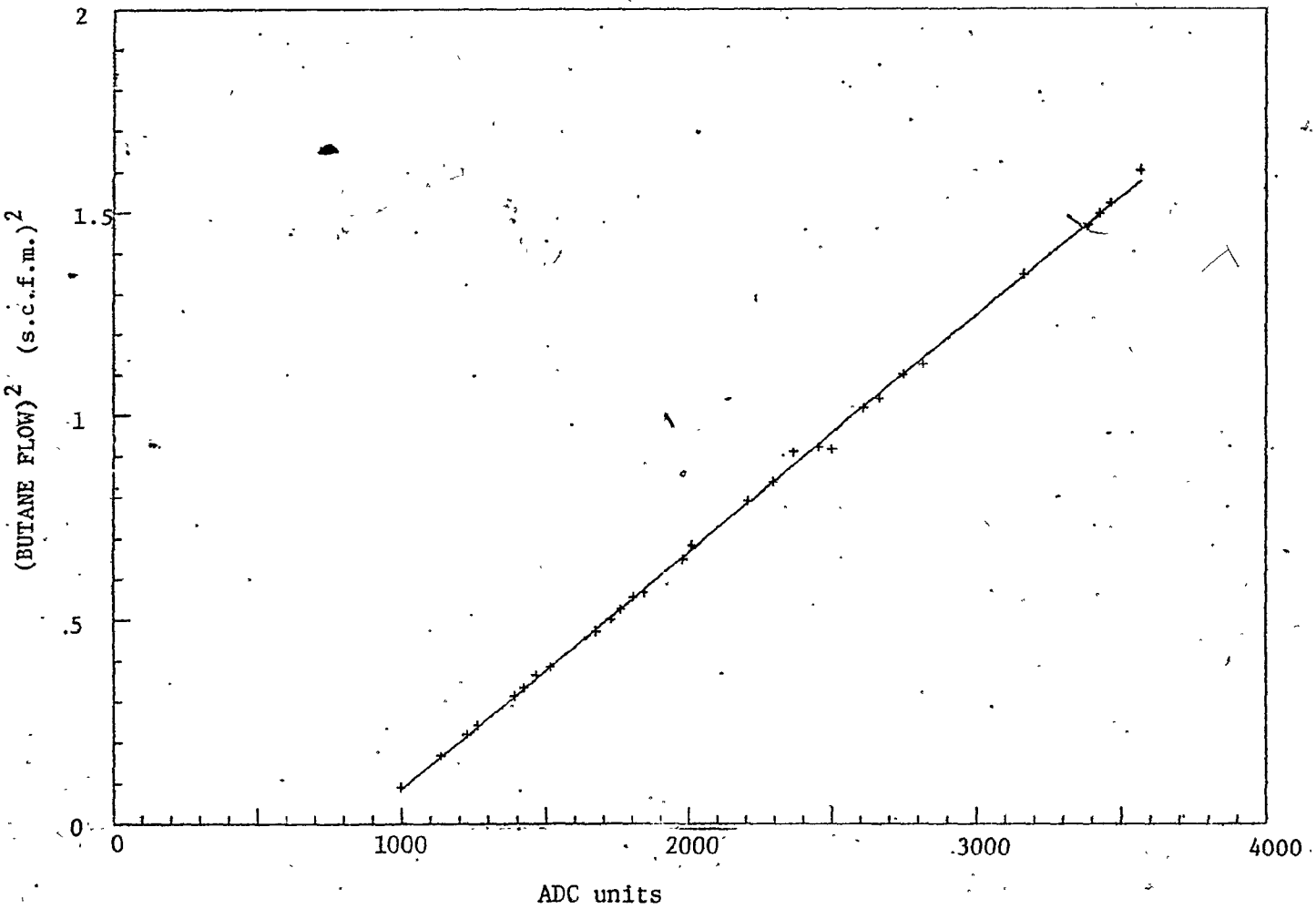

FIGURE A2.2 Computer Calibration Plot for n-Butane Flow

HYDROGEN CALIBRATION

For flows up to 2.4 s.c.f.m. a wet test meter was used for hydrogen calibration. Hydrogen exiting the wet test meter was vented to the exhaust fan. For higher flows, nitrogen and a precision nozzle (Cox Instruments) was used. The range of flows for hydrogen was between .5 and 5.3 s.c.f.m. The zero and span on the P transmitters were adjusted to produce approximately 1 and 9 volts respectively across the dropping resistor on the output of the P transmitters, corresponding to these flows.

The rotameter calibration curve is shown in Figure A2.3 and the calibration data used to fit the calibration equation are shown in Figure A2.4. The straight line fit to the data in Figure A2.4 give the calibration equation:

$$(H_2 \text{ flow})^2 = \beta_1 + \beta_0 \text{ (ADC units)}$$

$\beta_0 = -8.7230$ S.E. = .1780

$\beta_1 = 8.9892$ S.E. = $.8605 \times 10^{-4}$

where H_2 flow is in s.c.f.m.

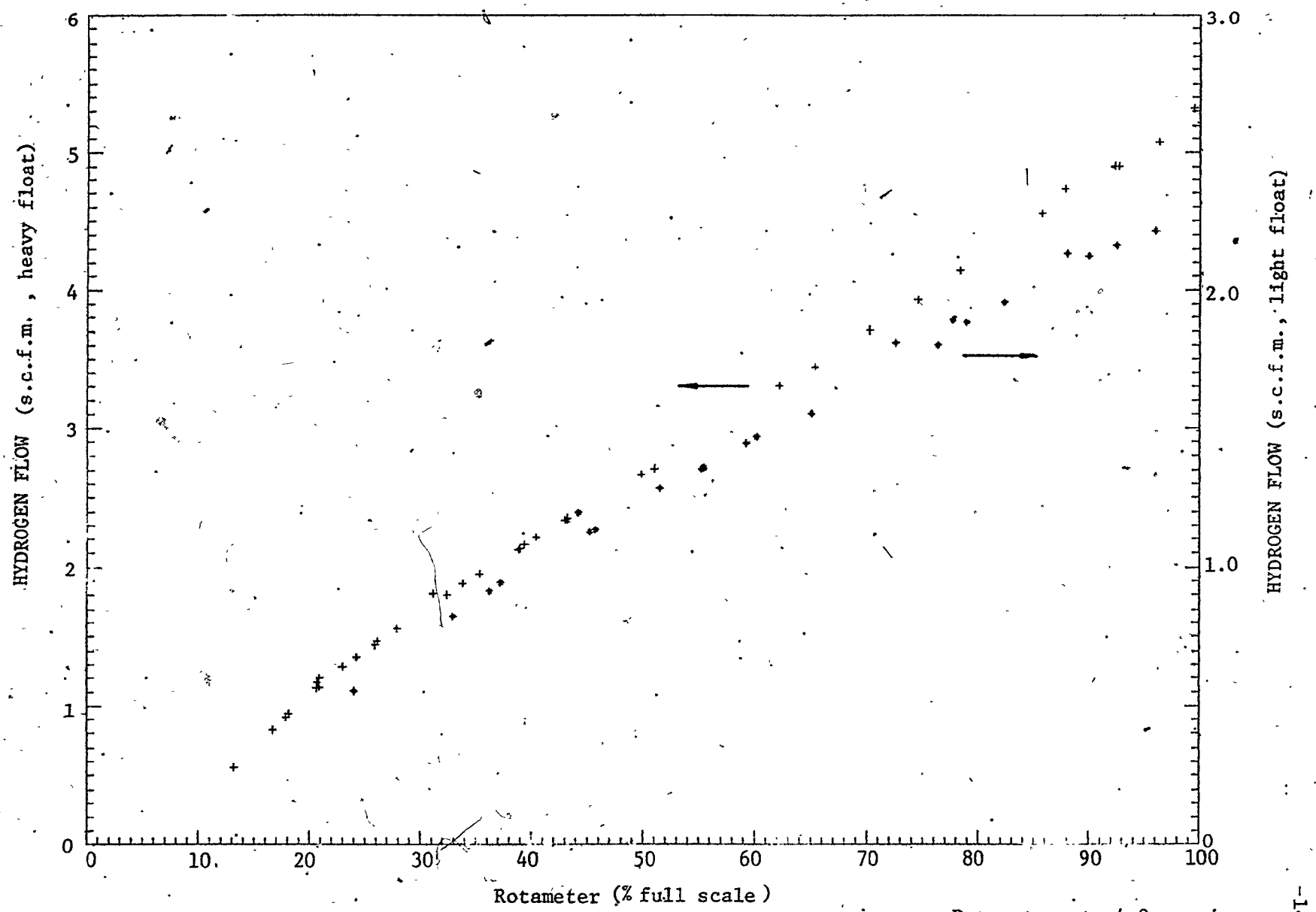

FIGURE A2.3 Rotameter Calibration for hydrogen flow

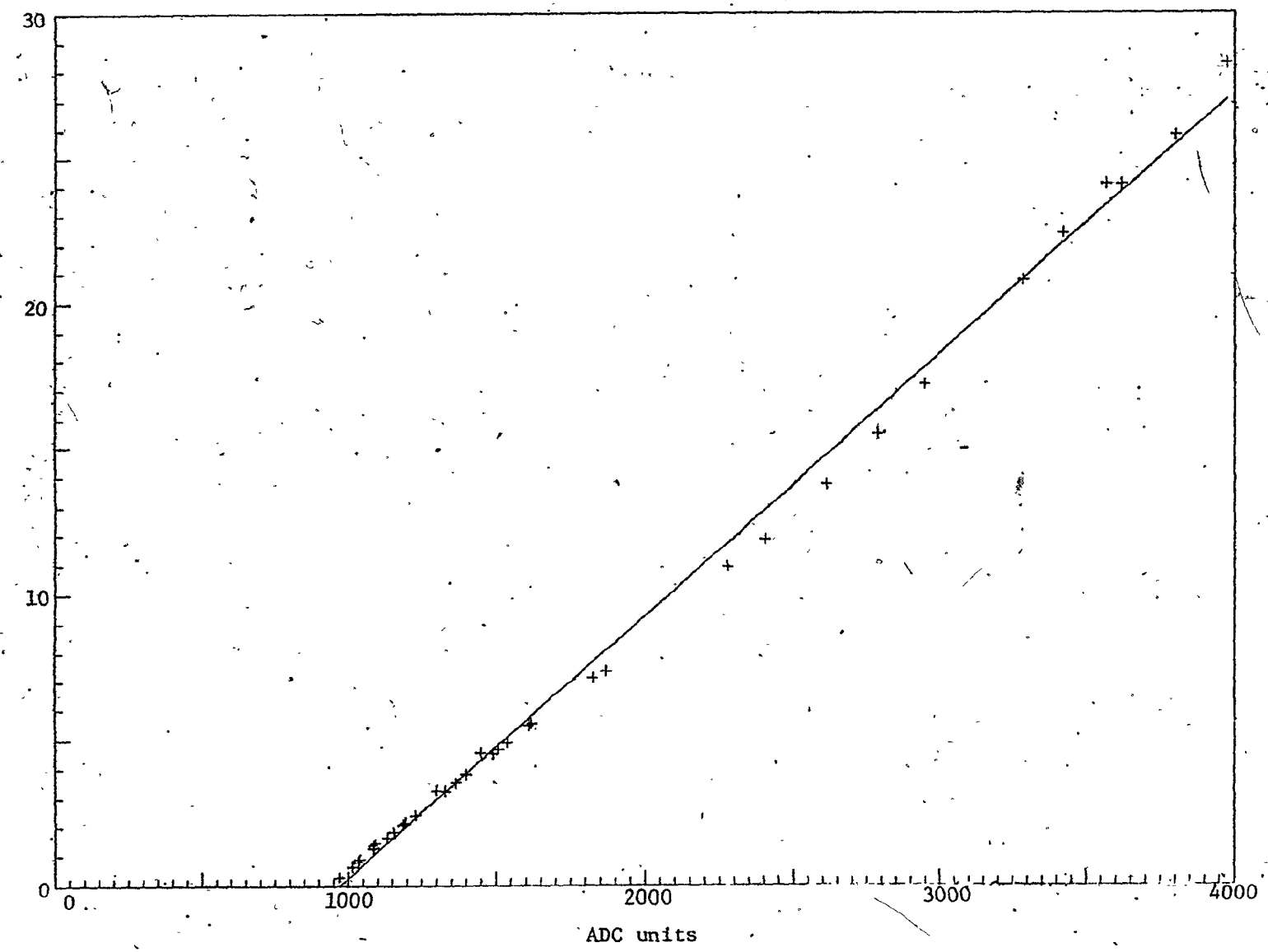

FIGURE A2.4 Computer Calibration Plot for hydrogen flow

APPENDIX A2.9 Adjustment and calibration procedure for the Beckman Model 6700 Gas Chromatograph

The procedures described below have been compiled from three sources:

1. Beckman Model 6700 Electronic Maintenance and Troubleshooting Manual (17)

2. Tremblay (16)

3. Packed bed operating manual (the section on analyzer flow adjustment has been reproduced here)

Several stages of adjustment are required to prepare the chromatograph for on-line operation:

A Analyzer flow adjustment

B Adjustment of Analyzer electronics

C Adjustment of Programmer electronics

C.1 Zeroing of Programmer amplifiers

C.2 Zeroing of Integrator amplifier

C.3 Programming of the four component boards, the digital timer board and the dual valve board

C.4 Adjustment of Component Area long term amplifier gains

D Complete calibration procedure

D.1 Adjustment of each component area amplifier

D.2 Preparation of calibration equations

E Verification of calibration

Depending on the circumstance, not all of these steps need be performed. Listed below are some typical situations and the corresponding steps, in order of execution, which are suggested.

1. start up of the chromatograph after a long period, or after replacement of faulty components which would suggest a total readjustment and calibration is necessary.

   STEPS A-D

2. the chromatograph has been calibrated recently, for a particular pilot plant but has been idle, waiting for a run.

   STEPS A,B,E

3. switching the chromatograph from either pilot plant to the other (it is assumed that the range of expected component concentrations is different for each pilot plant, necessitating re-calibration)

   STEPS A,B, C.3, C.4, D.1, D.2, E

   (in C.3, component and valve timing require verification only, but component gains might require readjustment, C.1 and C.2 can be checked if desired, but normally once set they should not need readjustment)

Before proceeding, it is important to study the procedure

outlined in Tremblay's Ph.D. thesis beginning at his Step 1, page 246. Many of the details included by Tremblay have not been described here, but are nevertheless important. Modifications and explanations to his procedures and some operating conditions are given below, where necessary.

STEP A Analyzer flow adjustment.

The procedure as described in the Packed bed operating manual as reproduced here: 'It is important to ensure that there is enough carrier gas in the cylinder which is supplying the gas chromatograph. Normally it should be replaced when the tank pressure drops below 200 lbs. on the gauge. The regulator on the tank should be set to 50 p.s.i.g. The carrier gas is hydrogen from a single cylinder which is mounted on the cylinder rack. After verification that the carrier gas is properly connected to the gas chromatograph, i.e. the connections at both the cylinder and the chromatograph ends have been made, the chromatograph may be checked. To check actual gas flows to the chromatograph, the flexible tubes that may be found on the outlet of the oven can be connected to the bubble flow meter. The bubble flow meter is used to measure chromatograph gas flow rates. The first flow rate to verify is that of the reference carrier gas which should be set to 1 cm^3 per second (or 15 cm^3 in 15 seconds). If this flow is not correct the carrier gas pressure regulator within the chromatograph in the top section should be adjusted to obtain that flow.' [Another needle valve, located inside the oven, and connected directly in front of the

filament housing, also adjusts this flow. Once this valve is set, it should not require readjustment, and the regulator alone is used to adjust flow.] The normal pressure of this regulator is approximately 14 p.s.i.g. Once the reference gas flow rate has been properly adjusted the column vent flowrate should be checked. This flowrate should be 1 cm^3 per second. To adjust the column vent flowrate two separate valves which are located in the oven must be adjusted. Since these valves are both in series and in parallel with the column, calibration is difficult and must be done carefully. The first adjustment is made with the detector measurement valve (series flow) which must be adjusted when injection switching valves A and B are de-energized, i.e. OFF position. Individual switches for the injection valves are located within the chromatograph programmer. With these valves off, i.e. in center position, detector measurement valve must be adjusted to obtain a flow of 1 cm^3 per second, as measured by the bubble flowmeter. Once this flow is adjusted, valve B must be energized. Energization will be indicated by a lamp which will be illuminated on the front of the chromatograph. The by-pass valve may now be adjusted for a flow rate of 1 cm^3 per second. Having adjusted all these flows, valves A and B are de-energized and the gas chromatogrph flowrate calibration has been completed'.

STEP B Adjustment of Analyzer electronics.

Before beginning these adjustments, check the operating conditions of the filament bridge and oven temprature:

filament current:	150 ma. (as indicated on the milliamp meter inside the analyzer cabinet)
filament bridge voltage:	adjusted to achieve desired filament current, ≈ 25V, measured between TB2-1 and TB2-2.
preregulated voltage from programmer:	29.9V, not to exceed approximately 5 volts greater than the filament bridge voltage (measured between TB2-4 and TB2-2)
oven temperature:	110°C by mercury thermometer

The correct filaments for our application are 'High Tempco' Beckman order no. 95970 (approximately 20 Ω at 70°C). Beckman recommends a maximum operating filament current of 110 ma. However, this is too low for our application because of insufficient sensitivity for accurate determination of low concentration components ethane and propane. A filament current of approximately 150 ma was found to be adequate. Running at higher currents is expected to reduce the operating lifetime of the filament.

The procedure for adjustment of the analyzer electronics as described in Section 1.1.4 of the Electronic Maintenance and Troubleshooting Manual (2) is satisfactory, with the following comments.

step 2: It is more convenient to simply place the 'Range' switch on the programmer front panel to X1 for this step.

step 4: After completing step 4 check that the auto zero amplifier is operating in the middle of its range (so that it is able to compensate equally for positive or negative baseline drift). To do this place the 'Monitor Select' switch on the programmer front panel to the 'Auto zero' position. Place the 'Auto zero' switch to 'on'. If the front panel meter is not reading roughly midscale, adjust R21 to bring it to this position. During actual operation, check the auto zero periodically in this way, and adjust R21 as required.

STEP C Adjustment of Programmer electronics

This stage of adjustment is described in Tremblay's Ph.D thesis, page 247 starting at his Step 2. Tremblay's Step 1 is described in more detail in A and B above.

C.1 Zeroing of Programmer amplifier: Trembley's step 2

C.2 Zeroing of Integrator amplifier: Trembley's step 3

Added comments: - For this step, all other cards except the universal component board 632181, the integrator board 63218# and the digital timer board 632196 must be removed from the programmer chassis.

- R18 is the 'calibrate/adjust' potentiometer
- 'calibrate/adjust' switch should read 'Zero/calibrate' switch

C.3 Programming of the four component boards, the digital timer board, and the dual valve board.

Before proceeding to the 'Adjustment of Component Area long term amplifier gains' it is necessary to program the four component boards, the digital timer board and the dual valve board.

Digital timer board This has been set to a cycle timer of 360 seconds in 1 cycle steps, and should not require readjustment.

Dual valve board Refer to Tremblay's Ph.D. thesis page 88 for an explanation of the timing requirements for these valves. The critical valve times are valve B 'on' and valve B 'off' times. Valve B 'on' must not be less than the time required for methane and ethane to be completely eluded into column 2, and not greater than the time at which propane begins to elute from column #1. When valve B is energized, methane and ethane are trapped in column #2, while allowing propane and butane to elute from column #1 directly into the detector. Valve B 'off' time must not be set less than the time at which butane has been completely eluted from column #1 and has passed through the detector. Valve A 'on' time is set at 2 seconds and need not be changed. Valve A 'off' time is not critical and has been set arbitrarily at 65 seconds.

To verify the valve B 'on' and 'off' times, run a representative sample mixture manually through column #1 only, and observe the times at which ethane and butane are completely eluted from the column, and the time at which propane begins to elute from column #1. Before starting the analysis cycle place switches as follows:

- 'Component disable' switch to 'on'
- on the front panel, all switches to the left most position except the 'Range' switch which is set to X1
- 'Monitor Select' switch to 'amplifier out'
- manual valve A to 'off' (middle) position
- manual valve B to 'on' (left) position

With the sample mixture flowing through the sample line, start a single analysis cycle from the front panel in the usual manner. At t=2 seconds, activate valve A by placing the manual valve A switch to the 'on' (left) position. On the front panel meter observe the times at which the components elute from column 1 (alternatively, connect a strip chart recorder to the BARGRAPH + and BARGRAPH - terminals at the rear of the programmer, or to the 'test output' jack on the front panel). Typically observed times are 33 seconds for ethane and 177 seconds for butane to be completely eluted from column #1 and approximately 42 seconds when propane begins to elute. Valve B 'on' and 'off' times have been set accordingly to 33 seconds and 195 seconds, respectively, as shown in Table A.1.

TABLE A.1 PROGRAMMER BOARD SETTINGS

Digital Timer cycle time: 360 seconds in 1 cycle steps.

Dual Valve Board

VALVE	ON TIME	OFF TIME
A	2	65
B	33	195

UNIVERSAL COMPONENT BOARDS.

COMPONENT	ON TIME	OFF TIME	AUTO ZERO	MEMORY	RANGE
CH_4	212	279	ON	1	x10
C_2H_6	300	348	ON	2	x 1
C_3H_8	39	74	ON	3	x 1
$n\text{-}C_4H_{10}$	95	195	ON	4	x10

All component boards were programmed with POLARITY REVERSE at OFF and amplifier range at LOW.

Component boards

Each component board requires unique programming of Component 'on' and 'off' times, Auto zero 'enable' or 'disable', Memory Select, and Range selection. Current programming for fluidized bed sampling is given in Table A10.1. The Memory Select settings have been set and should not be changed. To determine component 'on' and 'off' times, run

a sample as was done when verifying valve times, described above. Proceed as before, but this time put the manual valve switches both in the 'auto' (right) positions and leave them in these positions for the analysis cycle. On the programmer meter (or on a stripchart recorder) observe the time at which each component enters the detector and the time at which it has passed completely through the detector.

When programming the component 'on' and 'off' times note that actual time 'on' (i.e. when integration begins, as indicated by the 'component on' lamp at the upper right hand side of the front panel) occurs 2 seconds after the programmed time on, for the case when the 'Auto zero' is disabled for that particular component. This increases to 4 seconds when 'Auto zero' is enabled. Note, however, that the 'Range' is automatically switched at the programmed 'on' time. Therefore, program the 'on' time so that integration begins not after the time at which the component first enters the detector, and the 'off' time (integration ends at the programmed 'off' time) not earlier than the time at which all of the component has passed through the detector.

All component boards are programmed with 'polarity reverse' (on the component board) at 'off' and the 'amplifier range' at 'low'. The integrator functions are set to 'readout', 'integrate' and 'automatic'.

C.4 Adjustment of Component Area long term amplifier gains.

Follow Tremblay's Step. 4, beginning with the 2nd paragraph (pg. 249).

D Complete Calibration Procedure

A calibration procedure different from that used by Tremblay and other packed bed workers has been adopted here. Before beginning the calibration procedure, it is assumed that steps A and B have been completed satisfactorily and that the settings and adjustments in Step C are also satisfactory.

In the procedure to follow, it is assumed that a constant pressure sample is available to the analyzer. Since the sample volume is constant, integrated area (as indicated by programmer out voltage) for each component will be directly proportional to the component's mole fraction in the sample mixture. A calibration equation relating mole fraction and A/D computer units (indicating programmer out voltage) will be prepared for each component.

The first step of the calibration procedure is adjustment of each component's area amplifier.

D.1 Adjustment of each component's area amplifier.

The purpose here is to adjust each component's area amplifier so that a voltage of approximately 8-9 volts appears at the programmer output when a sample containing the maximum expected mole fraction of the particular component is analyzed. The A/D inputs at the DGDAC read up to 10 volts but the adjustment is made to 8-9 volts to allow a margin of error in the estimated maximum expected quantity (i.e., mole fraction) for each component. Prepare a calibration mixture which has the maximum expected mole fractions for each component. Since hydrogen

is not measured, this might be possible with one mixture, otherwise use two mixtures. For the fluidized bed, a mixture was prepared as follows:

$$x_{H_2} = 1-(x_{C_4} + x_{C_3} + x_{C_2} + x_{C_1})$$
$$x_{C_4} = .149$$
$$x_{C_3} = .0216$$
$$x_{C_2} = .0203$$
$$x_{C_1} = .447$$

Analysis of the mixture is performed with all programmer automatic functions enabled. Initiate a single analysis cycle in the usual manner.

At the end of the cycle, note the volages at the programmer outputs for each component. Adjust R1 of each component integrator control for a voltage of approximately 8.0 volts for that particular component. Note that the adjustment of R1 is extremely non-linear. Counterclockwise adjustment reduces the output voltage. After an adjustment is made, the sample mixture must be re-analyzed and the output voltage noted. An output voltage of around 12.3 V indicates that R1 is out of its working range and a large adjustment in the counterclockwise direction is required.

D.2 Preparation of Calibration equations

For each component, a calibration equation of the form

$$x = a + b\ (\text{ADC units}) + C\ (\text{ADC units})^2$$

where x is the absolute mole fraction of the component in the sample,

is required. Prepare a number (3 or 4 should be sufficient) of calibration mixtures which reflect the range of expected concentrations for each component. Analyse each mixture from the computer using program GCTEST.RM, with the programmer placed in the 'Computer' mode (see Section 2.4). Mixtures typically used for the fluidized bed are

x_{C_1}	.19	.418	.460
x_{C_2}	.0186	.0169	.00545
x_{C_3}	.016	.00885	.020
x_{C_4}	.065	.0389	.1353
x_{H_4}	.708	.517	.7937

At the end of each analysis cycle, GCTEST.RM prints to console the chromatograph analysis in computer units.

E. Verification of calibration

Immediately prior to a run, the chromatograph calibration should be verified. Steps A and B must be completed to do this. A known sample mixture is prepared and analyzed in the 'Computer' mode using GCTEST.RM. The resulting analysis in computer units is checked with the calibration equations to verify that the correct mole fractions have been predicted.

APPENDIX A3.1 Listing of subroutines TYPE 1 (REAC01), ORCMIX and HREACT.

```
      SUBROUTINE TYPE 1
      COMMON/CCN/IG,KLOOP,NCOMP,NC5,DELT,NE,TIME(30),NS,NPR,TOLL,TOLU,
     1  EMAX,NPOL,TMAX,NCOUNT,JM,KJ,MPR,NGIM
      COMMON/MAT/MP(20,8),EP(20,5),S(2,50,20),EX(100)
      COMMON/UNIT/IM,NMP
      COMMON/FPRINT/MPRINT
      COMMON/MTESTB/MTEST
      COMMON/C40/IPASS
      DIMENSION FEED(5),RM(5),HEAT(3),OUT(5)
      DATA MTEST/0/

C     FLUIDIZED BED REACTOR MODULE
C     WRITTEN APRIL 30,1979, R. MCFARLANE
C     CONCENTRATION DYNAMICS ARE ASSUMED TO BE AT PSEUDO STEADY
C     STATE WRT TO REACTOR CONTENTS THERMAL DYNAMICS.
C     MASS BALANCE SOLVED USING ORCMIX PROGRAM OF SHAW(PHD THESIS
C     MCMASTER UNIV.,.1974) WHICH IS BASED ON STEADY STATE TWO-PHASE
C     MODEL OF ORCUTT ET AL, CHEM ENG PROG SYMP SER,38, NO 58,1(1962)
C     EMULSION PHASE PERFECTLY MIXED

C     STREAM LIST
C     1  STREAM NO
C     2  FLAG
C     3  TOTAL FLOW  G/SEC
C     4  TEMP  DEG C
C     5  PRESSURE  ATM
C     6  MASS FLOWRATE CH4  G/SEC
C     7  MASS FLOWRATE C2H6
C     8  MASS FLOWRATE C3H8
C     9  MASS FLOWRATE C4H10
C     10 MASS FLOWRATE H2
C     11 MASS FLOWRATE OIL IN HEATING/COOLING SYSTEM  G/SEC
C     12 MASS FLOWRATE AIR TO OIL COOLER G/SEC

C     INFORMATION STREAM,  REQUIRES UNIQUE DEFINITION
C     1  STREAM NO
C     2  FLAG
C     3  TOIL, MEAN BULK TEMP OF OIL IN COOLING COIL  DEG C
C     4  TW, AVERAGE WALL TEMP OVER BED HEIGHT  DEG C
C     5  TR, REACTION TEMPERATURE DEG C
C     6  S1  SELECTIVITY OF METHANE
C        (MOLES METHANE PRODUCED/MOLES BUTANE REACTED)
C     7  S2  SELECTIVITY ETHANE
C     8  S3  SELECTIVITY PROPANE
C     9  CONV  CONVERSION OF BUTANE

      IF(TIME(2) .NE. 0.)GO TO 10

C     FETCH EQUIPMENT PARAMETERS

      WB=EP(IM,1)
      HAW=EP(IM,3)
      HAC=EP(IM,4)
      QLOSS=EP(IM,5)
      CPMW=EX(MP(IM,8))
      CPI=EX(MP(IM,8)+1)
      CPB=EX(MP(IM,8)+2  )
      MPRINT=EX(MP(IM,8)+3)
      IPASS=EX(MP(IM,8)+4)

      CPOIL=.74
      FAC1=WB*CPB
      FAC2=HAW/CPMW
      FAC3=HAC/CPMW
```

```
      CACT=EP(IM,2)
      HO=47.6
      XFAC=.426
      F=0.9
      RHOS=.957
      EMF=.557
      RM(1)=16.
      RM(2)=30.
      RM(3)=44.
      RM(4)=58.
      RM(5)=2.

C     GET INLET AND OUTLET STREAMS

      IOILI=MP(IM,3)
      IFEED=MP(IM,4)
      ICILO=-MP(IM,5)
      IEXIT=-MP(IM,6)
      INFO=-MP(IM,7)
   10 CONTINUE

C     SOLVE WALL DYNAMICS

C     CALCULATE DERIVATIVE

      TOIL=S(IG,INFO,3)
      D=FAC2*(S(IG,INFO,5)-S(IG,INFO,4))+FAC3*(TOIL-S(IG,INFO,4))
     1-QLOSS

C     IF THIS IS CORRECTOR STEP GET TW AT TN+1, WHICH WAS ESTIMATED
C     ON PREDICTOR STEP. IF THIS IS PREDICTOR STEP USE CURRENT TW

      IF(IG .EQ. 1)X=S(1,INFO,4)
      TW=Y1(1,S(2,INFO,4),D,X)
      S(1,INFO,4)=TW

C     PREPARE FOR CALL TO ORCMIX
C     ASSUME INLET GAS CONTAINS ONLY BUTANE AND HYDROGEN

      FEED(1)=0.
      FEED(2)=0.
      FEED(3)=0.
      TREACT=S(IG,INFO,5)
      RF4=S(IG,IFEED,9)/RM(4)
      RF5=S(IG,IFEED,10)/RM(5)
      RFT=RF4+RF5
      FEED(4)=RF4*S(IG,IFEED,5)/RFT
      FEED(5)=RF5*S(IG,IFEED,5)/RFT

C     FEED(1) - (5) ARE THE INLET PARTIAL PRESSURES, ATM
C     CALCULATE THE TOTAL VOLUMETRIC INLET FLOWRATE,ACFM
C     ASSUME IDEAL GAS BEHAVIOUR

      TFEED=S(IG,IFEED,4)
      VF4=RF4*(TFEED +273.1)*.17387/S(IG,IFEED,5)
      VF5=RF5*(TFEED +273.1)*.17387/S(IG,IFEED,5)
      FLOW=VF4+VF5
      TSEND=TREACT*9./5. + 32.1
      IF(IPASS .EQ. 0)GO TO 600
      CALL ORCMIX(CACT,FEED,FLOW,TSEND,OUT,RB,RP2,RE2,S1,S2,S3,CONV)

C     OUT  CONTAINS THE OUTLET PARTIALS PRESSURES, ATM
C     RB IS THE NET RATE OF REACTION OF BUTANE, MOLES/UNIT VOLUME
C     EMULSION PHASE-SEC
C     RP2 IS THE NET RATE OF REACTION OF PROPANE
```

APPENDIX A3.1 cont'd

```
C     RE2 IS THE NET RATE OF REACTION OF ETHANE

C     SOLVE ENTHALPY BALANCE
C     ENTHALPY BALANCE REQUIRES REACTION RATES ON A WEIGHT OF CATALYST
C     BASIS, MAKE THE CONVERSION

      FAC4=1./(PHOS*(1.-EMF))
      RB=RB*FAC4
      RP2=RP2*FAC4
      RE2=RE2*FAC4
C     THE ABOVE ARE NET RATES OF REACTIONS OF THE HYDROCARBONS
C     WE REQUIRE THE RATES OF THE ACTUAL REACTIONS WHICH ARE PRODUCING
C     HEAT

      RP=RB*F - RP2
      RE=RP+2.*(1.-F)*RB-RE2
C     RB IS THE RATE OF THE FIRST REACTION
C     RP IS THE RATE OF THE 2ND REACION
C     RE IS THE RATE OF THE 3RD REACTION

C     HEATS OF REACTION ARE CALCULATED USING HEATS OF FORMATION
C     REF  ≠THERMODYNAMIC CALCULATIONS ON AN ELECTRONIC DIGITAL
C     COMPUTER≠, JORGEN KJAER, AKADEMISK FORLAG, COPENHAGEN, 1963.

      CALL HREACT(TREACT,HEAT)

C     CALCULATE THE TOTAL HEAT LIBERATED

      THEAT=HEAT(1)*RB + HEAT(2)*RP + HEAT(3)*RE
  600 IF(IPASS .EQ. 0)THEAT=0.

C     PROCEED WITH ENTHALPY BALANCE
C     CALCULATE DERIVATIVE

      FEEDGM=S(IG,IFEED,9)+S(IG,IFEED,10)
      D=(FEEDGM          *CPI/FAC1)*(S(IG,IFEED,4)-S(IG,INFO,5))
     1   + (HAW/FAC1)*(S(IG,INFO,4)-S(IG,INFO,5))+(THEAT/CPB)

C     IF THIS IS CORRECTOR STEP USE REACTOR TEMP PREDICTED PREVIOUSLY
C     USE CURRENT REACTOR TEMP ON PREDICTOR STEP

      IF(IG .EQ. 1)X=S(1,INFO,5)
      T=Y1(1,S(2,INFO,5),D,X)
      S(1,INFO,5)=S(1,IEXIT,4)=T

C     CALCULATE MASS FLOWRATES IN OUTLET STREAM, GIVEN PARTIAL
C     PRESSURES FROM ORDMIX

      IF(IPASS .EQ. 0)GO TO 601
      PT=0.
      DO 120 I=1,5
  120   PT=PT+OUT(I)
      S(1,IEXIT,5)=PT

C     RECALL TOTAL MOLAR IN IS EQUAL TO RFT
C     REACTION IS EQUIMOLAR

      OUTT=0.
      DO 122 I=1,5
      S(1,IEXIT,I+5)=RFT*OUT(I)*RM(I)/PT
  122   OUTT=OUTT+S(1,IEXIT,I+5)
      S(1,IEXIT,3)=OUTT
  601 CONTINUE

C     OUTT IS THE TOTAL MASS FLOWRATE OUT
```

```
C     SOLVE COOLING COIL

      TIN=S(IG,IOILI,4)
      FLOWDIV=S(IG,IOILI,3)/3.
      SNTU=HAC/(FLOWDIV*CPOIL)
      EFF=1.-EXP(-SNTU)
      TRISE=EFF*(S(IG,INFO,4)-TIN)
      TOIL=TIN+TRISE/2.

C     TOIL IS THE AVERAGE BULK TEMP OF OIL IN THE COOLING
C     COIL. STORE IN INFO STREAM FOR FUTURE REFERENCE

      S(1,INFO,3)=TOIL
      S(1,IOILO,4)=TIN + TRISE


C     PLACE SELECTIVITIES AND CONVERSION INTO INFO STREAM

      S(1,INFO,6)=S1
      S(1,INFO,7)=S2
      S(1,INFO,8)=S3
      S(1,INFO,9)=CONV
      IF(IG .EQ. 2 .OR. MPRINT .EQ. 0)GO TO 156
      PRINT *,≠CPB,CPI,HAW,HAC,CPOIL,CPMW  ≠,CPB,CPI,HAW,HAC,CPOIL,CPMW
      PRINT *,≠FEED(4),FEED(5), FLOW  ≠,FEED(4),FEED(5),FLOW
      PRINT *,≠INLET VOL FLOW BUTANE , H2  ACFM  ≠, VC4H10,VH2
      PRINT *,≠RB,RP2,RE2 (GM MOLES/GM CATALYST-SEC)  ≠,RB,RP2,RE2
      PRINT*, ≠PB,RP,RE, RATES OF 3 IND RXNS(GM MOLES HC/GM CATALYST-SEC
     1)  ≠,RB,RP,RE
      PRINT *,≠TREACT(DEG K),HEAT(1,2,3) , HEATS OF RXNS  ≠,TREACT,
     1HEAT
      PRINT *,≠TOTAL HEAT LIBERATED(CAL/SEC)  ≠,THEAT
      PRINT *,≠OUTLET P.P.(ATM)  ≠,OUT
      PRINT *,≠S1,S2,S3, CONVERSION  ≠,S1,S2,S3,CONV
  156 RETURN
      END


      SUBROUTINE ORCMIX(CACT,FEED,FLOW,T,OUT,RB,RP2,RE2,S1,S2,S3,CONV)
      INTEGER P
      DIMENSION A(13),OUT(5),FEED(5)
      DATA ITEST/0/
      IF(ITEST .GT. 0)GO TO 911
      ITEST=1
      A(1)=5.1E04
      A(2)=4.0E04
      A(3)=3.0E04
      A(4)=1.6E04
      A(5)=15.6604
      A(6)=10.6322
      A(7)=12.2229
      A(8)=6.8140
      A(9)=-2.155
      A(10)=-2.0753
      A(11)=2.6E04
      A(12)=4.5208
      A(13)=-2.2115
      A(5)=10.**A(5)
      A(6)=10.**A(6)
      A(7)=10.**A(7)
      A(8)=10.**A(8)
      A(12)=10.**A(12)
      HO=47.6
      XFAC=0.426
      GRAV = 980.0
      OBMAX = 10.0
      UMF = 0.77
```

```
      HN = 20.0
      RHOS = 0.957
      DP = 0.01
  911 CONTINUE
      U = FLOW*1.46042
      TEMP = (T-32.)*(5./9.) + 273.1
      UEMUL = UMF
      HMF = HO*1.043
      DO = 0.3261*(((U-UEMUL)*HN)**0.4)
      G1 = 1.0
      UX = U/G1
      HDBMAX = (DBMAX-DO)*UMF/(1.4*RHOS*DP*L)
      DBMEAN = DBMAX - 0.9
    2 HT = HMF*(1.0 + (U-UEMUL)/(0.711* SQRT(980.*DBMEAN)))
      DBSAVE = DBMEAN
      DBMEAN = ((DBMAX-DO)*0.5*HDBMAX + DBMAX*(HT-HDBMAX))/HT
      IF( ABS(DBSAVE-DBMEAN).GT.0.0001)GO TO 2
      Q = XFAC*11.0/DBMEAN
      X = 0*HT/(0.711* SQRT(GRAV*DBMEAN))
      NH2 = 0
      NSW=1
      MSW = 1
      TOL=0.000001
      RTT=1.99*TEMP
      FAC = (1.0-0.557)/(1.0-0.449)
      RKB=CACT*FAC*A(5)* EXP(-A(1)/RTT)
      RKP1=CACT*FAC*A(6)* EXP(-A(2)/RTT)
      RKP2=A(7)* EXP(-A(3)/RTT).
      RKE2 = CACT*FAC*A(12)* EXP(-A(11)/RTT)
      RKE=A(8)* EXP(-A(4)/RTT)
      EXPX = EXP(X)
      GAM = (U*(1.0-(1.0-UEMUL/L)/EXPX))/(82.06*TEMP*HMF)
      P5 = FEED(5)
C
C     REACTION KINETICS FOR EMULSION WHERE THE ONLY REACTION OCCURS
  800 Y2 = P5**A(9)
      P42 = (FEED(4)*GAM)/(GAM + RKB*Y2)
      RB = RKB*P42*Y2
      Z1=0.9*RB
      Z3 = RKP1*(P5**A(10))
      P32 = (Z1+FEED(3)*GAM*(1.0+RKP2))/(Z3+GAM*(1.0+RKP2))
      PP2=(Z1-Z3*P32)/(1.0+RKP2)
      Z4 = RKE2*(P5**A(13))
      P22 = (1.1*RB-PP2+(1.0+RKE)*GAM*FEED(2))/(Z4+(1.0+RKE)*GAM)
      RE2 = (1.1*RB-PP2-Z4*P22)/(1.0+RKE)
      P12=(4.0*RB-3.0*PP2-2.0*RE2)/GAM
      P52 = (FEED(5)*GAM - 3.0*RB + 2.0*PP2 + RE2)/GAM
C     SEARCH SO THAT GUESSED H2 WILL BE THE SAME AS THE CALCULATED H2
      PDIF=P5-P52
      IF(NSW.EQ.2)  GO TO 703
      IF(PDIF.LE.0.0) GO TO 700
      MSW = 2
      PRT=P5
      P5 = P5 - 0.10
      DIFR=PDIF
      IF(P5.GE.0.0)  GO TO 800
      P5 = 0.0001
      IF(NH2.EQ.0) GO TO 701
      P52 = 0.0001
      IPRINT = -999
      GO TO 704
  701 NH2 = 1
      GOTO800
  700 IF(MSW.EQ.1) WRITE(6,996) IPRINT,P5,P52,PDIF
      PLT=P5
```

APPENDIX A 3.1 cont'd

```
      DIFL=PDIF
      NSW=2
      GO TO 750
  703 IF( ABS(PDIF).LT.TOL) GO TO 704
      IF( ABS(PDIF).LT. ABS(DIFR).OR. ABS(PDIF).LT. ABS(DIFL))GO TO 710
      WRITE(6,999) IPRINT,P5,P52,PLT,PRT,PDIF,DIFL,DIFR
  710 IF( ABS(DIFR).LT. ABS(DIFL)) GO TO 730
      IF(PLT.GT.P5)  GO TO 715
      PRT = P5
      DIFR = PDIF
      GO TO 750
  715 PRT = PLT
      DIFR = DIFL
      PLT = P5
      DIFL = PDIF
      GO TO 750
  730 IF(PRT.LT.P5)  GO TO 735
      PLT = P5
      DIFL = PDIF
      GO TO 750
  735 PLT = PRT
      DIFL = DIFR
      PRT = P5
      DIFR = PDIF
  750 P5 = PLT - DIFL*(PRT-PLT)/(DIFR-DIFL)
      GOTO800
C
  704 PB1 = P12 + (FEED(1)-P12)/EXPX
      PB2 = P22 + (FEED(2)-P22)/EXPX
      PB3 = P32 + (FEED(3)-P32)/EXPX
      PB4 = P42 + (FEED(4)-P42)/EXPX
      PB5 = P52 + (FEED(5)-P52)/EXPX
      F1 =  UEMUL/U
      F2 =  (U-UEMUL)/U
      OUT(1)=F1*P12+PB1*F2
      OUT(2)=F1*P22+PB2*F2
      OUT(3)=F1*P32+PB3*F2
      OUT(4)=F1*P42+PB4*F2
      OUT(5)=F1*P52+PB5*F2
  380 IF(FEED(4) .EQ. 0.)GO TO 390
      F=FEED(4)
      DD=FEED(4)- OUT(4)
      S3=OUT(3)/DD
      S2=OUT(2)/DD
      GO TO 410
  390 IF(FEED(3) .EQ. 0.)GO TO 400
      F=FEED(3)
      DD=FEED(3) - OUT(3)
      S3=0.
      S2=OUT(2)/DD
      GO TO 410
  400 F=FEED(2)
      DD=FEED(2)-OUT(2)
      S3=0.
      S2=0.
  410 CONV=100.*DD/F
      S1=OUT(1)/DD
      EMULH2=P52
  996 FORMAT(1X, 40HNEGATIVE ON FIRST STEP OF SEARCH FOR P52, 5X,I3,3F15
     ,.4)
  999 FORMAT( 1X, 45H THE ORCUTT SEARCH MAY BLOW UP FOR IPRINT =  ,I4,
     17E11.4)
      RETURN
      END
```

APPENDIX A3.1 cont'd

```
      SUBROUTINE HREACT(TR,HEAT)

      COMMON/CCN/IG,KLCCP,NCOMP,NC5,DELT,NE,TIME(30),NS,NPR,TOLL,TCLU,
     1  EMAX,NPCL,TMAX,NCOUNT,JP,KJ,MPR,NGIR
      DIMENSION FORM(5),HEAT(3), PP(5,5)
      DATA IFIX/0/

C       CONSTANTS FOR THE POLYNOMIALS USED IN CALCULATING HEATS OF
C       FORMATION ARE STORED IN PP(5,5)
      IF(IFIX .GT. 0)GO TO 105
      IFIX=1
      WRITE(6,101)
  101 FORMAT(//,1X,*HEAT OF FORMATION CONSTANTS*/)
      DO 10 I=1,5
      DO 10 J=1,5
      READ(5,100)PP(I,J)
   10 WRITE(6,100)PP(I,J)
  100 FORMAT(E16.6)
      F=0.9
  105 CONTINUE
      TR=TR+273.1
      DO 50 I=1,5
   50  FORM(I)=PP(I,1)+PP(I,2)*TR + PP(I,3)*TR**2
     1  +PP(I,4)*TR**3 + PP(I,5)*TR**4
      HEAT(1)=FORM(4)+FORM(5)-F*FORM(3)-2.*(1.-F)*FORM(2)-F*FORM(1)
      HEAT(2)=FORM(3)+FORM(5)-FORM(2)-FORM(1)
      HEAT(3)=FORM(2)+FORM(5)-2.*FORM(1)
      RETURN
      END
```

APPENDIX A3.2 Listing of subroutine TYPE 3 (OILHEAT).

```
      SUBROUTINE TYPE 3
      COMMON/CCN/IG,KLCOP,NCOMP,NC5,DELT,NE,TIME(30),NS,NPR,TOLL,TOLU,
     1  EMAX,NPCL,TMAX,NCOUNT,JM,KJ,MPR,NGIM
      COMMCN/MAT/MP(20,8),EP(20,5),S(2,50,20),EX(100)
      COMMON/UNIT/IM,NMP

C     OIL HEATER MODULE, WRITTEN JUNE 14/79, R MCFARLANE
C     MAXIMUM HEAT INPUT FROM ELECTRICAL HEATERS IS 2031 CAL/SEC

C     STREAM LIST
C     1.  STREAM NO.
C     2.  FLAG
C     3.  TOTAL FLOW  G/SEC
C     4.  TEMP  DEG C
C     5.  PRESSURE  ATM
C     6.  MASS FLOWRATE CH4  G/SEC
C     7.                C2H6
C     8.                C3H8
C     9.                C4H10
C     10.               H2
C     11. MASS FLOWRATE OIL  G/SEC
C     12. MASS FLOWRATE AIR G/SEC

      IF(TIME(2) .NE. 0.)GO TO 105

C     GET INLET AND OUTLET STREAMS

      INOIL=MP(IM,3)
      IOILO=IABS(MP(IM,4))

C     GET UNIT PARAMETERS FROM EP MATRIX

      CPOIL=EP(IM,1)
      RHOV=EP(IM,2)
      QLOSS=EP(IM,4)
      WOIL=EP(IM,5)
  105 CONTINUE
      QE=EP(IM,3)
      FAC2=QE/(RHOV*CPOIL)
      S(IG,INOIL,11)=WOIL
      FAC1=S(IG,INOIL,11)/RHOV

C     CALCULATE DERIVATIVES USING APPROPRIATE STREAM VALUES
C     IE., IG=1 ON CORRECTOR STEP, IG=2 ON PREDICTOR STEP

      D=FAC1*(S(IG,INOIL,4)-S(IG,IOILO,4))+FAC2  -QLOSS

C     IF THIS IS CORRECTOR STEP GET TANK TEMP PREDICTED PREVIOUSLY
C     IF THIS IS PREDICTOR STEP USE CURRENT TANK TEMP

      IF(IG .EQ. 1)X=S(1,IOILO,4)
      TTANK=Y1(1,S(2,IOILO,4),D,X)
      S(1,IOILO,4)=TTANK
      RETURN
      END
```

APPENDIX A3.3 Listing of subroutine TYPE 2 (AIRCOOL).

```
      SUBROUTINE TYPE 2
      COMMON/CON/IG,KLOOP,NCOMP,NC5,DELT,NE,TIME(30),NS,NPR,TOLL,TOLU,
     1   EMAX,NPCL,TMAX,NCOUNT,JM,KJ,MPR,NGIM
      COMMON/MAT/MP(20,8),EP(20,5),S(2,50,20),EX(100)
      COMMON/UNIT/IM,NMP

C     AIR COOLER MODULE WRITTEN JUNE 19 79 R MCFARLANE
C     STREAM LIST
C     1.  STREAM NO.
C     2.  FLAG
C     3.  TOTAL FLOW  G/SEC
C     4.  TEMP  DEG C
C     5.  PRESSURE  ATM
C     6.  MASS FLOWRATE CH4  G/SEC
C     7.                C2H6
C     8.                C3H8
C     9.                C4H10
C     10.               H2
C     11.  MASS FLOWRATE OIL  G/SEC
C     12.  MASS FLOWRATE AIR  G/SEC

      IF(TIME(2) .NE. 0.)GO TO 10

C     RETRIEVE UNIT PARAMETERS FROM EP MATRIX

      UA=EP(IM,1)
      CPAIR=EP(IM,2)
      CPOIL=EP(IM,3)

C     DEFINE INLET AND OUTLET STREAMS

      INAIR=MP(IM,4)
      INOIL=MP(IM,3)
      IAIRO=IABS(MP(IM,6))
      IOILO=IABS(MP(IM,5))
   10 CONTINUE

C     BECAUSE OF THE LARGE DRIVING FORCE BETWEEN THE AIR AND OIL,OIL
C     TEMP CHANGES ALMOST INSTANTANEOUSLY WITH CHANGES IN AIR FLOW.
C     THEREFORE THIS MODULE IS WRITTEN AS AN ALGEBRAIC ONE, IGNORING
C     THE DYNAMICS OF THE COOLER. ALGEBRAIC MODULES ARE EXECUTED ONLY
C     AFTER DYNAMIC ONES, AND THEREFORE OPERATE ONLY ON S(1,-,-) STREAM
C     VALUES

C     CALCULATE EFFECTIVENESS FACTOR

      RNTU=UA/(S(1,INAIR,12)*CPAIR)
      R=(S(1,INAIR,12)*CPAIR)/(S(1,INOIL,11)*CPOIL)
      FAC1=EXP(-RNTU*(1.-R))
      EPS=(1.-FAC1)/(1.-(R*FAC1))

C     CALCULATE AIR OUTLET TEMP

      TO=EPS*(S(1,INOIL,4)-S(1,INAIR,4))+S(1,INAIR,4)
      S(1,IAIRO,4)=TO

C     CALCULATE OIL OUTLET TEMP

      TIN=S(1,INOIL,4)-R*(TO-S(1,INAIR,4))
      S(1,IOILO,4)=TIN
      RETURN
      END
```

APPENDIX A3.4 Listing of subroutine MODEL1

```
      SUBROUTINE MODEL1(TR1,TW1,TOIL1,TFEED1,TFEED2,TOILIN1,TOILIN2,
     1H2SCFM1,H2SCFM2,C4SCFM1,C4SCFM2,TRP,TWP,TOILP)
      COMMON/CON/IG,KLOOP,NCOMP,NCS,DELT,NE,TIME(30),NS,NPR,TOLL,TOLU,
     1   EMAX,NPOL,TMAX,NCOUNT,JM,KJ,MPR,NGIM
      COMMON/MAT/MP(20,8),EP(20,5),S(2,50,20),EX(100)
      COMMON/UNIT/IM,NMP
      COMMON/BKV/NBV,BV(2,200)
      COMMON/PTAB/  IGFLAG,PP(10,10)
      COMMON/PLT/  NPLOTS,PLOTIME,PLOTS(20,4),PLOTT
      COMMON/PRED/S1,S2,S3,CON
      COMMON/AREA4/IFLAG
      DATA ITEST/0/

C     GIVEN CURRENT AND ONE STEP AHEAD INPUT INFORMATION, THIS SUB
C     -ROUTINE DIRECTS INTEGRATION OF REACO1 OVER ONE TIME INTERVAL

      MAXNS=50
      MAXNE=20

C     IF THIS IS FIRST CALL TO MODEL1, READ AND VERIFY IC DATA

      IF(ITEST .GT. 0)GO TO 500
      CALL DYN1(MAXNE,MAXNS,MP,EP,S,EX,BV)
      EMAX=0.
      CALL OUTPUT(MAXNE,MAXNS,MP,EP,S)
      ITEST=1
  500 CONTINUE

C     IF THIS IS THE BEGINNING OF A NEW INTEGRATION FROM TIME ZERO,
C     INITIALIZE BV MATRIX AN TIME VECTOR TO ZERO, AND SET INITIAL
C     VALUES OF DEPENDENT RESPONSES
      IF(IFLAG .GT. 0)GO TO 501
      IFLAG=1
      IG=2
      KLOOP=0

      DO 13 I=1,200
      BV(1,I)=0.
   13 BV(2,I)=0.

      DO 14 I=1,30
   14 TIME(I)=0.

      S(1,5,5)=S(2,5,5)=TR1
      S(1,5,4)=S(2,5,4)=TW1
      S(1,5,3)=S(2,5,3)=TOIL1

  501 CONTINUE

C     INTEGRATE MODULES OVER ONE TIME INTERVAL
C     SET CURRENT AND ONE STEP AHEAD INPUT VARIABLES

C     BUTANE AND HYDROGEN FEEDRATES

      FAC=(TFEED2+273.)/273.
      H2ACFM1=H2SCFM1*FAC
      H2ACFM2=H2SCFM2*FAC
      FAC1=(TFEED2+273.)*.17387
      H2GM1=((H2ACFM1*1.136)/FAC1)*2.
      H2GM2=((H2ACFM2*1.136)/FAC1)*2.
      S(1,2,10)=H2GM1
      S(2,2,10)=H2GM2
```

APPENDIX A3.4 cont'd

```
      C4ACFM1=C4SCFM1*FAC
      C4ACFM2=C4SCFM2*FAC
      C4GM1=((C4ACFM1*1.136)/FAC1)*58.
      C4GM2=((C4ACFM2*1.136)/FAC1)*58.
      S(1,2,9)=C4GM1
      S(2,2,9)=C4GM2
C     FEED TEMP
      S(1,2,4)=TFEED1
      S(2,2,4)=TFEED2
C     OIL IN TEMP
      S(1,1,4)=TOILIN1
      S(2,1,4)=TOILIN2
C     INTEGRATE MODULES
      TIME(1)=TIME(2)+DELT
      KLOOP=KLOOP+1
      CALL DYN2(MP,MAXNE)
      IG=1
      CALL DYN2(MP,MAXNE)
      IG=2
C     RETURN PREDICTIONS TO CALLING PROGRAM
C     RETRIEVE PREDICTED SELECTIVITIES AND CONVERSIONS FROM THE
C     INFORMATION STREAMS OF REAC01 AND PMIX01
C     SELECTIVITIES AND CONVERSION HAVE BEEN PLACED IN COMMON
      TRP=S(1,5,5)
      TWP=S(1,5,4)
      TOILP=S(1,5,3)
      S1=S(1,5,6)
      S2=S(1,5,7)
      S3=S(1,5,8)
      CON=S(1,5,9)
C     THIS COMPLETES ONE INTEGRATION STEP
C     UPDATE THE S MATRIX FOR NEXT INTEGRATION STEP
      DO 180 I=1,NS
      S(1,I,1)=S(2,I,1)
      S(1,I,2)=S(2,I,2)
      DO 180 J=3,NCS
  180 S(2,I,J)=S(1,I,J)
C     UPDATE TIME VECTOR
      DO 190 I=1,29
      II=30-I
  190 TIME(II+1)=TIME(II)
 1000 CONTINUE
      RETURN
      END
```

APPENDIX A3.5 Listing of main program for closed loop PI control of T_R.

```
      PROGRAM ABC(INPUT, OUTPUT,PI1,TAPE5=INPUT, TAPE6=OUTPUT,
     1TAPE3=PI1)
      DIMENSION TRSET(200),S3SET(200)
      DIMENSION TR(200),TW(200),TOIL(200)
      DIMENSION TFEED(200),TOILIN(200),H2SCFM(200),C4SCFM(200),
     1RATIO(200)
      DIMENSION VS1(200),VS2(200),VS3(200),VCON(200)
      COMMON/PRED/S1,S2,S3,CON
      COMMON/AREA4/IFLAG

C     MAIN PROGRAM TO SIMULATE PI FEEDBACK CONTROL FROM REACTION TEMP
C     TO RATIO OF HYDROGEN TO N-BUTANE FEEDRATES
C     NDELT IS THE INTEGRATION STEPSIZE AND MUST CORRESPOND TO THE
C     STEPSIZE DEFINED IN THE DYNSYS INPUT DATA
C     NSTEP IS THE NUMBER OF INTEGRATION STEPS REQUIRED
C     TRSET(I), I=1,NSTEP IS THE VECTOR OF DESIRED TR SETPOINTS

C     S3SET(I), I=1,NSTEP IS THE VECTOR OF DESIRED S3 SETPOINTS


      NDELT=30
      NSTEP=100

C     INFORM SUBROUTINE MODEL1 THAT A NEW INTEGRATION HAS BEEN INITIATED

      IFLAG=0
C     DEFINE INITIAL TR TW AND TOIL

      TR1=260.
      TW1=253.
      TOIL1=247.4

C     DEFINE DESIRED TOTAL VOL FLOWRATE TO REACTOR

      SCFM=3.5

C     DEFINE VECTOR OF INPUTS , TFEED AND TOILIN

      DO 1000 I=1,NSTEP
      TFEED(I)=260.
      TOILIN(I)=247.
 1000 CONTINUE

C     DEFINE INITIAL FEED FLOWS

      RATIO1=8.
      C4SCFM1=SCFM/(RATIO1+1)
      C4SCFM2=C4SCFM1
      H2SCFM1=SCFM-C4SCFM1
      H2SCFM2=H2SCFM1

      RATIO(1)=RATIO1
      C4SCFM(1)=C4SCFM1
      H2SCFM(1)=H2SCFM1
C     DEFINE CONTROLLER PARAMETERS

      C1=2.68
      C2=-1.


C     DEFINE VECTOR OF TR SETPOINTS
      ALPHA=0.
      PHI=.6
```

APPENDIX A3.5 cont'd

```
      TRSET(1)=260.
      TRSET(2)=260.
      DO 1003 I=3,NSTEP
      IF(I .EQ. 30)ALPHA=1.2
      IF(I .EQ. 60)ALPHA=-1.2
      TRSET(I)=(1.+PHI)*TRSET(I-1)  - PHI*TRSET(I-2) + ALPHA
      ALPHA=0.
 1003 CONTINUE
C     INITIAL PAST VALUE OF ERROR FOR RATIO CONTROLLER
      E2=0.

C     PROCEED WITH NSTEP-1 INTEGRATIONS, APPLYING CONTROL ACTION
C    AFTER EACH STEP
      NUMB=NSTEP-1
      DO 2000 I=1,NUMB

C     DEFINE CURRENT AND ONE STEP AHEAD INPUTS
C     2 IS CURRENT TIME, 1 IS ONE STEP AHEAD
      TFEED1=TFEED(I+1)
      TFEED2=TFEED(I)

      TOILIN1=TOILIN(I+1)
      TOILIN2=TOILIN(I)

C     INTEGRATE MODULES OVER ONE TIME INTERVAL
      CALL MODEL1(TR1,TW1,TOIL1,TFEED1,TFEED2,TOILIN1,TOILIN2,
     1H2SCFM1,H2SCFM2,C4SCFM1,C4SCFM2,TRP,TWP,TOILP)
C     STORE THE PREDICTIONS IN THE APPROPRIATE PREDICTION VECTORS
      VS1(I)=S1
      VS2(I)=S2
      VS3(I)=S3
      VCON(I)=CON
      TR(I)=TRP
      TW(I)=TWP
      TOIL(I)=TOILP
C     ***************************************************************
C     TAKE CONTROL ACTION
C     ***************************************************************
      E1=TRSET(I+1) - TRP
      E1=-E1
      RATIO1=RATIO1 + C1*E1     +C2*E2
C     BASED ON THIS NEW RATIO SET C4 AND H2 FEEDRATES, SCFM
      IF(RATIO1 .LE. 3.)RATIO1=3.
      C4SCFM1=SCFM/(RATIO1+1.)
      C4SCFM2=C4SCFM1
      H2SCFM1=SCFM-C4SCFM1
      H2SCFM2=H2SCFM1
C     UPDATE FOR NEXT CONTROL INTERVAL
      E2=E1
C     RECORD NEW RATIO C4SCFM AND H2SCFM
      C4SCFM(I+1)=C4SCFM1
      H2SCFM(I+1)=H2SCFM1
      RATIO(I+1)=RATIO1
```

```
C     ***************************************************************
C     END OF CONTROLLER
C     ***************************************************************
 2000 CONTINUE
C     THIS IS THE END OF NSTEP-1 INTEGRATIONS, OUTPUT TO LINE
C     PRINTER AND DISC

      WRITE(6,110)
  110 FORMAT(//3X,≠TIME≠,4X,≠TR≠,6X,≠TW≠,6X,≠TOIL≠,9X,≠S1≠,8X,≠S2≠,7X,
     1≠S3≠,5X,≠CON≠,4X,≠C4SCFM≠,3X,≠H2SCFM≠,3X,≠RATIO≠,3X,≠TFEED≠,
     13X,≠TOILIN≠,4X,≠TRSET≠,5X,≠S3SET≠,//)
      TIME=0.
      WRITE(6,107)TIME,TR1,TW1,TOIL1
  107 FORMAT(1X,F6.0,3F9.4)
      DO 1011 I=1,NUMB
      TIME=I*NDELT
      J=I+1
      WRITE(3,108) TIME,TR(I),TW(I),TOIL(I),VS1(I),VS2(I),VS3(I),
     1VCON(I),C4SCFM(J),H2SCFM(J),RATIO(J),TFEED(J),TOILIN(J)
     1,TRSET(J),S3SET(J)
 1011 WRITE(6,108) TIME,TR(I),TW(I),TOIL(I),VS1(I),VS2(I),VS3(I),
     1VCON(I),C4SCFM(J),H2SCFM(J),RATIO(J),TFEED(J),TOILIN(J)
     1,TRSET(J),S3SET(J)
  108 FORMAT(1X,F6.0,14F9.4)
      STOP
      END
```

```
BEGIN
COMPS       7.
IN/OUT      5.
DELTAT      30.
PROCESS
REAC01      1.
            1.          2.          -3.         -4.         -5.
            7000.       1.870       21.41       17.3E       .0165
EXTRA       5.
            3000.00     0.64        0.25        0.          1.
END
STREAMS     5.
EXPLICIT
            1.          5.          565.7       247.00      1.1
            0.          0.          0.          0.          0.
            565.7       0.
            2.          5.                      260.00      1.1
            0.          0.          0.
            0.          0.
            3.          5.          565.7
            0.          0.          0.          0.          0.
            565.7       0.
            4.          5.          0.                      1.0
            0.            0.        0.          0.          0.
            0.          0.
            5.          11.         247.4       253.00      260.
            0.          0.          0.          0.          0.
            0.          0.
END
PROPERTIES  0.
  -19625.11
  3.35959530
  8.4959047E-003
  -7.112638.2E-07
  -2.5486782E-10
  -22148.55
  -0.10380823
  2.4080342E-002
  -7.7818629E-06
  1.1441622E-009
  -27396.10
  -1.26541850
  3.6877433E-002
  -1.2849924E-05
  1.9768954E-009
  -33721.76
  -0.57401823
  4.6665211E-002
  -1.6016282E-05
  2.3949331E-009
  -1909.88
  5.84681958
  2.0631049E-003
  -6.5971584E-07
  8.4704866E-011
```

APPENDIX A4.1 Listing of main program for UWHAUS, and subroutines MODEL and DYN.

```
      PROGRAM ABC(INPUT,OUTPUT,PES4A,DAT4,TAPE5=INPUT,TAPE6=OUTPUT,
     1TAPE3=PES4A,TAPE4=DAT4)
      DIMENSION TH(1),SIGNS(1),DIFF(1),SCRAT(1374)
      DIMENSION H2SCFM(45),C4SCFM(45),E(135)
      COMMON/FINISH/FINAL(135)
      COMMON/AREA1/NOB,T(45,16),H2GM(45),C4GM(45),E(135)

      EXTERNAL MODEL

C     MAIN PROGRAM FOR CATALYST ACTIVITY ESTIMATION
C     THE VECTOR OF OBSERVED RESPONSES IS FORMED BY CONCATENATING
C     THE VECTORS TR(I),TW(I),TOIL,AVG(I)  I=1,NOB
C     NOB=NO. OF OBSERVATIONS
C     TEMPERATURE AND FLOW DATA ARE READ FROM PERMANENT FILE DAT4
C     REACTOR TEMPS IN T(I,2),T(I,4),T(I,5)   I=1,NOB
C     WALL TEMPS IN T(I,9),T(I,10)
C     FEED TEMP IN T(I,8)
C     OIL IN TEMP IN T(I,12)
C     HYDROGEN INLET FLOWRATE(SCFM) IN T(I,15)
C     BUTANE INLET FLOWRATE(SCFM) IN T(I,16)

C     READ AND VERIFY DATA FROM DAT4
C     NOB=70

      NOB=70
      WRITE(6,500)
  500 FORMAT(//1X,*DAT4 DATA*,//)
      DO 1000 I=1,NOB
      READ(4,900)IJ,IK,IM
  900 FORMAT(2X,3I3)
      READ(4,901)(T(I,J),J=1,6)
      READ(4,901)(T(I,J),J=7,12)
  901 FORMAT(1X,6F9.2)
      READ(4,902)(T(I,J),J=13,16),H2SCFM(I),C4SCFM(I)
  902 FORMAT(1X,4F9.2,2F9.5)
      IF(C4SCFM(I).LT. .19)C4SCFM(I)=0.

      WRITE(6,40)IJ,IK,IM
   40 FORMAT(1X,3I4)
      WRITE(6,41)(T(I,J),J=1,6)
      WRITE(6,41)(T(I,J),J=7,12)
   41 FORMAT(1X,6F9.2)
      WRITE(6,42)(T(I,J),J=13,16),H2SCFM(I),C4SCFM(I)
   42 FORMAT(1X,4F9.2,2F9.5)

 1000 CONTINUE


C     CREATE THE OBSERVED DEPENDENT VARIABLE E(I), I=1,3*NOB
C     (TR,TW,TOIL)
C     DO NOT USE THERMOCOUPLE DATA FROM DISTRIBUTOR PLATE

      DO 100 J=1,NOB
      TR=(T(J,2)+T(J,4)+T(J,5))/3.
  100 E(J)=TR

      I1=NOB+1
      I2=2*NOB
      DO 101 I=I1,I2
      IK=I-NOB
      TW=(T(IK,9)+T(IK,10))/2.
  101 E(I)=TW
```

APPENDIX A4.1 cont'd

```
      I1=2*NOB+1
      I2=3*NOB
      DO 102 I=I1,I2
      IK=I-2*NOB
      TOIL=(T(IK,12)+T(IK,13))/2.
  102 E(I)=TOIL
      WRITE(6,300)
  300 FORMAT(//20X,'DEPENDENT RESPONSES',//1X,
     15X,'TR',10X,'TW',10X,'TOIL,AVG',//)
      DO 502 I=1,NOB
      INN=2*NOB
  502 WRITE(6,503)E(I),E(I+NOB),E(I+INN)
  503 FORMAT(1X,F10.5,5X,F10.5,5X,F10.5)

C     CONVERT INLET VOLUMETRIC FLOWRATE TO MASS FLOWRATE
      DO 550 J=1,NOB
      FAC=(T(J,8)+273.)/273.
      H2ACFM=H2SCFM(J)*FAC
      C4ACFM=C4SCFM(J)*FAC
      H2GM(J)=((H2ACFM*1.136)/((T(J,8)+273.)*.17387))*2.
  550 C4GM(J)=((C4ACFM*1.136)/((T(J,8)+273.)*.17387))*58.

C     PRINT INLET FLOW CONDITIONS

      WRITE(6,560)
  560 FORMAT(//1X,'INLET FLOW CONDITIONS')
      WRITE(6,561)
  561 FORMAT(//1X,7X,'TFEED',7X,'H2SCFM',7X,'H2GM',7X,'C4SCFM',7X
     1,'C4GM')
      DO 562 I=1,NOB
  562 WRITE(6,563)T(I,8),H2SCFM(I),H2GM(I),C4SCFM(I),C4GM(I)
  563 FORMAT(1X,5F12.6)

C     CALL UWHAUS

      MIT=20
      FLAM=.01
      FNU=10.
      NOBS=3*NOB
      NPARS=1
      TH(1)=1.
      DIFF(1)=.01
      SIGNS(1)=1.
      EPS1=0.
      EPS2=.0001
      SCRAT=1074.
      CALL UWHAUS(1,MODEL,NOBS,E,NPARS,TH,DIFF,SIGNS,EPS1,EPS2,MIT,
     1FLAM,FNU,SCRAT)

      WRITE(6,118)
  118 FORMAT(//1X,7X,'TR OBS',7X,'TW OBS',7X,'TOIL OBS',7X,
     1'TR PRED',7X,'TW PRED',7X,'TOIL PRED',//)
      DO 116 I=1,NOB
      WRITE(3,117)E(I),E(I+NOB),E(I+INN),FINAL(I),FINAL(I+NOB),
     1FINAL(I+INN)
  116 WRITE(6,117)E(I),E(I+NOB),E(I+INN),FINAL(I),FINAL(I+NOB),
     1FINAL(I+INN)
  117 FORMAT(1X,6F12.6)
      STOP
      END
      SUBROUTINE MODEL(NPROB,TH,F1,NOB2,NP)
      DIMENSION TH(1),F1(135),F(135)
      COMMON/AREA2/PAR(1)

      PAR(1)=TH(1)


      CALL DYN(F)
      DO 100 I=1,NOB2
  100 F1(I)=F(I)
      RETURN
      END
```

```
      SUBROUTINE DYN(F)
      DIMENSION F(1)
      COMMON/AREA1/NOB,T(45,16),H2GM(45),C4GM(45),E(195)
      COMMON/AREA2/PAR(1)
      COMMON/CON/IG,KLOOP,NCOMP,NCS,DELT,NE,TIME(30),NS,NPR,TOLL,TOLU,
     1   EMAX,NPOL,TMAX,ACOUNT,JM,KJ,MPP,NGIM
      COMMON/MAT/MP(20,8),EP(20,5),S(2,50,20),EX(100)
      COMMON/UNIT/IM,NMP
      COMMON/BKV/NBV,BV(2,200)
      COMMON/PTAB/  IGFLAG,PP(10,10)
      COMMON/PLT/  NPLOTS,PLOTIME,PLOTS(20,4),PLOTT
      DATA ITEST/0/
      MAXNS=50
      MAXNE=20
C     IF THIS IS 1ST CALL TO DYN READ AND VERIFY IC DATA
      IF(ITEST .GT. 0)GO TO 500
      CALL DYN1(MAXNE,MAXNS,MP,EP,S,EX,BV)
      EMAX=0.
      CALL OUTPUT(MAXNE,MAXNS,MP,EP,S)
      ITEST=1
  500 CONTINUE
      IG=2
      KLOOP=0

C     INITIALIZE BV MATRIX TO ZERO

      DO 13 I=1,200
      BV(1,I)=0.
   13 BV(2,I)=0.

C      INITIALIZE TIME VECTOR

      DO 14 I=1,30
   14 TIME(I)=0.

C     BEFORE BEGINNING INTEGRATION, INITIALIZE DEPENDENT RESPONSES
C     TR,TW AND TOIL,  AND RETRIEVE CURRENT PARAMETERS

      IM=1
      EP(IM,2)=PAR(1)

      IOQ=2*NOB+1
      S(1,5,5)=S(2,5,5)=E(1)
      S(1,5,4)=S(2,5,4)=E(NOB+1)
      S(1,5,3)=S(2,5,3)=E(IOQ)


C     THE FIRST ELEMENT OF THE PREDICTION VECTOR FOR MODEL IS THE
C     REACTOR INITIAL CONDX TR
C     THE (NOB+1) ELEMENT IS TW INITIAL
C     THE (2*NOB+1) ELEMENT IS TOIL,INITIAL
      F(1)=E(1)
      F(NOB+1)=E(NOB+1)
      F(IOQ)=E(IOQ)
C     INTEGRATE MODEL EQUATIONS OVER NOB TIME INTERVALS


      NUMB=NOB-1
      DO 1000 K=1,NUMB
      TIME(1)=TIME(2)+DELT
      KLOOP=KLOOP+1

C     GET CURRENT INDEPENDENT VARIABLES AND PUT INTO APPROPRIATE
C     STREAM POSITIONS
C     (IG=2= CURRENT TIME,   IG=1=FUTURE TIME)

      S(1,2,9)=C4GM(K+1)
      S(2,2,9)=C4GM(K)
      S(1,2,10)=H2GM(K+1)
      S(2,2,10)=H2GM(K)
```

```
C       OIL IN TEMP

        S(1,1,4)=T(K+1,12)
        S(2,1,4)=T(K,12)

C       FEED TEMP
        S(1,2,4)=T(K+1,8)
        S(2,2,4)=T(K,8)
C       NOW PROCEED WITH INTEGRATION

        CALL DYN2(MP,MAXNE)
        IG=1
        CALL DYN2(MP,MAXNE)
        IG=2

C       PREDICTED RESPONSES ARE IN S(1,-,-)
C       PUT THESE INTO PREDICTION VECTOR FOR RETURN
C       TO MODEL
C       TR IS IN S(1,5,5)
C       TW IS IN S(1,5,4)
C       TOIL IS IN S(1,5,3)

        F(K+1)=S(1,5,5)
        F(NOB+K+1)=S(1,5,4)
        IRS=2*NOB+1+K
        F(IPS)=S(1,5,3)

C       UPDATE THE S MATRIX FOR NEXT INTEGRATION STEP

        DO 180 I=1,NS
        S(1,I,1)=S(2,I,1)
        S(1,I,2)=S(2,I,2)
        DO 180 J=3,NOS
  180   S(2,I,J)=S(1,I,J)

C       UPDATE TIME VECTOR

        DO 190 I=1,29
        II=30 - I
  190   TIME(II+1)=TIME(II)

 1000   CONTINUE

C       THIS COMPLETES ONE PASS THRU THE MODEL WITH THE CURRENT PARAMETRS
C       RETURN TO MODEL WITH VECTOR OF PREDICTED RESPONSES F(3*NOB)
C       CONTAINING PREDICTED RESPONCES OF TR,TW AND TOIL

        WRITE(6,160)
  160   FORMAT(//1X,7X,'TR PRED',7X,'TWPRED',7X,'TOIL PRED',//)
        INN=2*NOB
        DO 170 I=1,NOB


  170   WRITE(6,171)F(I),F(NOB+I),F(INN+I)
  171   FORMAT(1X,3F12.6)
        RETURN
        END
```

REFERENCES

1. Shaw, I.D., "Modelling and Discrimination Studies in a Catalytic Fluidized Bed Reactor", Ph.D. Thesis, McMaster University, Hamilton, Ontario (1974).

2. Tremblay, J.P., "Real Time Computer Data Acquisition and Control Systems: An Application to Model Reference Adaptive Control of a Packed Bed Tubular Reactor", Ph.D. Thesis, Mcmaster University, Hamilton, Ontario (1977).

3. Foss, A.S., AIChE J., 19 (2), 209 (1973).

4. Lee, W. and Weekman, V.W., AIChE J., 22 (1), 27 (1976).

5. Orcutt, J.C., Davidson, J.E. and Pigford, R.L., Chem. Eng. Prog. Symp. Sci., 58 (38), 1 (1962).

6. Partridge, B.A. and Rowe, P.N., Trans. Inst. Chem. Engrs. 44, T349 (1966).

7. Kunii, D., Levenspiel, O., Ind. Eng. Chem. Des. and Development, 7 (4), 481 (1968).

8. Kato, K., Wen, C.Y., Chem. Eng. Sci., 24, 1351 91969).

9. Orlickas, A., "Kinetic Study of the Hydrogenolysis of n-Butane on Nickel Catalyst", M.Eng. Thesis, McMaster University, Hamilton, Ontario (1970).

10. Orlickas, A., Hoffman, T.W., Shaw, I.D., and Reilly, P.M., Can. J. Chem. Eng., 50, 628 (1972).

11. Shaw, I.D., Hoffman, T.W., Orlickas, A. and Reilly, P.M., Can. J. Chem. Eng., 50, 637 (1972)

12. Shaw, I.D., Hoffman, T.W., and Reilly, P.M., AIChE Symp. Ser., 70 (141), 41 (1974).

13. Kjaer, J., Thermodynamic Calculations on an Electronic Digital Computer, Akademisk Forlag, Copenhagen, 1963.

14. Bobrow, S., DYNSYS – A Digital Computer Program for Studying the Transient Behaviour of Systems using a Modular Apporach", M. Eng. Thesis, McMaster University, Hamilton, Ontario (1969)

15. Marquardt, D.W., J. Soc. Ind. Appl. Math., 2, (1963).

16. Beckman Instruments Inc.; Operating Manual for Model 6700 Process Gas Chromatograph, 1973.

17. Beckman Instruments Inc., Electronic Maintenance and Troubleshooting Manual, Model 6700 Process Gas Chromatograph, 1975.

18. Dahlin, E.B., Instruments and Control Systems, 41 (6), 77 (1968)